

AD-A168 829

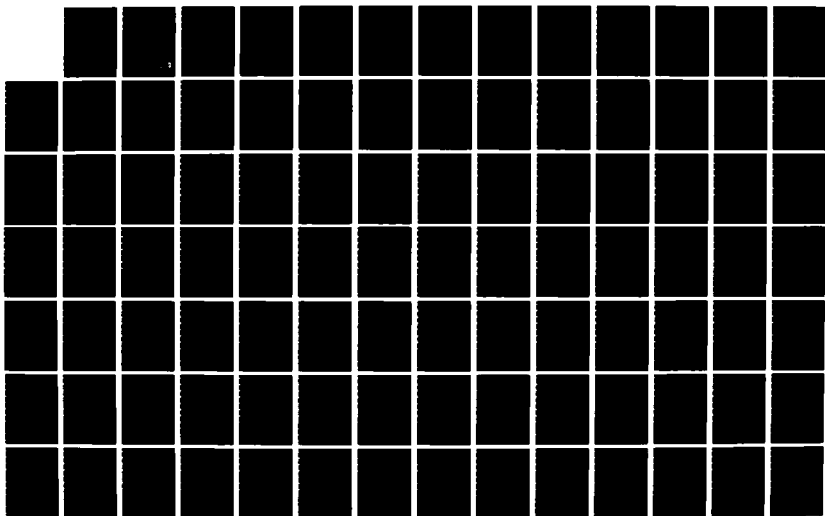
A MODEL OF INHALED GAS AND VAPOR TRANSPORT IN THE HUMAN
LUNG(U) AIR FORCE INST OF TECH WRIGHT-PATTERSON AFB OH
M L SHELLEY 1985 AFIT/CI/NR-85-143D

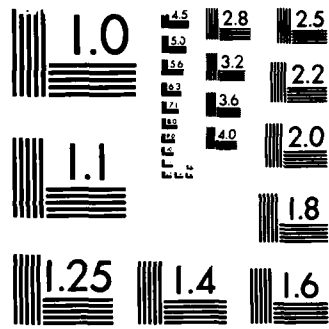
1/2

UNCLASSIFIED

F/G 6/16

NL





MICROCOPY RESOLUTION TEST CHART
NATIONAL BUREAU OF STANDARDS-1963-A

UNCLASS

SECURITY CLASSIFICATION OF THIS PAGE (When Data Entered)

REPORT DOCUMENTATION PAGE

READ INSTRUCTIONS BEFORE COMPLETING FORM

1. REPORT NUMBER AFIT/CI/NR 85-143D		2. GOVT ACCESSION NO. AD-A160 829	3. RECIPIENT'S CATALOG NUMBER
4. TITLE (and Subtitle) A Model Of Inhaled Gas And Vapor Transport In The Human Lung		5. TYPE OF REPORT & PERIOD COVERED THESIS/DISSERTATION	
7. AUTHOR(s) Michael L. Shelley		6. PERFORMING ORG. REPORT NUMBER	
9. PERFORMING ORGANIZATION NAME AND ADDRESS AFIT STUDENT AT: The University of North Carolina		8. CONTRACT OR GRANT NUMBER(s)	
1. CONTROLLING OFFICE NAME AND ADDRESS AFIT/NR WPAFB OH 45433-6583		10. PROGRAM ELEMENT, PROJECT, TASK AREA & WORK UNIT NUMBERS	
14. MONITORING AGENCY NAME & ADDRESS (if different from Controlling Office)		12. REPORT DATE 1985	
		13. NUMBER OF PAGES 123	
		15. SECURITY CLASS. (of this report) UNCLASS	
		16a. DECLASSIFICATION/DOWNGRADING SCHEDULE	

6. DISTRIBUTION STATEMENT (of this Report)
APPROVED FOR PUBLIC RELEASE; DISTRIBUTION UNLIMITED

17. DISTRIBUTION STATEMENT (of the abstract entered in Block 20, if different from Report)

18. SUPPLEMENTARY NOTES
APPROVED FOR PUBLIC RELEASE: IAW AFR 190-1

Lynn E. Wolaver
LYNN E. WOLAVER *Director*
Dean for Research and Professional Development
AFIT, Wright-Patterson AFB

19. KEY WORDS (Continue on reverse side if necessary and identify by block number)

20. ABSTRACT (Continue on reverse side if necessary and identify by block number)

ATTACHED

DTIC
ELECTE
NOV 04 1985
S E D

DD FORM 1 JAN 73 1473

EDITION OF 1 NOV 65 IS OBSOLETE

UNCLASS

SECURITY CLASSIFICATION OF THIS PAGE (When Data Entered)

AD-A160 829

DTIC FILE COPY

ABSTRACT

MICHAEL L. SHELLEY. A Model of Inhalation Gas and Vapor Transport in the Human Lung. (Under the direction of DR. ROBERT L. HARRIS)

The transport of inhaled gas or vapor in the human lung is theoretically modeled to determine the fraction of inhaled gas or vapor absorbed through the bronchial walls in the conductive zone and the fraction entering alveolated space and undergoing blood/gas exchange. An iterative-analytical approach is used, rather than a numerical one, to generate a large amount of data over a wide range of gas or vapor solubilities and diffusivities. The model applies to gases or vapors of low solubility. Simple analytical expressions are fitted to model results, expressing fractional bronchial absorption and alveolar uptake in terms of gas or vapor solubility and diffusivity. Typical physiological parameters are assumed and only physical properties of the gas or vapor are required for input. Methods are presented which allow estimation of these input values.

↑

Accession For	
NTIS GRA&I	<input checked="" type="checkbox"/>
DTIC TAB	<input type="checkbox"/>
Unannounced	<input type="checkbox"/>
Justification	
By	
Distribution/	
Availability Codes	
Dist	Avail and/or Special
A-1	



A MODEL OF INHALED GAS AND
VAPOR TRANSPORT IN THE
HUMAN LUNG

by

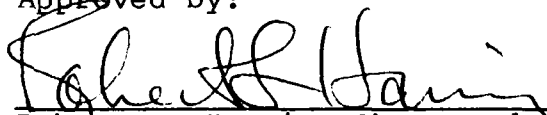
Michael L. Shelley

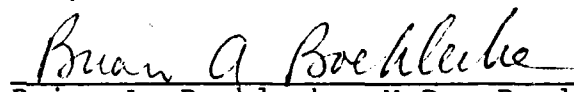
A Dissertation submitted to the faculty of The University of
North Carolina at Chapel Hill in partial fulfillment of the
requirements for the degree of Doctor of Philosophy in the
Department of Environmental Sciences and Engineering.

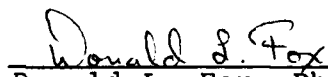
Chapel Hill

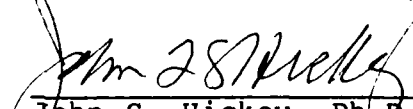
1985

Approved by:


Robert L. Harris, Ph.D., Adviser


Brian A. Boehlecke, M.D., Reader


Donald L. Fox, Ph.D., Reader


John S. Hickey, Ph.D., Reader


Cass T. Miller, Ph.D., Reader

85 11 04 002

ACKNOWLEDGEMENTS

I wish to express my deep love and appreciation to my wife, Sherry, and my children, Maria, Ashley, and Joshua, for their untiring love, support, and encouragement during this research.

I especially appreciate my father whose advice and continual support was invaluable.

In all things, and above all, I am grateful for the Grace and Strength of my Lord Jesus Christ who has given me life, purpose, and motivation in my work.

I acknowledge also the Institute for Computational Studies and the National Institutes of Health for their computational resource support.

CONTENTS

<u>TITLE</u>	<u>PAGE</u>
I. CHAPTER 1 INTRODUCTION	1
II. CHAPTER 2 HUMAN LUNG STRUCTURE	8
Airways of the Conductive Zone	9
Air Flow Patterns	13
Structure and Composition of the Bronchial Wall	21
III. CHAPTER 3 MASS TRANSPORT	27
IV. CHAPTER 4 PHYSICAL PROPERTIES OF INHALED GASES AND VAPORS	37
Solubility	38
Air Diffusion Coefficient	43
Water Diffusion Coefficient	44
V. CHAPTER 5 A LUNG MASS TRANSPORT MODEL	49
VI. CHAPTER 6 RESULTS	65
Conclusions	80

<u>TITLE</u>	<u>PAGE</u>
VII. APPENDIX A LAMINAR FLOW VELOCITY PROFILE IN A CIRCULAR TUBE	84
VIII. APPENDIX B EQUATIONS OF CHANGE FOR TURBULENT AIR FLOW	89
IX. APPENDIX C FORTRAN SOURCE LISTING, TRANSPORT MODEL	93
X. APPENDIX D TABULATED MODEL RESULTS	107
XI. APPENDIX E BRONCHIAL ABSORPTION UPTAKE, MODEL RESULTS vs PREDICTED	111
XII. APPENDIX F ALVEOLAR UPTAKE, MODEL RESULTS vs PREDICTED	115
XIII. APPENDIX G ESTIMATION OF SOLUBILITY PARAMETERS	119
XIV. REFERENCES	123

LIST OF FIGURES

<u>TITLE</u>	<u>PAGE</u>
FIGURE 1.1 SYSTEMIC DISTRIBUTION MODEL	4
FIGURE 1.2 SYSTEMIC MODEL WITH LUNG PARTITIONING	6
FIGURE 2.1 BIFURCATING AIRWAY PATTERN	10
FIGURE 2.2 PATTERNS OF DICHOTOMY	11
FIGURE 2.3 INHALATION/EXHALATION FLOW FUNCTION	15
FIGURE 2.4 NON-TURBULENT FLOW PATTERNS	17
FIGURE 2.5 TAYLOR DISPERSION	19
FIGURE 2.6 BRONCHIAL WALL FLUID LAYERS	23
FIGURE 2.7 BRONCHIAL MASS TRANSPORT REGIONS	25
FIGURE 3.1 AIR PHASE MASS BALANCE	28
FIGURE 3.2 FLUID AND EPITHELIAL MASS BALANCE	32
FIGURE 4.1 VAPOR-LIQUID EQUILIBRIA	40

<u>TITLE</u>	<u>PAGE</u>
FIGURE 4.2 ESTIMATING SOLUBILITY AND DIFFUSIVITY	47
FIGURE 5.1 CONVECTIVE-DIFFUSIVE TRANSPORT	51
FIGURE 5.2 SIMPLIFIED AIRWAY MODEL	54
FIGURE 5.3 FLUID AND EPITHELIAL MODEL	55
FIGURE 5.4 BRONCHIAL AIR CONCENTRATION	58
FIGURE 5.5 TRANSPORT MODEL OVERVIEW	61
FIGURE 5.6 MODEL ASSUMPTIONS	62
FIGURE 6.1 LUNG UPTAKE	69
FIGURE 6.2 EPITHELIAL ABSORPTION	70
FIGURE 6.3 PREDICTED EPITHELIAL ABSORPTION	71
FIGURE 6.4 ALVEOLAR UPTAKE	73
FIGURE 6.5 PREDICTED ALVEOLAR UPTAKE	74
FIGURE 6.6 MUCO-CILIARY CLEARANCE	75

<u>TITLE</u>	<u>PAGE</u>
FIGURE 6.7 SUMMARY OF CONCLUSIONS	82
FIGURE A.1 LAMINAR FLOW MOMENTUM BALANCE	85

Chapter 1

INTRODUCTION

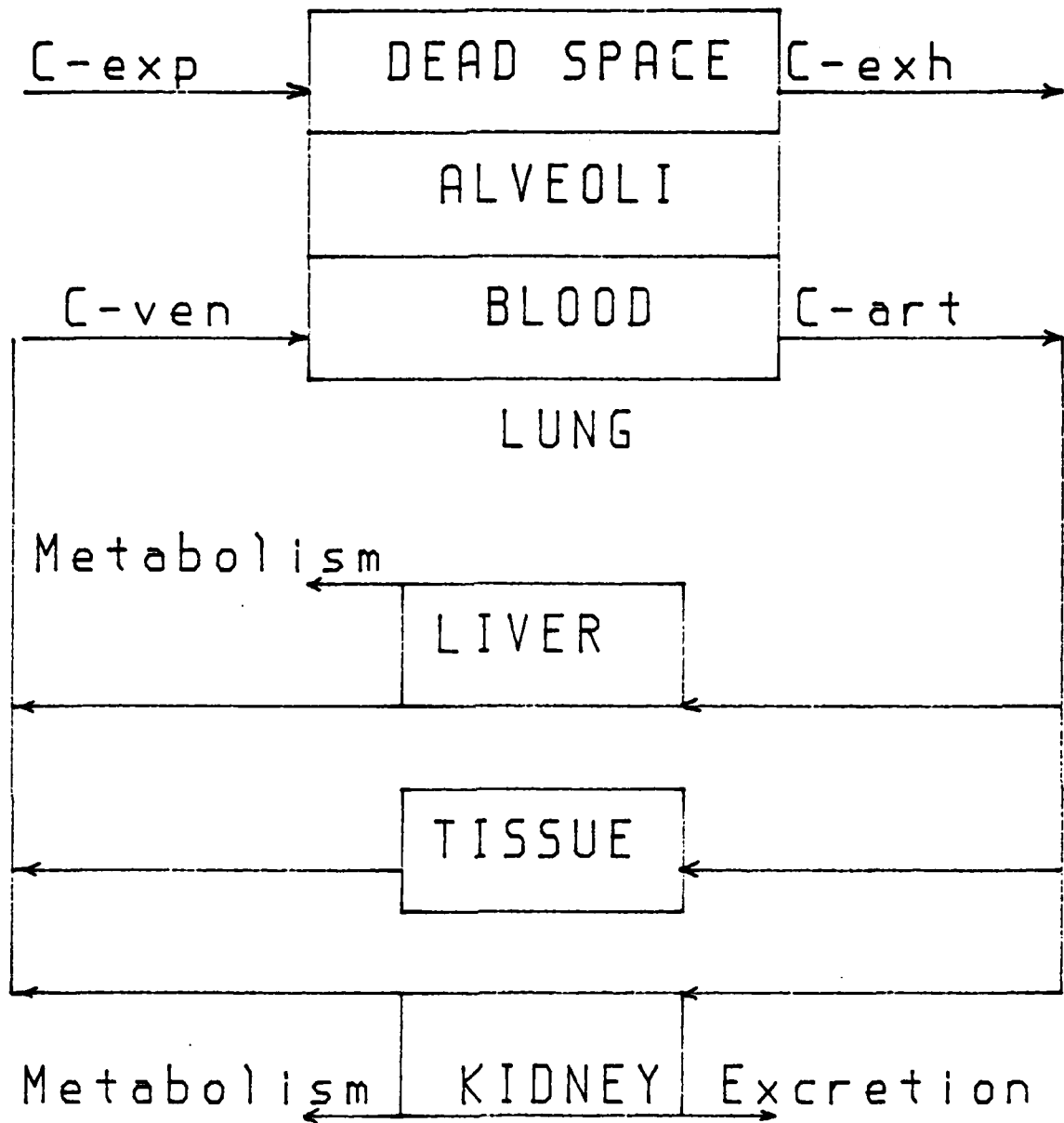
The modeling of inhalation exposure to gases and vapors has received much attention in the literature, particularly in the anesthesiology field. Models have been rigorously developed for alveolar gas exchange, distribution to various tissue types, and clearance from these tissues under varying physiological conditions. Application of these mathematically derived relations to in-vivo laboratory experiments has allowed the establishment of important physiological constants for many exposure gases (blood/gas and tissue/blood partition coefficients, tissue clearance rates, etc.). These data provide a tool for predicting body burdens, half life, and pharmacological effects of particular gaseous insults at various inhalation exposure concentrations. In large part, these constants are based on direct measurement of blood and tissue concentrations, urine excretion, ventilation, etc. as well as certain indirect measurements such as analysis of end-exhalation expired air representing alveolar concentration. Measurement of alveolar concentration in this way probably provides a reasonably accurate estimation when dealing with large exposure concentrations such as those of interest in

anesthesiology.

In public health, one is more often concerned with relatively low exposure concentrations of many types of gases with a wide range of solubilities. Under these conditions, distribution of gas within the lung must be considered in a different light, with particular attention to the significance of the muco-ciliary clearance mechanism and absorption through the epithelial wall of the conductive zone of the lung prior to reaching the alveolar region. Conceptually, one must envision a mass balance which distributes the inhaled mass of gas into the known pulmonary clearance mechanisms of exhalation, alveolar gas exchange, bronchial wall absorption, and mucus discharge to the GI tract. Gas exchanged at the bronchial epithelium beneath the mucus blanket should ultimately enter the same physiological compartment as that exchanged in the alveoli but with a different rate of uptake and with an opportunity to undergo metabolism in lung tissue prior to entering the blood stream for further distribution. Sixteen different enzymatic systems involved in metabolism have been reported in lung tissue.⁸ The mixed function oxidase systems in the lung are similar to those in the liver. Enzymatic activity in the lung is small relative to that in the liver, but considerable metabolism might be expected due to higher exposure to inhalation agents, the lung acting as a gateway for systemic entry.

An understanding of the distribution partitioning described above is essential in relating exposure concentration to blood concentration as well as estimating the GI insult due to ciliary clearance. Yet, such a model, using this mass balance approach, to date has not been presented in the literature. The complexities of gas exchange back and forth across the air/liquid interface on the bronchial wall, together with the uncertainties of the structure and composition of the mucus blanket and the lack of computer methods to generate data consistent with lung morphology, hindered such efforts prior to the early 50's when existing inhalation models were developed. Construction of a model which would properly distribute exposure in the lung relative to applicable physical and physiological parameters is now within reach and would constitute a significant contribution to the study of gaseous inhalation exposure.

For example, consider the conceptual model in figure 1.1 which is of the type often used by systemic distribution modelers. In this model, the inhaled mass entering the dead space (conductive zone) and the alveoli (respiratory zone) is partitioned into the two compartments of blood and exhalation. The mass partitioned into the blood compartment is based on complete air/blood equilibration of all mass entering the alveolar region in accordance with the alveolar ventilation rate and blood perfusion rate. This assumes that the mass entering the alveolar region is at the same

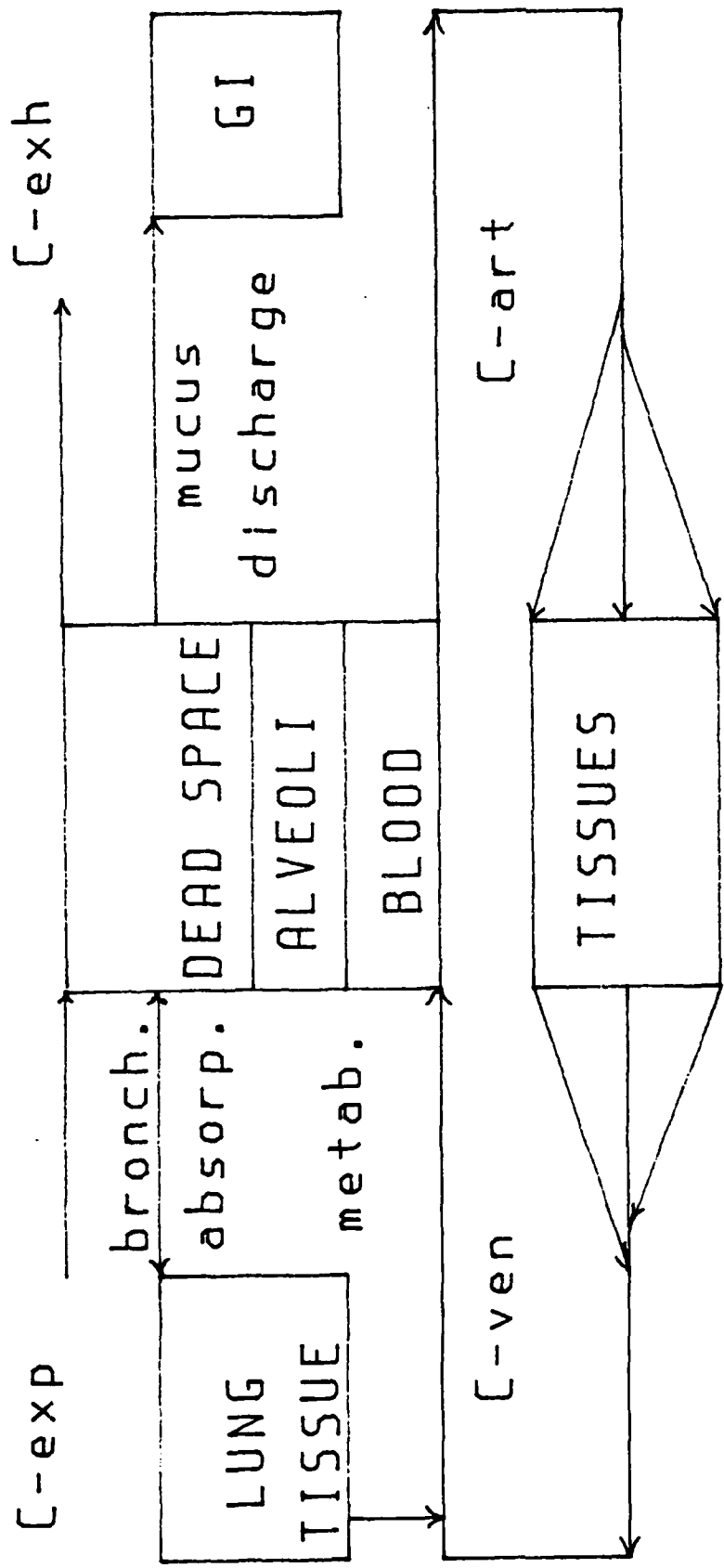


SYSTEMIC DISTRIBUTION MODEL

FIGURE 1.1

concentration as that of the environment (allowing for minor differences due to body temperature and humidity). The equilibrated blood concentration thus arrived at is the basis of subsequent uptake and elimination determination in the various tissue types. (Note: Ketty¹⁵ presents several approaches to this type of model, reviewing previous work by Zunts, von Schroder, Widmark³⁰, Haggard¹⁰, Teorell²⁶, Morales and Smith¹⁷, and Copperman. Fiserova-Bergerova⁸ also presents a fundamental review of the principles involved.) For the case of low concentration exposure to an environmental agent, a more desirable model is depicted in figure 1.2 and includes a more detailed partitioning within the lung. Here, rather than all mass passing through the conductive zone reaching the alveoli, two additional compartments are added: bronchial wall absorption to lung tissue and mucus discharge at the top to the GI tract. Exposure to the GI tract via this route may or may not be significant. Partitioning to lung tissue would limit the rate of transport to blood and provide the opportunity for metabolism prior to reaching other tissue types.

Partitioning to lung tissue or discharge to GI tract, however, is not as simple as assuming complete equilibration with that compartment. One must describe the transport process in terms of the gas solubility and diffusivity through the medium. If such a description can be achieved, the behavior of the gas in the lung could be predicted without experimental data based on the physical constants of



SYSTEMIC MODEL WITH LUNG PARTITIONING

FIGURE 1.2

the gas. The relative significance of exposure via blood/gas exchange, bronchial wall absorption, and GI ingestion by mucus discharge could then be analyzed with confidence, possessing a valuable tool in estimating the potential toxicity of the exposure.

The present work examines the fundamentals involved in creating a model to partition inhaled gas or vapor into the four compartments of blood/gas exchange, bronchial epithelium absorption, mucus discharge, and exhalation. First, the architecture of the conductive zone of the human lung is examined and pathways for mass transport are considered. Air flow patterns in light of this structure are studied. Next, the theory of mass transport is presented and applied to human lung structure. Differential equations of change are derived for various transport regions involved in lung partitioning. Next, physical properties of inhaled gases and vapors are discussed in relation to their impact on mass transport models. Methods for estimating solubilities and diffusivities are provided. Finally, a simplified model of inhaled mass partitioning in the lung is presented, using an iterative-analytical approach. Results of the model over a range of exposure substances allow formulation of simple expressions to calculate fractional partitioning into compartments proceeding from the lung.

Chapter 2

HUMAN LUNG STRUCTURE

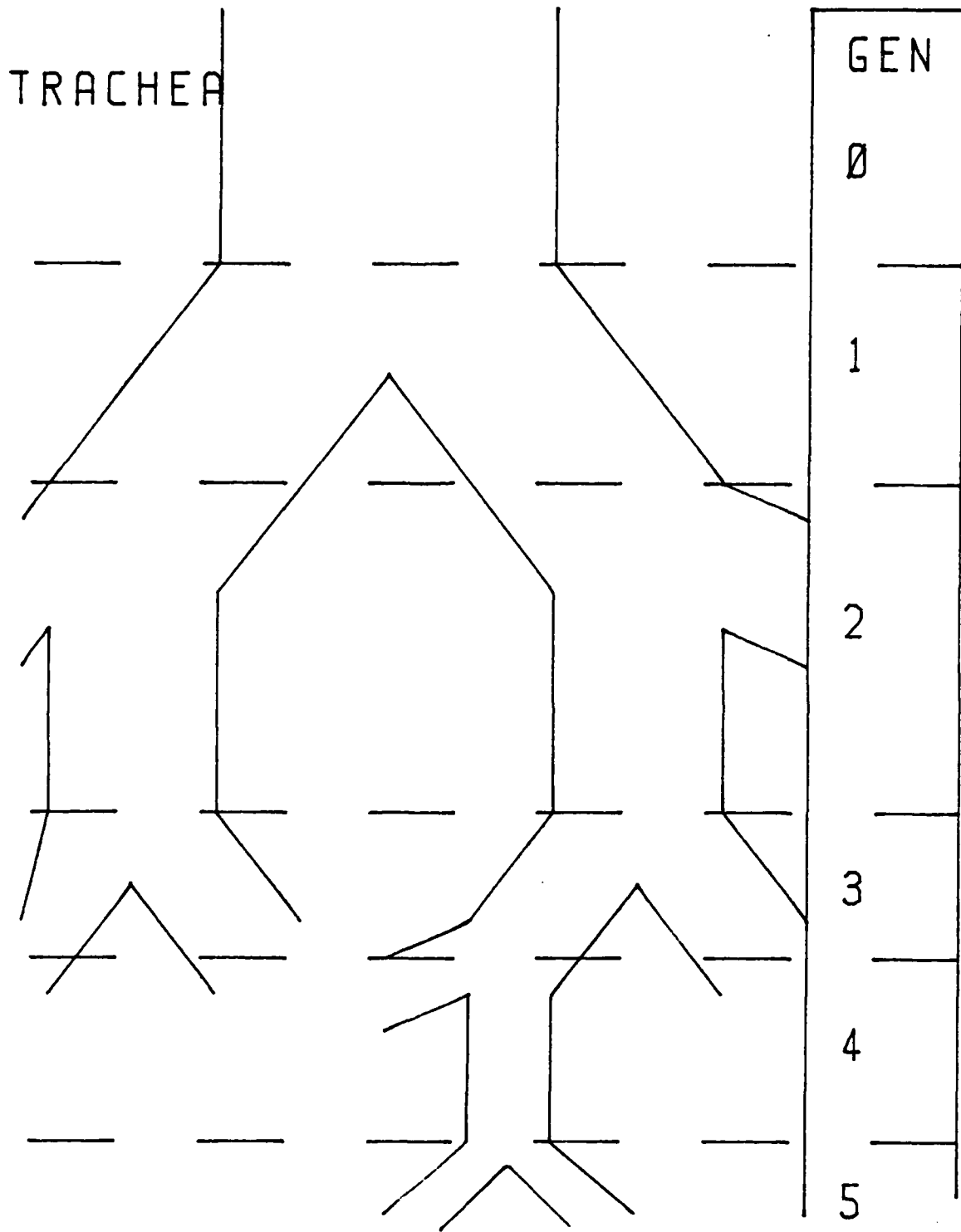
Any mass transport model must make precise assumptions concerning the structure of the transport medium. In the human lung, this can be quite complicated with the number of bifurcating bronchi increasing geometrically as one proceeds from the trachea toward the alveolar spaces. The length, diameter, and angle of bifurcation of the bronchi affect air flow patterns and transfer of mass to the bronchial walls, thus affecting absorption rates. These dimensions vary widely from bronchial generation to generation as well as from individual to individual. Once absorbed at the bronchial wall surface, further mass transport of a gas or vapor into various fluid and tissue layers again depends on the geometry and dimensions of these regions which also may have wide variations. A subset of structural models is required which will characterize the dimensions within a particular bronchial generation and represent an average over a normal population. A well known empirical model of human airway dimensions (Weibel²⁹) is available and is based on extensive morphological study. The structure of the mucosa and sub-mucosa comprising the bronchial walls is less systematically characterized, and one must make assumptions

based on limited experimental data.

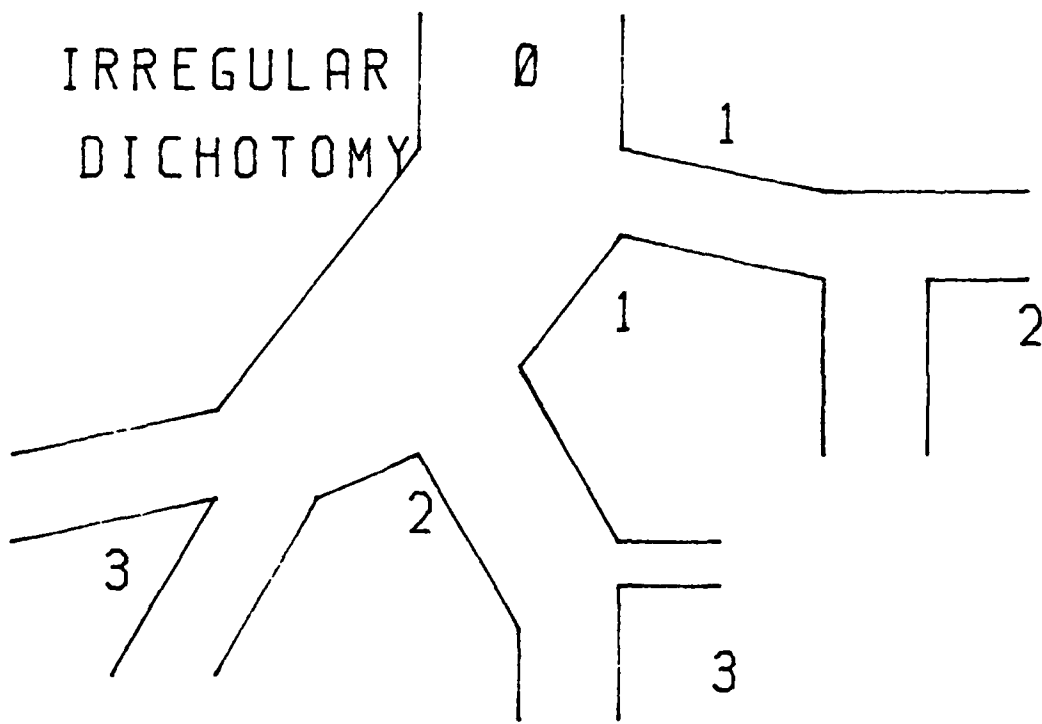
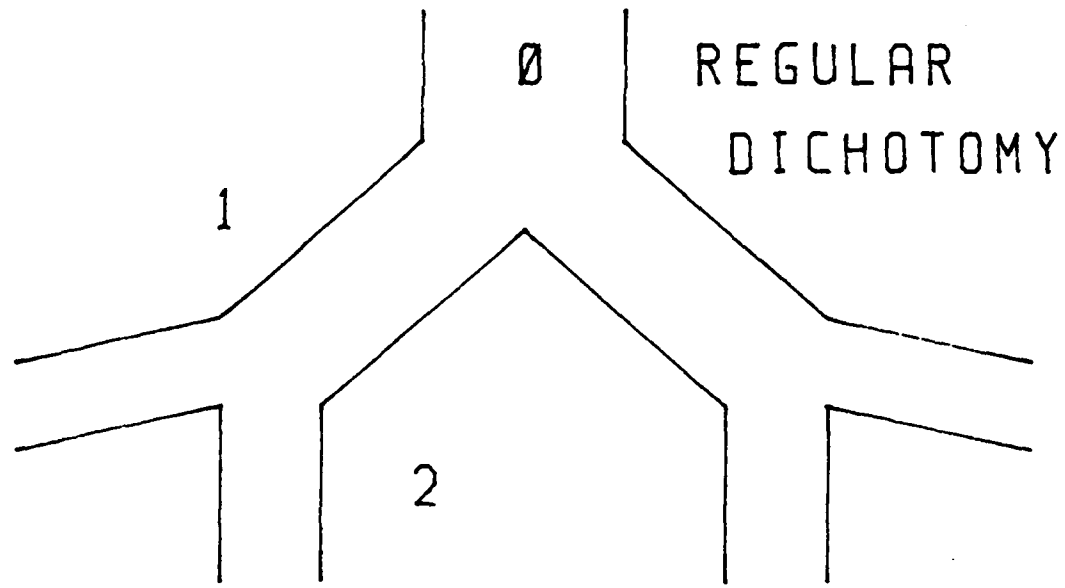
Airways of the Conductive Zone

The system of airway branching in the conductive zone of the human lung serves to distribute air from the trachea to the 300 million alveoli. The airways are organized in a tree-like system, each generation branching by dichotomy (dividing into two daughter branches). Figure 2.1 depicts this bifurcating system and illustrates the generation numbering convention, the trachea being generation '0' and numbering up with each successive bifurcation. The conductive zone extends to approximately generation 16, the walls of which are relatively smooth consisting of varying degrees of cartilage and smooth muscle. Beyond generation 16 lie the transitory and respiratory zones where bronchial walls become 'spotted' with alveoli becoming more and more dense until the walls become completely alveolated. Airways terminate in alveolar sacs at approximately generation 23.

Two systems of dichotomy are depicted in figure 2.2: 'regular' and 'irregular'. In the case of irregular dichotomy the angle of bifurcation, diameter, and length of the two daughter bronchi are unequal, whereas with regular dichotomy the bifurcation is completely symmetric. It has been shown²⁰ that the human lung branches by irregular dichotomy. Weibel²⁹ has presented simple expressions for airway diameter and length which fit his morphological data



BIFURCATING AIRWAY PATTERN
FIGURE 2.1



PATTERNS OF DICHOTOMY
FIGURE 2.2

for a regular dichotomy assumption. Although regular dichotomy rarely occurs in nature and is less representative of reality, it is more simply described and more amenable to computer methods employed in distribution of gases in the lung than in irregular dichotomy.

Weibel's regular dichotomy expressions for the diameter and length of airways in generations 0 thru 3 are exponential functions of the tracheal diameter and length, respectively:

$$D_{\text{GEN}} = D_0 \exp(-0.388 \text{ GEN}) \quad (2.1)$$

$$L_{\text{GEN}} = L_0 \exp(-0.92 \text{ GEN}) \quad (2.2)$$

where D_0 = tracheal diameter = 1.8 cm

and L_0 = tracheal length = 12 cm

Generations 4 thru 16 require empirical values for D_0 and L_0 :

$$D_{\text{GEN}} = D'_0 \exp[-(0.293 - 0.0062 \text{ GEN})\text{GEN}] \quad (2.3)$$

$$L_{\text{GEN}} = L'_0 \exp(-0.17 \text{ GEN}) \quad (2.4)$$

where D'_0 = 1.3 cm

and L'_0 = 2.5 cm

Since the airways branch by dichotomy, the total number of branches within a generation is given by

$$N_{\text{GEN}} = 2 N_{(\text{GEN}-1)} = 2^{\text{GEN}} \quad (2.5)$$

Combinations of equations 2.1 thru 2.5 allow complete description of the gross airway dimensions of the conductive zone. Table 2.1 tabulates some key dimensions for this region.

Air Flow Patterns

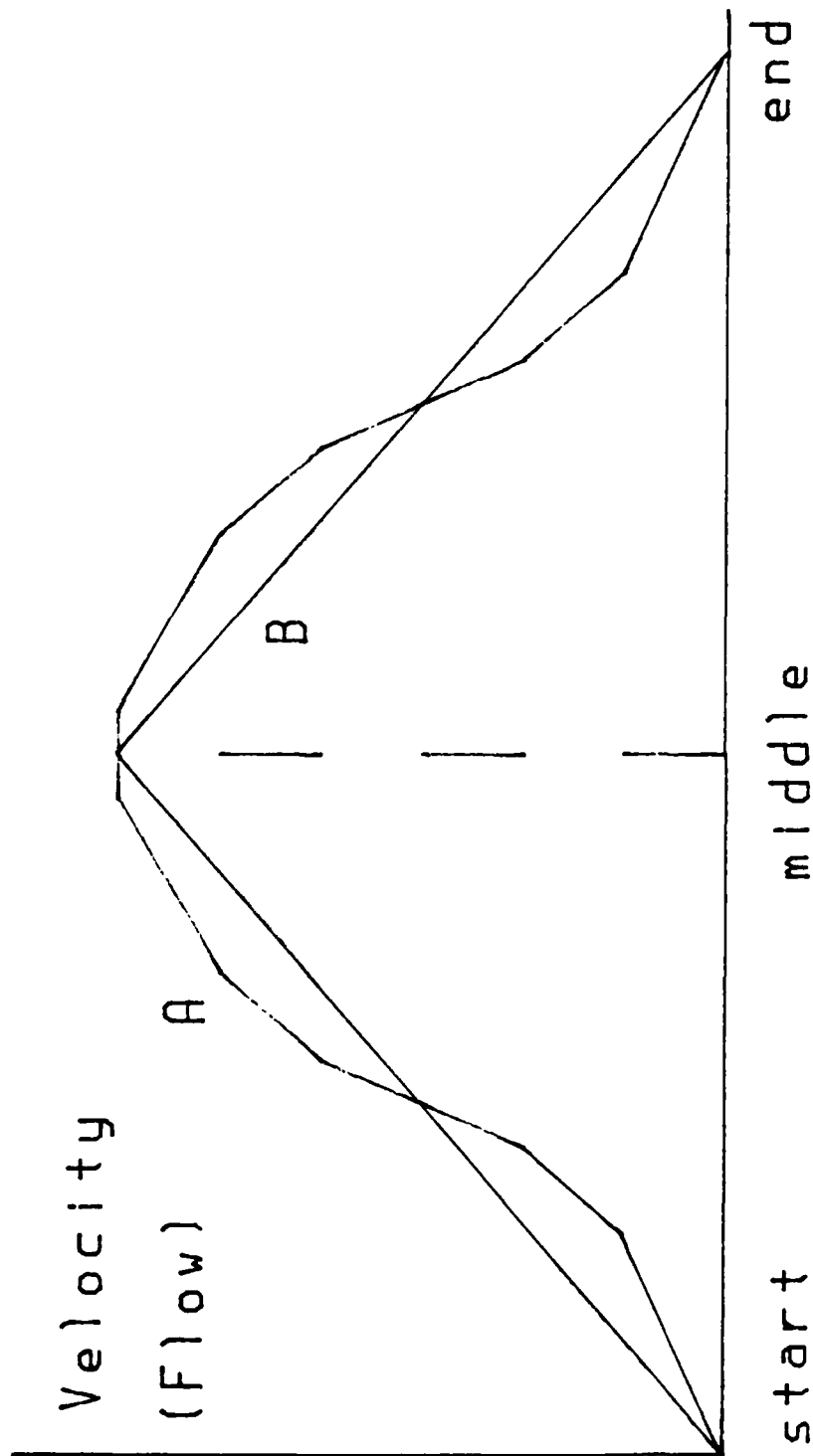
The structural model described above assumes a system of ideally bifurcating tubes of ideal shape (right circular cylinders). Flow patterns within such systems have been extensively studied and discussed.^{18,23} Flow patterns, of course, depend not only on pathway structure but on local flow velocity. During breathing this is particularly complicating due to the oscillating breathing process. As illustrated in figure 2.3 (curve A), the flow velocity is near zero at the beginning and end of inhalation or exhalation and maximum near the middle. Since, during normal breathing, inhalation is generally a forced process while exhalation is passive, the curve, in reality, may be expected to be slightly skewed in varying degrees from inhalation to exhalation. However, for purposes of modeling, one may consider the velocity curve to be triangular (curve B) with the maximum velocity at mid inhalation or exhalation dependent on the tidal volume and respiratory rate.

Given the path structure and local velocity, transport of a particular gas is by convection (with the flow of air),

AIRWAY DIMENSIONS OF CONDUCTIVE ZONE
(Regular Dichotomy)

<u>GEN</u>	<u>NUMBER</u>	<u>DIA (cm)</u>	<u>LENGTH (cm)</u>	<u>TOTAL VOLUME (cm)</u>
0	1	1.8	12.0	30.50
1	2	1.22	4.76	11.25
2	4	0.83	1.90	3.97
3	8	0.56	0.76	1.52
4	16	0.45	1.27	3.46
5	32	0.35	1.07	3.30
6	64	0.28	0.90	3.53
7	128	0.23	0.76	3.85
8	256	0.186	0.64	4.45
9	512	0.154	0.54	5.17
10	1024	0.130	0.46	6.21
11	2048	0.109	0.39	7.56
12	4096	0.095	0.33	9.82
13	8192	0.082	0.27	12.45
14	16384	0.074	0.23	16.40
15	32768	0.066	0.20	21.70
16	65536	0.060	0.165	29.70

TABLE 2.1

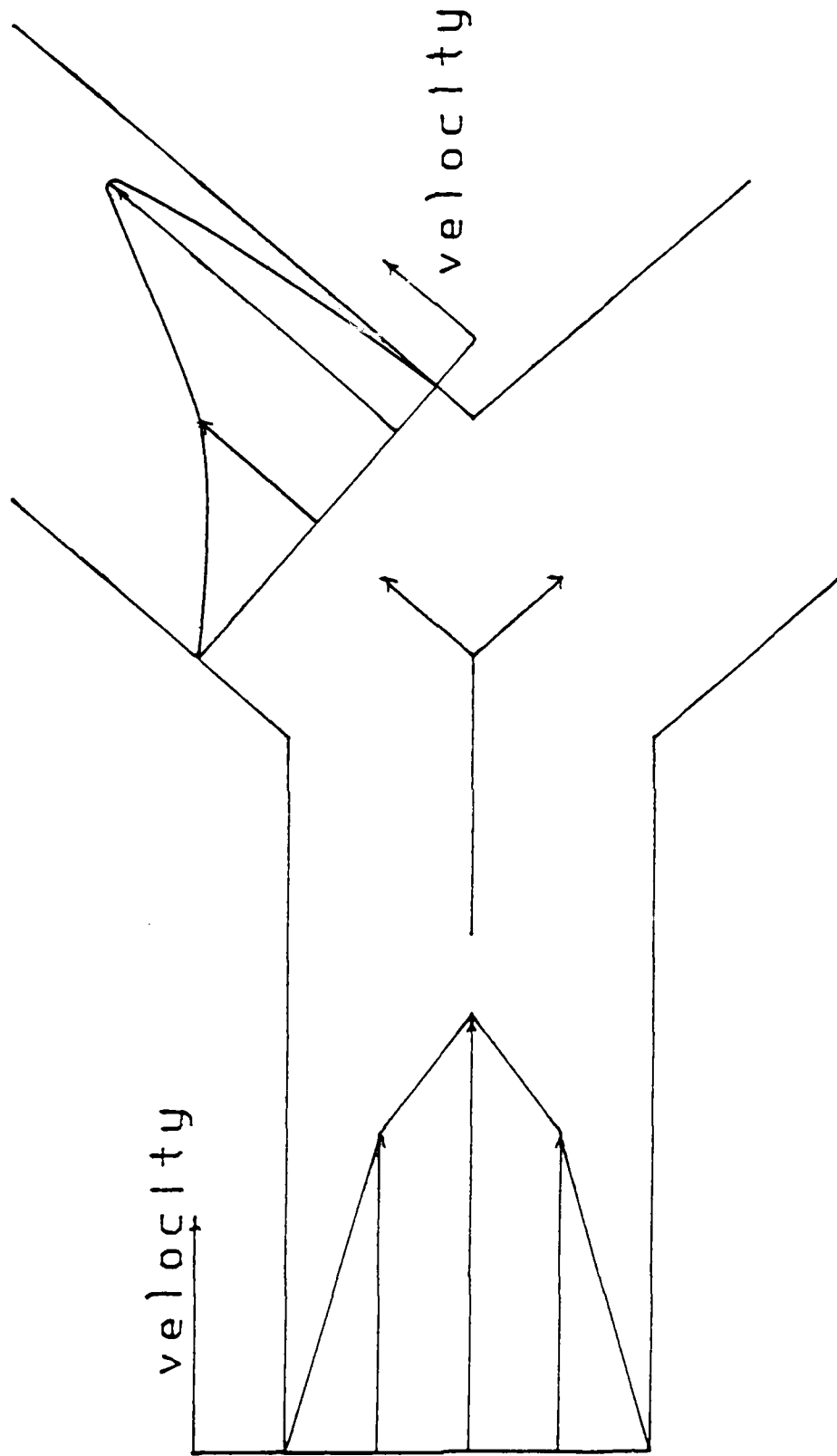


INHALATION/EXHALATION FLOW FUNCTION

FIGURE 2.3

molecular diffusion, and absorption at the surface of the tube wall. Molecular diffusion is assumed to proceed in accordance with Fick's Law (dependent on concentration gradients) while absorption at the surface depends on concentration gradients and the solubility of the gas at the prevailing temperature. Convection (described by flow patterns) influences the development of concentration gradients and thus impacts all phases of transport.

Within the convective process, flow velocity determines the nature of the velocity profile (i.e. turbulent or non-turbulent). Although turbulent conditions can occur with some extreme physiological conditions in the first three or four generations, velocity profiles throughout the lung are generally considered non-turbulent, taking on a parabolic shape. Figure 2.4 illustrates some aspects of this type of flow. A parabolic velocity profile is established due to frictional resistance at the walls and a radial transfer of momentum. There is near zero velocity at the walls and maximum velocity at the centerline which will be shown in appendix A to be twice that of the average velocity in any bronchial generation. Since mass is convectively transported at different rates depending on radial distance from the center, concentration gradients controlling molecular diffusion are thus affected to varying degrees. Additionally, the right side of figure 2.4 illustrates a further complicating factor. Depending on the angle of bifurcation and assuming that the velocity profile is

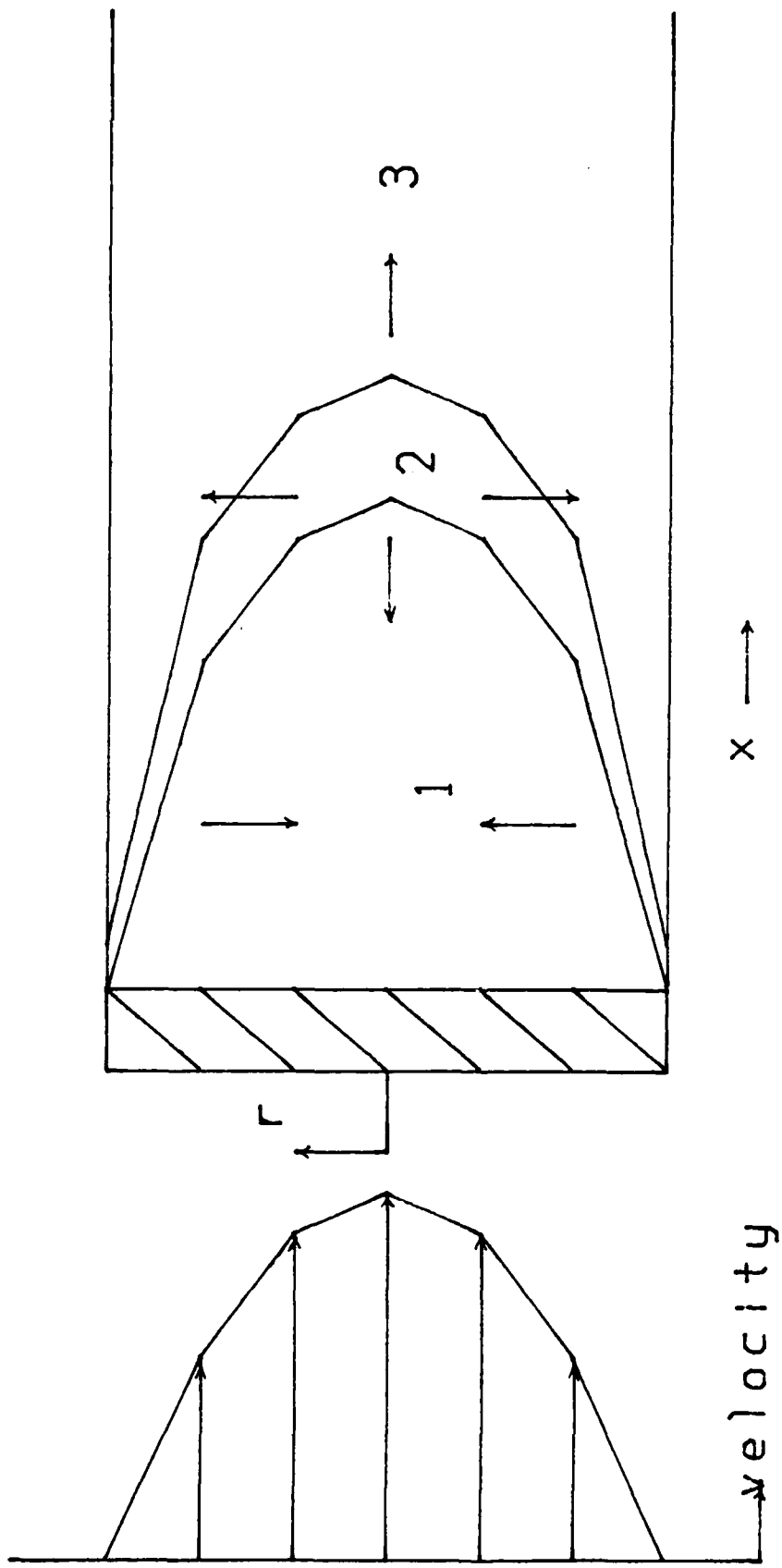


NON-TURBULENT FLOW PATTERNS

FIGURE 2.4

relatively undisturbed across bifurcations, an axial asymmetry may be expected to occur in the daughter branches as the velocity profile is split at the centerline with the maximum velocity in the daughter branches off-set from center toward the point of bifurcation. Schroter and Sudlow²³ also discuss the occurrences of vortices in the air flow pattern at bifurcations which appear to have differing patterns from inhalation to exhalation.

In addition to the above aspects of convection, studies have shown^{22,27} that longitudinal dispersion occurs, described by a dispersion coefficient which is clearly greater than the molecular diffusion coefficient alone. This effect is commonly termed 'the Taylor effect'. Taylor dispersion is simply illustrated in figure 2.5. Assume an initial plug of uniform concentration (hatched area) is introduced at the entrance of a cylindrical tube. In the absence of molecular diffusion, a parabolic velocity profile will advance the plug to occupy region 2 at some time later with zero concentration in regions 1 and 3. Without diffusion, the average cross-sectional concentration will thus reflect significant longitudinal dispersion. Molecular diffusion will further spread the mass from region 2 towards regions 1 and 3. Taylor²⁵ presents an expression describing the average concentration at a distance 'X' downstream at time 't' given a constant uniform concentration C_0 introduced at $X=0$ with a centerline velocity v :



TAYLOR DISPERSION

FIGURE 2.5

$$C/C_0 = 0.5 + 0.5 \operatorname{erf}(0.5 X_1 K^{-0.5} t^{-0.5}) \quad (X_1 \leq 0) \quad (2.6)$$

$$C/C_0 = 0.5 - 0.5 \operatorname{erf}(0.5 X_1 K^{-0.5} t^{-0.5}) \quad (X_1 > 0) \quad (2.7)$$

where $X_1 = X - 0.5 v t$

$$K = A^2 v^2 / (192 D)$$

A = tube radius

D = molecular diffusion coefficient

and erf = the error function

This formulation assumes that the radial 'smoothing out' of the concentration profile due to molecular diffusion is rapid compared to convective effects. It also assumes no absorption at the wall which limits its practical use in modeling highly soluble mass transport in the human lung. Taylor also cautions that this expression should be applied only at some finite time and distance downstream from the tube entrance after 'stabilization' of the assumed convective-diffusive conditions. Attempts have been made to circumvent this restriction by employing time-dependent dispersion coefficients. For a detailed discussion, the reader is referred to Gill and Sankarasubramanian⁹. However, most modeling efforts of mass transport in tubes assume an infinite tube length ignoring entrance and exit effects.

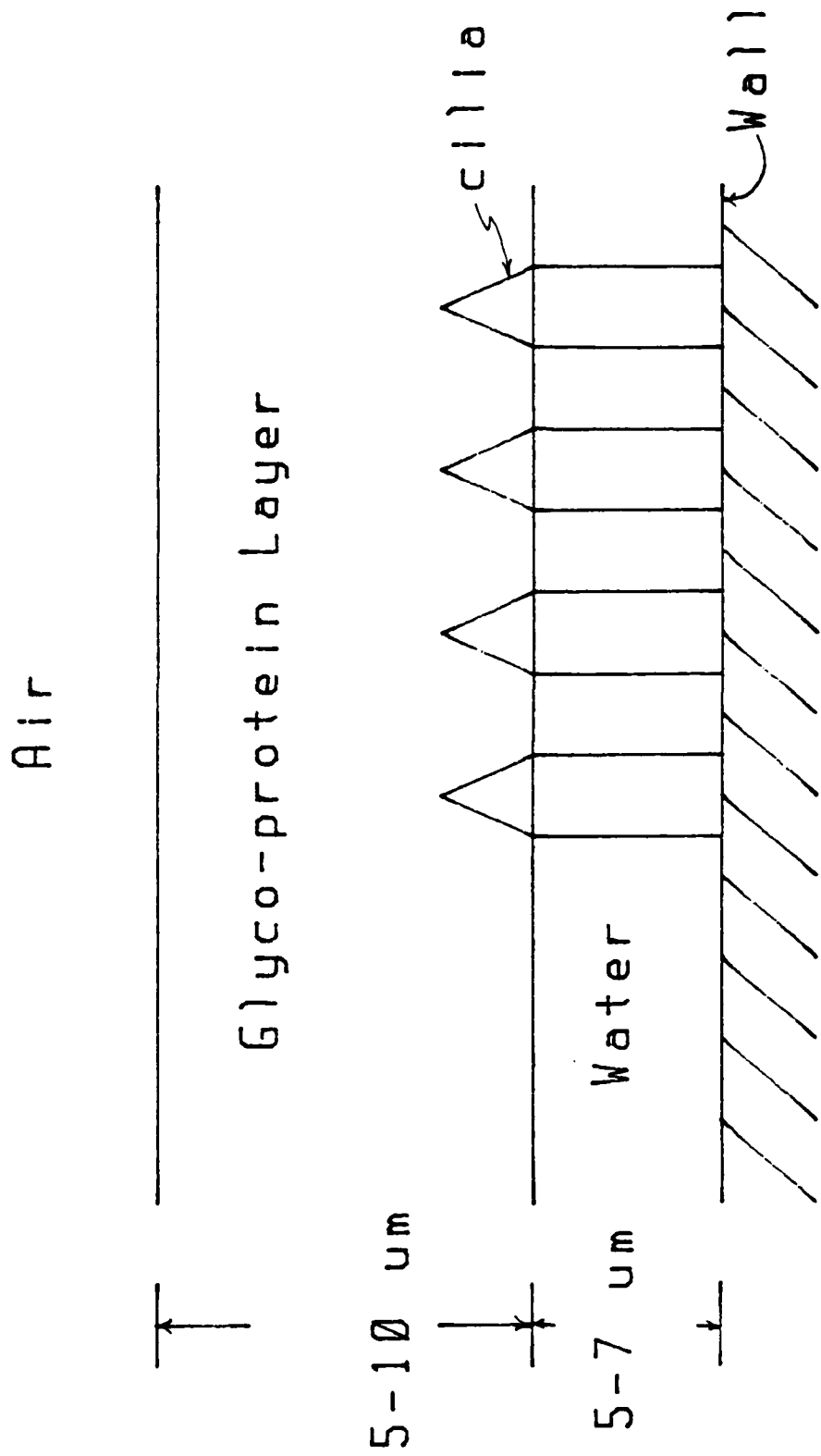
An excellent summary of air flow patterns in bifurcating tubes is provided by Overton, pages 93-102 of Miller and Menzel¹⁶.

Structure and Composition of the Bronchial Wall

Once molecules have been absorbed by the bronchial wall, further absorption is influenced not only by solubility and concentration gradients in the air phase but also by the rate of transport in the liquid or tissue phase away from the surface and deeper into the wall. Diffusion kinetics are active here as well and the structure and dimensions of regions beneath the surface must be defined.

The surface of the airways is bathed with a fluid known to be active in the capture and clearance of particulate matter in the conductive zone. Ciliated cells lining the epithelial wall move the fluid blanket upward toward the tracheal opening where it is expelled to the GI tract. Wanner²⁸ has published a detailed review of the structure and function of this muco-ciliary clearance mechanism. The airway epithelium consists of several types of ciliated and non-ciliated cells, some or all of which are involved in the secretion of fluid for the mucus blanket. The relative number of ciliated and secretory cells generally decrease from the trachea downward suggesting a systematic variation from generation to generation of fluid thickness, velocity, and composition. These variations have not been clearly defined, but average values have been established which are perhaps more representative of the upper than of the lower airways.

Figure 2.6 depicts a longitudinal view of a bronchial wall segment. The cilia (approximately 6 micro-meters in length) are surrounded by a watery layer of fluid just above the epithelial wall. Above the watery layer is a second fluid layer with a high glyco-protein content. The presence of these molecules gives this layer a viscous consistency. The glyco-protein layer rides above the watery layer and is propelled toward the top of the trachea by interaction with the tips of the cilia. The direction of motion of the watery layer beneath is undefined and it is expected to be in a turbulent state due to the rapid and sudden motion of the cilia. Particulate matter inhaled into the conductive zone which is captured and absorbed by the glyco-protein layer would be expected to remain captured there traveling with the layer and finally expelled to the GI tract perhaps hours later. Gaseous molecules, on the other hand, when captured and absorbed into the glyco-protein layer would continue to pass into and out of various fluid or tissue regions (or back into air) depending on prevailing concentration gradients and the diffusivity of the gas. Beneath the watery layer, the epithelial wall itself consists of layers of surface, intermediate, and basal cells totalling approximately 30 micro-meters in thickness prior to reaching well-perfused lung tissue where the gas concentration would be in equilibrium with blood flow to the area.



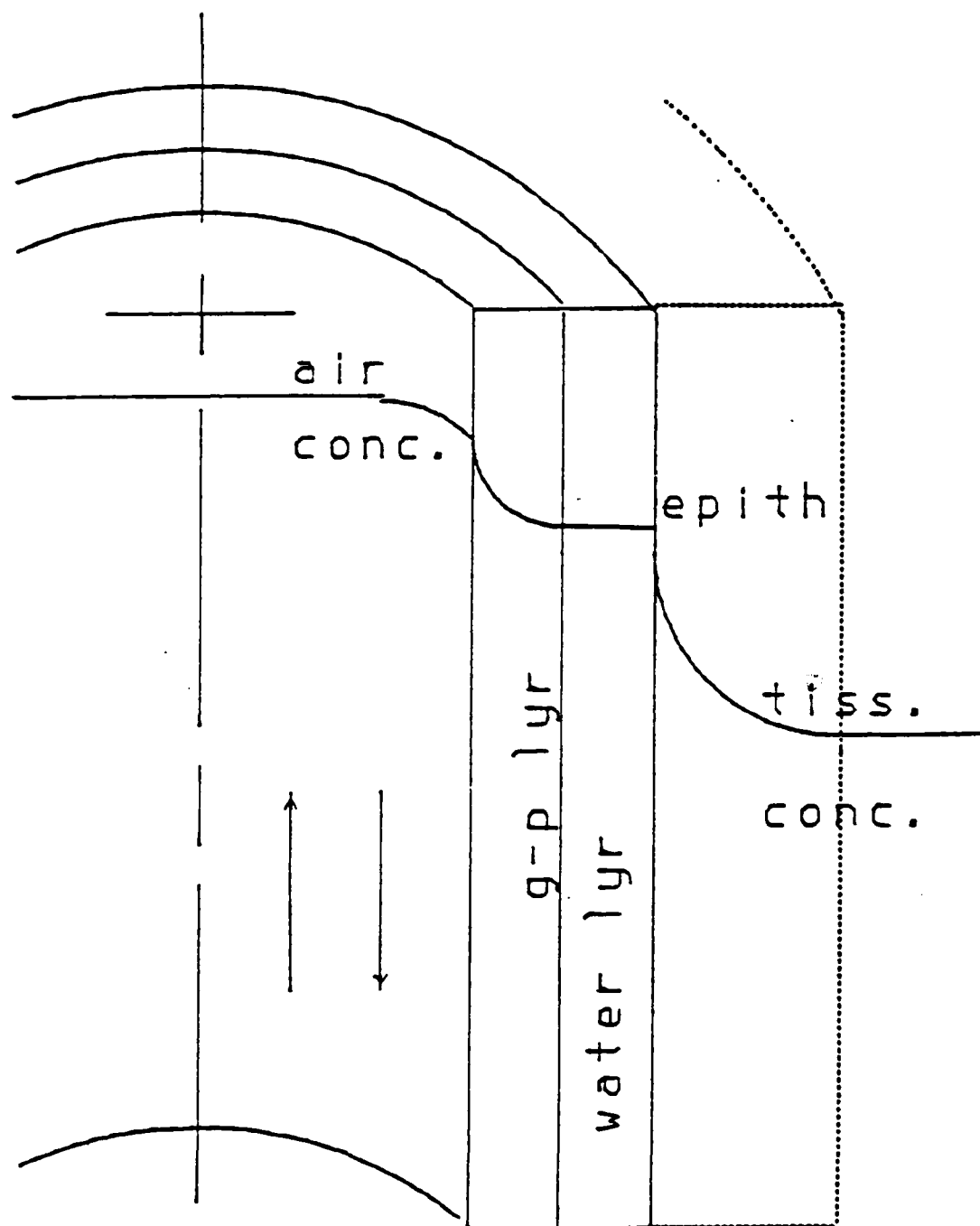
BRONCHIAL WALL FLUID LAYERS

FIGURE 2.6

There is some evidence that the mucus blanket (glyco-protein layer) may be discontinuous toward the distal end of the respiratory tract, existing as patches or not existing at all. Components of both fluid layers may be secreted and re-absorbed into the epithelium in response to varying physiological stimuli. In the absence of concrete data, it is best for modeling purposes to assume a continuous blanket of uniform thickness within each bronchial generation.

Figure 2.7 summarizes the regions involved in mass transport of inhaled gases within a single bronchial segment. A concentration profile is illustrated which, in this case, depicts a gradient from the air phase toward lung tissue. Molecules are convectively transported in and out of the lung with varying velocity in the air (lumen) while experiencing radial diffusion as well. Once absorbed by the glyco-protein layer predominant transport is by molecular diffusion with a distinct concentration profile likely developing within this viscous layer. A slight convective component would also be involved here as the layer is cilia-propelled intact at a rate of approximately 3 to 10 mm/min. Rapid turbulent mixing in the watery layer would predominate over any diffusive effects, resulting in a uniform concentration profile. Within the epithelium, again a distinct profile develops depending on the relatively uniform tissue concentration beyond.

The suggested structural model above should allow a practical description of transport in the conductive zone of



MASS TRANSPORT REGION
FIGURE 2.7

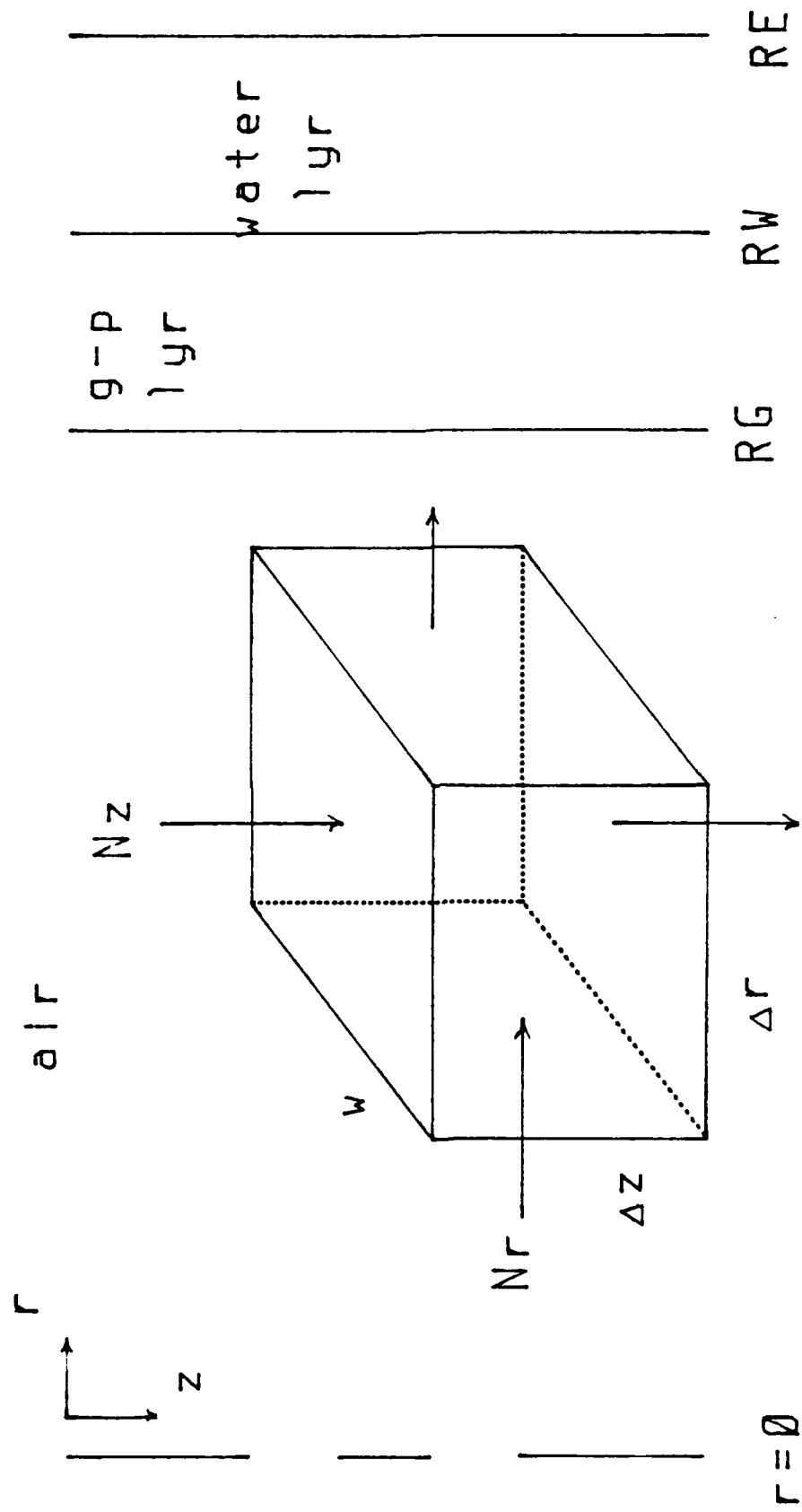
the human lung given knowledge of the contaminant gas diffusivity in the various regions and its solubility which would define the partitioning of gas between air and liquid phases at the air-liquid interface. Development of transport expressions and models in subsequent chapters will refer to the structural model depicted in figure 2.7.

Chapter 3

MASS TRANSPORT

As demonstrated in chapter 2, the airways of the human lung are arranged in a complicated tree-like expansion, bifurcating into thousands of daughter branches of varying dimensions. Simplifying assumptions allow consideration of a 'regular dichotomy' model in which all branches of a particular generation have identical dimensions. In this way a relatively simple algorithm may be employed to model the transport of a gas or vapor simply relating the concentration leaving a generation to the concentration entering an adjacent generation. Prior to this step, however, transport must be described in detail on the level of a single bronchial segment, in accordance with a reasonable structural model like that depicted in figure 2.7. This chapter will present equations of change which describe the transport phenomenon within each transport region.

To describe transport in the air phase (lumen of the bronchiole), consider the elemental volume shown in figure 3.1. We will take the elemental volume to be a ring of height Δz , depth Δr , and width $w = 2\pi r$. If we assume that there is no net mass flux in the w direction, then mass



AIR PHASE MASS BALANCE

FIGURE 3.1

enters and leaves the elemental volume in the r direction by molecular diffusion (given non-turbulent air flow) and in the z direction by molecular diffusion and convection. Using the notation ' $N_z|z$ ' to denote mass flux in the z direction evaluated at the point ' z ', we can write the following mass balance for the elemental volume:

$$[N_z 2\pi r \Delta r]|_z - [N_z 2\pi r \Delta r]|_{z+\Delta z} + [N_r 2\pi r \Delta z]|_r - [N_r 2\pi r \Delta z]|_{r+\Delta r} = \frac{\partial C}{\partial t} [2\pi r \Delta r \Delta z] \quad (3.1)$$

The right hand side of the equation merely conserves mass. If the sum of the mass entering and leaving the element does not equal zero, the difference must reflect a change in total mass over the period; thus, a change in concentration (C) over time times the volume of the element. Dividing equation 3.1 by $2\pi r \Delta r \Delta z$, we have

$$\frac{N_z|_z - N_z|_{z+\Delta z}}{\Delta z} + \frac{[N_r r]|_r - [N_r r]|_{r+\Delta r}}{r \Delta r} = \frac{\partial C}{\partial t} \quad (3.2)$$

The terms on the left we recognize as the definition of the differential if we take the limit as Δz and Δr approach zero. Thus we have

$$-\frac{\partial N_z}{\partial z} - \frac{1}{r} \frac{\partial (N_r r)}{\partial r} = \frac{\partial C}{\partial t} \quad (3.3)$$

If we neglect molecular diffusion in the z direction as insignificant compared to convection, we may describe the mass flux as

$$N_z = v C$$

where $v =$ air flow velocity (3.4)

and, by Fick's Law

$$N_r = -DA \frac{\partial C}{\partial r} \quad (3.5)$$

where $DA =$ the gas diffusion coefficient in air.

Substituting equations 3.4 and 3.5 into equation 3.3

$$-v \frac{\partial C}{\partial z} + \frac{DA}{r} \frac{\partial [r \frac{\partial C}{\partial r}]}{\partial r} = \frac{\partial C}{\partial t} \quad (3.6)$$

or

$$-v \frac{\partial C}{\partial z} + DA \frac{\partial^2 C}{\partial r^2} + DA \frac{\partial C}{r \partial r} = \frac{\partial C}{\partial t} \quad (3.7)$$

Now we have a differential transport equation in terms of known parameters, except that in non turbulent flow, the velocity profile is parabolic, varying with r. For the case of laminar flow through a circular tube this profile can be derived in terms of a radial momentum balance and can be shown to be

$$v = 2 v_{AVG} [1 - (r/R)^2] \quad (3.8)$$

where R = the tube radius (RG in figure 3.1)

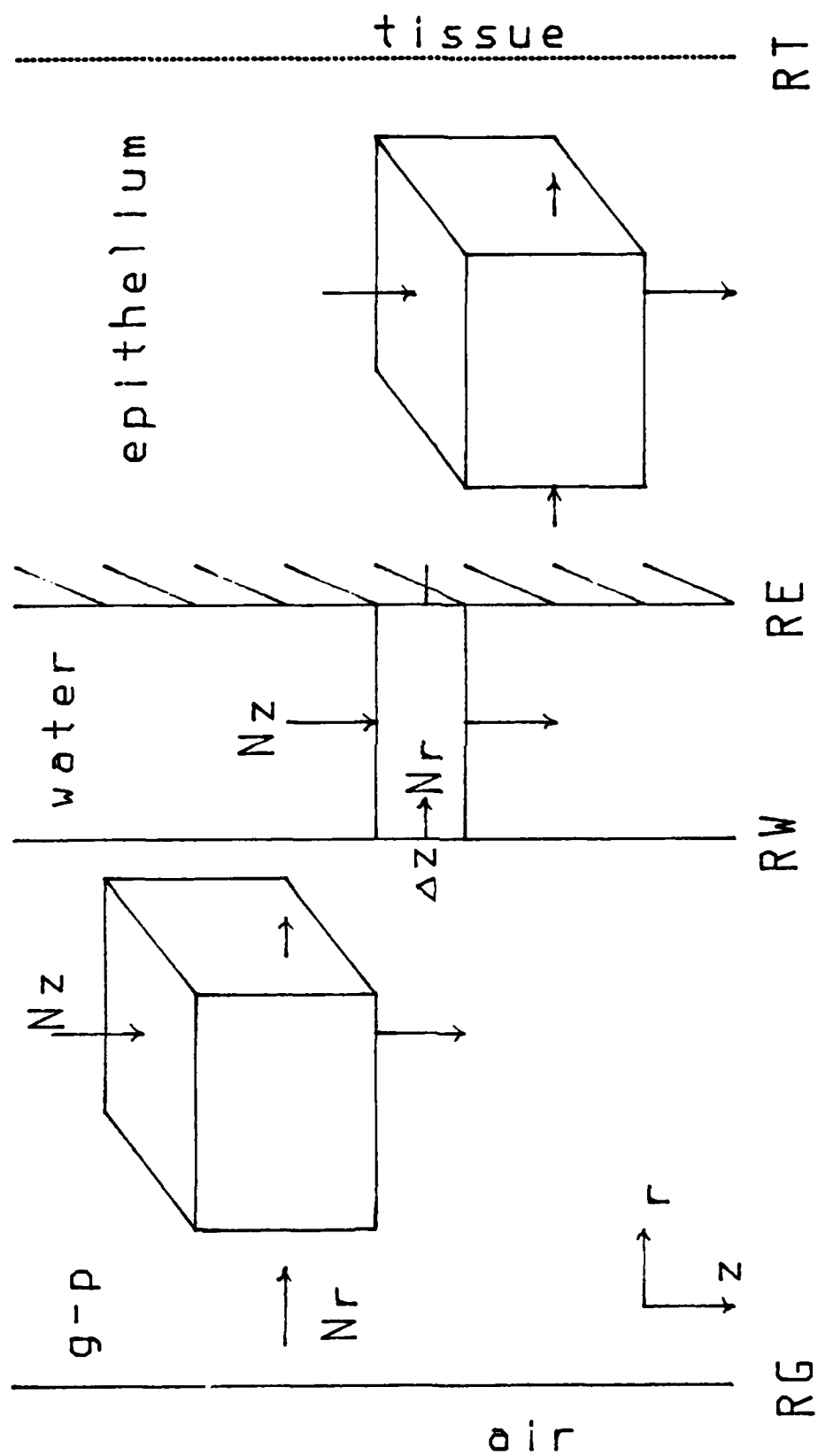
and v_{AVG} = the volumetric air flow rate divided by the tube cross-sectional area

(For a complete derivation, see Appendix A). Finally, substituting in equation 3.7, we have

$$-2 v_{AVG} [1 - (r/RG)^2] \partial C / \partial z + DA \partial^2 C / \partial r^2 + DA \partial C / r \partial r = \partial C / \partial t \quad (3.9)$$

which describes mass transport in the air phase. For the case of turbulent air flow (rare in the human lung), the equation becomes much more complicated and must be divided into two equations, one applicable to the turbulent core and one to the region near the wall. For a derivation of the turbulent case, the interested reader is referred to Appendix B.

For transport in the viscous glyco-protein region [$RG < r < RW$] we again refer to an elemental volume (figure 3.2). We begin with the mass balance of equation 3.1 reducing to the differential form of equation 3.3 as in the case of the air phase. Ciliary action in this region propels the mucus blanket upward (in the z direction) at a rate less than 0.5 cm per minute. This is a slow clearance process and may be considered distinct from the rapid transport process of air convection and molecular diffusion. Thus, the concentration in the glyco-protein region is predominantly influenced by the radial concentration gradient due to diffusion, and ciliary convection in the z direction is neglected. Thus,



FLUID AND EPITHELIAL MASS BALANCE

FIGURE 3.2

$$N_z = -DG \frac{\partial C}{\partial z} \quad (3.10)$$

$$\text{and } N_r = -DG \frac{\partial C}{\partial r} \quad (3.11)$$

where DG = the molecular diffusion coefficient of the gas in the glyco-protein medium.

Substituting in equation 3.3 and simplifying, we have

$$DG \frac{\partial^2 C}{\partial z^2} + DG \frac{\partial^2 C}{\partial r^2} + DG \frac{\partial C}{r \partial r} = \frac{\partial C}{\partial t} \quad (3.12)$$

In the water layer [$RW < r < RE$], rapid turbulent mixing distributes any entering mass uniformly across the region instantaneously (given the small distance across). Since the height of the region in the z direction is large compared to $(RE - RW)$, diffusion would remain a factor in that dimension. Thus, we consider an elemental ring of height z and width $(RE - RW)$ [figure 3.2] and write the mass balance as follows:

$$[N_z A_z] | z - [N_z A_z] | z + \Delta z + [N_r A_r] | RW - [N_r A_r] | RE = \frac{\partial C}{\partial t} V \quad (3.13)$$

$$\text{where } N_z = -DW \frac{\partial C}{\partial z} \quad (3.14)$$

$$N_r | RW = -DG \frac{\partial C}{\partial r} | RW \quad (3.15)$$

$$N_r | RE = -DE \frac{\partial C}{\partial r} | RE \quad (3.16)$$

$$A_z = \pi (RE^2 - RW^2) \quad (3.17)$$

$$A_r | RW = 2 \pi RW \Delta z \quad (3.18)$$

$$A_r | RE = 2 \pi RE \Delta z \quad (3.19)$$

$$V = \pi (RE^2 - RW^2) \Delta z \quad (3.20)$$

DE = diffusion coefficient in the epithelium

and DW = diffusion coefficient in water

Note that the flux in and out in the radial direction is coupled to transport in the adjacent regions and assumes conservation of mass across the boundaries. Forming the differential in the z direction and substituting in equation 3.13, we have

$$\begin{aligned} DW \frac{\partial^2 C}{\partial z^2} - DG [2 RW / (RE^2 - RW^2)] \frac{\partial C}{\partial r} \Big|_{RW} \\ DE [2 RE / (RE^2 - RW^2)] \frac{\partial C}{\partial r} \Big|_{RE} = \frac{\partial C}{\partial t} \end{aligned} \quad (3.21)$$

describing transport in the water layer.

The equation of change for transport in the epithelium is directly analogous to that for the glyco-protein region and may be written immediately by inspection of equation 3.12

$$\begin{aligned} DE \frac{\partial^2 C}{\partial z^2} + DE \frac{\partial^2 C}{\partial r^2} \\ + DE \frac{\partial C}{r} \frac{\partial r} = \frac{\partial C}{\partial t} \end{aligned} \quad (3.22)$$

To summarize, the final equations of transport for each region are re-written, representing a system of simultaneous partial differential equations which must be solved:

Air:

$$\begin{aligned} -2 v_{AVG} [1 - (r/RG)^2] \frac{\partial C}{\partial z} + DA \frac{\partial^2 C}{\partial r^2} \\ + DA \frac{\partial C}{r} \frac{\partial r} = \frac{\partial C}{\partial t} \end{aligned} \quad (3.9)$$

Glyco-protein:

$$\begin{aligned}
 DG \frac{\partial^2 C}{\lambda} \frac{\partial z^2}{\partial z^2} + DG \frac{\partial^2 C}{\lambda} \frac{\partial r^2}{\partial r^2} \\
 + DG \frac{\partial C}{\lambda r} \frac{\partial r}{\partial r} = \frac{\partial C}{\lambda} \frac{\partial t}{\partial t} \quad (3.23)
 \end{aligned}$$

Water:

$$\begin{aligned}
 DW \frac{\partial^2 C}{\lambda} \frac{\partial z^2}{\partial z^2} - DG [2 RW / (RE^2 - RW^2)] \frac{\partial C}{\lambda} \frac{\partial r}{\partial r} |_{RW} \\
 DE [2 RE / (RE^2 - RW^2)] \frac{\partial C}{\lambda} \frac{\partial r}{\partial r} |_{RE} = \frac{\partial C}{\lambda} \frac{\partial t}{\partial t} \quad (3.24)
 \end{aligned}$$

Epithelium:

$$\begin{aligned}
 DE \frac{\partial^2 C}{\lambda} \frac{\partial z^2}{\partial z^2} + DE \frac{\partial^2 C}{\lambda} \frac{\partial r^2}{\partial r^2} \\
 + DE \frac{\partial C}{r \lambda} \frac{\partial r}{\partial r} = \frac{\partial C}{\lambda} \frac{\partial t}{\partial t} \quad (3.25)
 \end{aligned}$$

Here, λ is an air/liquid partition coefficient which allows C to be expressed in terms of air concentration throughout. The partition coefficient, like the diffusion coefficient, is a characteristic of the transported gas and is related to its solubility. The above equations assume that the gas is partitioned across the air/liquid interface by the partition coefficient (i.e. air/liquid equilibrium exists at the surface). Solution of the above equations requires specification of boundary conditions which include description of the concentration entering the bronchiole, zero radial flux at the centerline, conservation of mass across region boundaries, and constant tissue concentration. The complexity of the system (even under simplifying assumptions under which it was derived) precludes the development of a single analytical expression representing a solution. Numerical analysis would generally be employed to

study the transport of one or two inhalation gases. A numerical approach is not trivial and would consume a great deal of computer resources. Alternatively, to gather a large amount of transport data over a broad range of inhalation gases and vapors, further simplifying assumptions can be made allowing the use of analytical expressions to describe portions of the transport problem and approximating overall results in an iterative-analytical approach. Such a model is described in chapter 5.

Chapter 4

PHYSICAL PROPERTIES OF INHALED GASES AND VAPORS

Regardless of the method used to describe mass transport in the conductive zone of the human lung, any model must depend on accurate values of inhaled gas or vapor physical characteristics: namely, its solubility and diffusivity. Ideally, one would hope to be able to reference experimentally derived values for a particular species in air and water. We assume here that solubility and diffusivity in the mucus layers and tissue is reasonably equivalent to that in water, water being the predominant constituent of composition. Attempts to estimate more accurate values based on an analysis of all possible chemical interactions between solute and small fractional components of the solvent would be difficult to justify in light of the benefit. Because such values are not readily available in the literature, reasonable estimates must be used unless one has the resources available to gather this data experimentally. This chapter presents suggested methods for estimating contaminant gas solubility and diffusivity with specific examples.

Solubility

In mass transport models describing transport across air/liquid interfaces, we assume that the concentration at the interface just to the liquid side is in equilibrium with the interface concentration just to the air side and that the ratio of these two concentrations is constant at a given temperature and pressure (within practical inhalation concentration ranges). Thus we consider a partition coefficient (α) which converts, for example, milligrams per liter of air (CA) at the interface to milligrams per liter of water (CW) at the interface:

$$CW = \alpha CA \quad (4.1)$$

Definition of this partition coefficient is less complicated in the lung since lung temperature and pressure do not vary enough to significantly affect it. Thus, α (for an air/water interface) may be considered to depend solely on the particular gas or vapor in question.

The partition coefficient is, of course, an indicator of the gas's solubility. Estimation of solubilities is not well developed due to the difficulty in describing all possible complicating interactions of solute and solvent molecules. In the ideal case, one would expect the air/liquid equilibrium to follow Raoult's Law:

$$Y_i P = X_i P_{vp} \quad (4.2)$$

where Y_i = mole fraction of solute in air

X_i = mole fraction of solute in liquid

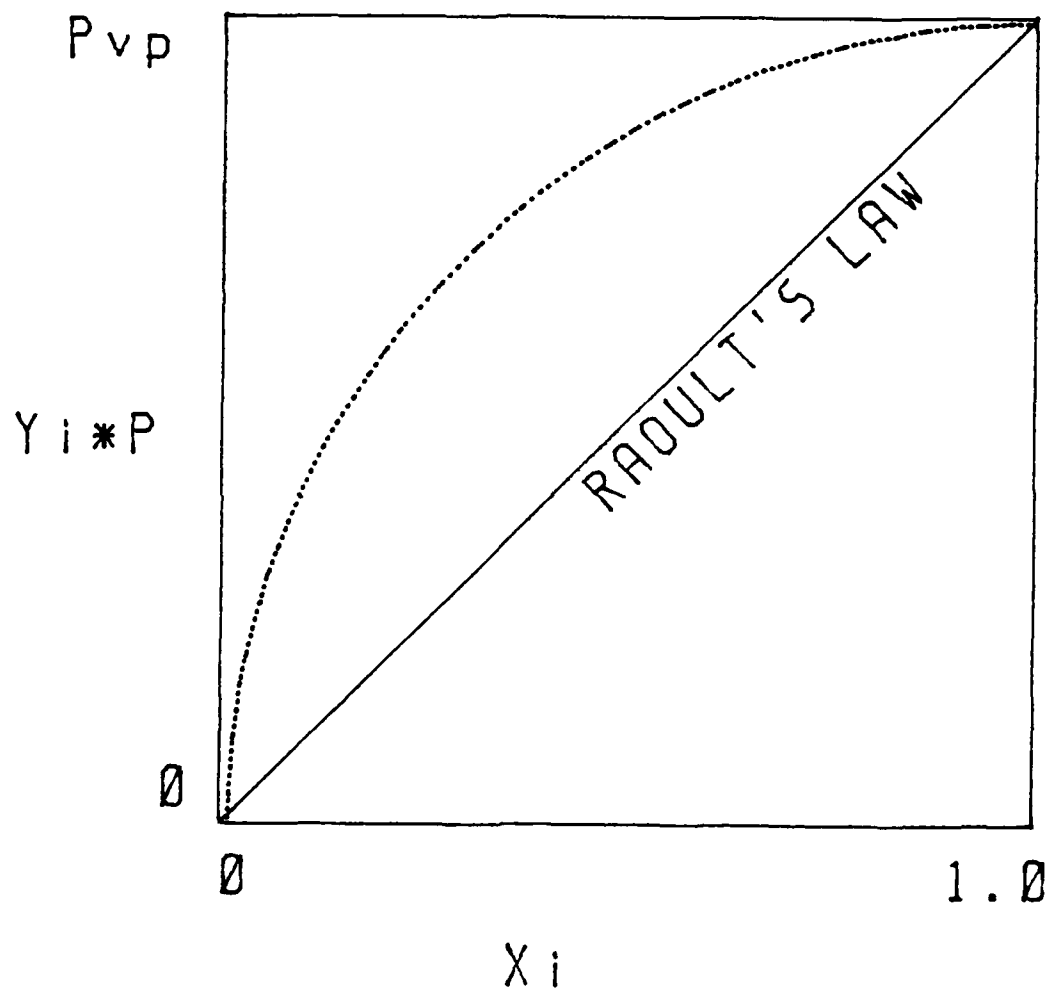
P = total pressure of system

and P_{vp} = saturation vapor pressure of solute
at the system temperature

This law, illustrated by the solid line in figure 4.1, simply states that the partial pressure exerted by solute in air approaches linearly the saturation vapor pressure of the solute as the mole fraction in liquid approaches 1.0 (pure solute). Molecular interactions between solute and solvent cause the equilibrium function to depart from the ideal. This is particularly true in the case of a polar solvent like water in which case the function may appear as that represented by the dashed line in figure 4.1. Thus, we require a correction factor γ , known as the activity coefficient which will adjust the slope of the curve from the ideal case for low concentrations encountered in the lung, such that

$$Y_i P = \gamma X_i P_{vp} \quad (4.3)$$

Reid, Prausnitz, and Sherwood²¹ review several methods of estimating activity coefficients for vapor-liquid equilibria. Combinations of empirical equations and equation coefficients are offered for classes of solutes and solvents in table 8-17 of their work. Table 8-21 also provides parameters for a more complicated series of calculations in a functional group additive contribution method. Both methods are semi-empirical: the first assumes



VAPOR-LIQUID EQUILIBRIA
FIGURE 4.1

that compounds of the same class will behave similarly while the second assumes that the contribution of functional groups is additive regardless of their combination with other groups. These methods apply only to vapor-liquid solubility and not to solubility of substances which are gaseous at standard conditions.

For the case of gases, Hayduk¹³ provides direct empirical values for some gases. His values, termed hydrogen-bonding factors (σ), effectively function as the inverse of the activity coefficient. That is,

$$Y_i P = X_i P_{vp}/\sigma \quad (4.4)$$

where σ (H-bonding factor) = the ratio of X_i to the predicted mole fraction in water according to Raoult's Law.

Appropriate tables, adapted from Reid, Prausnitz, and Sherwood²¹ and from Hayduk¹³ are reproduced in Appendix G.

Example: Determine the partition coefficient (α) for 1,1,1-trichloroethane and propane at an air/water interface at 37 degrees C and 1 atm pressure.

| If $C_W = \text{mg/l}$ in water and $C_A = \text{mg/l}$ in air,

| then we seek α satisfying:

$$C_W = \alpha C_A$$

$$Y_i = C_A / (1000 \text{ mol.wt.}) \text{ [gm-moles per liter]} \\ * 25.4 \text{ [liters per gm-mole at 37 deg C]}$$

$$= 0.0254 C_A / \text{mol.wt.}$$

| Since 1 liter of water is 55.49 gm-moles,

$$\begin{aligned} CW &= X_i (55.49) \text{ mol.wt. } (1000) \\ &= 55490 (\text{mol.wt.}) X_i \quad (\text{mg/l}) \end{aligned}$$

| and

$$X_i = CW / (55490 \text{ mol.wt.})$$

| For vapors,

$$\begin{aligned} \gamma &= Y_i / (X_i P_{vp}) = \frac{0.0254 \text{ CA/mol.wt.}}{P_{vp} CW / (55490 \text{ mol.wt.})} \\ &= 1409 \text{ CA} / (CW P_{vp}) \end{aligned}$$

$$CW = [1243 / (\gamma P_{vp})] \text{ CA}$$

| Thus, $\alpha = 1409 / (\gamma P_{vp})$

| For gases,

$$\sigma = X_i P_{vp} / Y_i = CW P_{vp} / (1409 \text{ CA}) \quad [\text{inverse of } \gamma]$$

$$CW = [1409 \sigma / P_{vp}] \text{ CA}$$

| Thus, $\alpha = 1409 \sigma / P_{vp}$

| For trichloroethane (a mono-alkyl chloride), table 8-17 of Reid, Prausnitz, and Sherwood²¹ allows calculation of the activity coefficient at 20 degrees C as 380.0. This is acceptable as a good estimate for 37 degrees C as well since the difference would be insignificant as shown by Hayduk¹³. The saturation vapor pressure (0.33 atm) is readily available

handbook data (interpolated for 37 degrees). Thus,
for 1,1,1-trichloroethane

$$\alpha = 1409 / (380.0 \times 0.33) = 11.2$$

For propane, the hydrogen bonding factor is
read directly from Hayduk (table 2) as 0.0326 and,
from handbook data, $P_{vp} = 14.8$ atm (interpolated to
37 deg.). Thus

$$\alpha = 1409 (0.0326 / 14.8) = 3.1$$

Air Diffusion Coefficient

Methods for estimation of diffusion coefficients are slightly more developed than for solubility. For air, several methods can be found in the literature²¹, all of which recognize the same fundamental components. Panwitz¹⁹ presents the following equation:

$$D_{FA} = 0.941077 T^{1.5} / [P W (0.5 d_A + 0.5 d_B)^2] * (1/M_A + 1/M_B)^{0.5} \quad (4.5)$$

where D_{FA} = diffusion coeff. in air (cm^2/sec)

T = 310 degrees K (body temperature)

M_A = 28.96 (mol.wt. of air)

M_B = mol.wt. of gas

d_A = 3.617 (dia of avg air molecule, angstr)

P = 1013.3 (pressure in mbar)

d_B = dia of gas molecule = $1.18 V_A^{1/3}$

VA = molar volume at boiling point = $0.285 V_C^{1.048}$

VC = critical volume of gas

and W = collision integral.

Reid, Prausnitz, and Sherwood²¹ presents the following expression, by Neufeld, for the collision integral:

$$W = A/S^B + C/\exp(DS) + E/\exp(FS) + G/\exp(HS) \quad (4.6)$$

where $S = KT/\xi$

K = Boltzman's constant

ξ = characteristic molecular energy

and

A = 1.06036;

B = 0.15610;

C = 0.19300;

D = 0.47635;

E = 1.03587;

F = 1.52996;

G = 1.76464;

H = 3.89411.

S can also be estimated in terms of the gas boiling point (BP) as

$$S = T/(111.55 \text{ BP})^{1/2} \quad (4.7)$$

Thus, diffusivity in air can be calculated from the molecular weight and boiling point (handbook data) and the critical volume, values of which are tabulated for a wide range of compounds in Reid, Prausnitz, and Sherwood²¹.

Water Diffusion Coefficient

The best and most widely used method for estimating diffusivity in water (DFW) is the Wilke-Chang method³¹

given by

$$DFW = 7.4 \times 10^{-8} (\phi M)^{1/2} T / (\eta V_A^{0.6}) \quad (4.7)$$

where $M = 18.02$ (mol.wt. of water)

$T = 310$ degrees K (body temperature)

$\eta = 0.6915$ cp (viscosity of water)

$V_A =$ gas molar volume (estimated from the critical volume as in the previous section)

and $\phi = 2.6$ (association factor for water)

Example: Determine the diffusion coefficient in air and water for benzene (MW = 78) at 37 deg C.

| From handbook data, the boiling point (BP) for benzene
| is 80 deg C and from Reid, Prausnitz, and Sherwood²¹
| the critical volume (VC) is 259 cc/gm-mole.

| For air:

| By eq'n 4.7,

$$\begin{aligned} | \quad S &= 310 / [111.55(353)]^{1/2} \\ | \quad &= 1.56 \end{aligned}$$

| and, by eq'n 4.6,

$$\begin{aligned} | \quad W &= 1.06036/1.560.15610 + \\ | \quad &0.193/\exp[0.47635(1.56)] + \\ | \quad &1.03587/\exp[1.52996(1.56)] + \\ | \quad &1.76464/\exp[3.89411(1.56)] \\ | \quad &= 1.18 \end{aligned}$$

$$| \quad V_A = 0.285(259)^{1.048} = 96.38$$

$$| \quad dB = 1.18(96.38)^{1/3} = 5.41$$

| Finally, by eq'n 4.5,

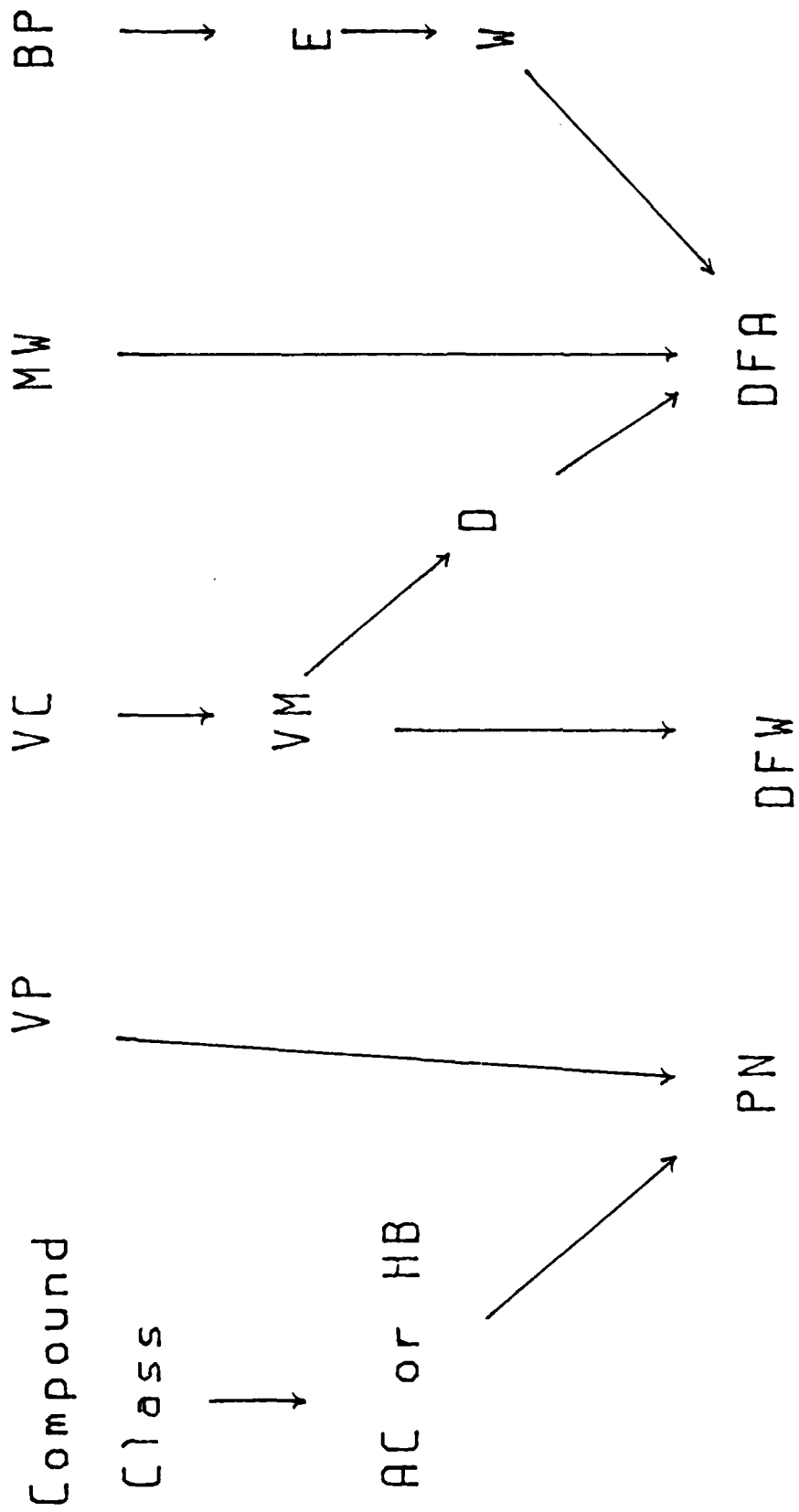
$$\begin{aligned}
 | \text{DFA} &= 0.941077(310)^{1.5} / \\
 | & \quad \{1013.3(1.18)[0.5(3.617) + 0.5(5.41)]^2\} * \\
 | & \quad [1/28.96 + 1/78]^{0.5} \\
 | & = 4.6\text{E-}2 \text{ cm}^2/\text{sec}
 \end{aligned}$$

| For water:

| By eq'n 4.8,

$$\begin{aligned}
 | \text{DFW} &= 7.4\text{E-}8 [2.6(18.02)]^{1/2} 310 / \\
 | & \quad [0.6915(96.38)^{0.6}] \\
 | & = 1.46\text{E-}5 \text{ cm}^2/\text{sec}
 \end{aligned}$$

In summary, mass transport modeling in the conductive zone of the lung requires values of air/liquid partition coefficients (α or PN), air diffusivity (DFA), and water diffusivity (DFW). In the absence of reliable experimental data, these values can be estimated by existing methods using readily available handbook data as illustrated in figure 4.2. Table 4.1 lists solubility and diffusivity data calculated by methods described in this chapter for some of the more common gases and vapors.



ESTIMATING SOLUBILITY AND DIFFUSIVITY

FIGURE 4.2

Table 4.1

WATER SOLUBILITY AND DIFFUSIVITY DATA FOR SOME
COMMON GASES AND VAPORS

<u>GAS/VAPOR</u>	<u>PARTITION COEFF. (PN)</u>	<u>cm²/sec DIFF. COEFF. (DFW)</u>
Acetone	348.0	1.67E-5
Acetylene	0.81	2.5E-5
Ammonia	237.0	3.26E-5
Benzene	4.6E-6	1.46E-5
Butane	17.2	1.48E-5
Carbon Tetrachloride	51.1	1.41E-5
Chloroform	32.2	1.54E-5
Dichlorethane	3.04	-
Dichloroethylene	5.32	-
Ethane	0.034	2.08E-5
Heptane	0.08	1.06E-5
Hexane	0.11	1.17E-5
1,1,1-Trichloroethane	11.2	1.35E-5
Methylene Chloride	16.6	1.76E-5
Methyl Ethyl Ketone	378.0	1.44E-5
Nitrous Oxide	0.48	2.71E-5
Octane	0.05	9.77E-6
Pentane	0.18	1.33E-5
Perchloroethylene	74.0	1.36E-5
Propane	3.1	1.71E-5
Sulfur Dioxide	24.0	2.35E-5
Toluene	4.0E-6	1.29E-5
Trichloroethylene	18.5	1.47E-5
Vinyl Chloride	1.6	1.9E-5
Xylene	3.2E-6	1.17E-5

Chapter 5

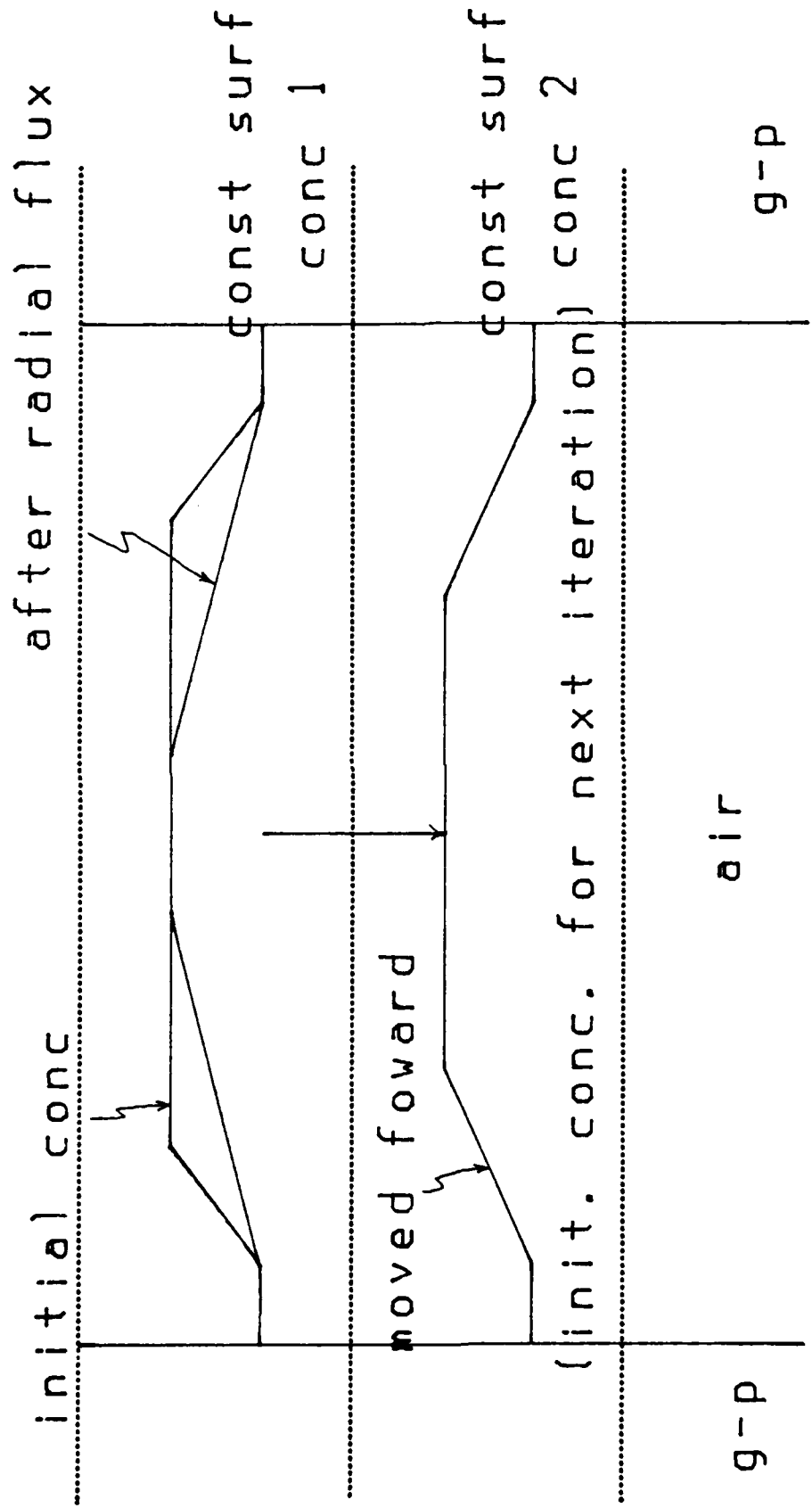
A LUNG MASS TRANSPORT MODEL

As discussed in chapter 3, an iterative-analytical model is desired which would track the transport of an inhaled gas or vapor in the conductive zone of the lung over a sufficiently long exposure time to determine routes of uptake. Specifically, over the course of an exposure, we wish to partition a volume of gas or vapor into fraction entering system through alveolar blood/gas exchange, fraction entering system through bronchial absorption in the conductive zone, fraction expelled to the GI tract, and fraction exhaled. If a large amount of such data is generated over a range of gases and vapors of varying physical characteristics, then these compartmental uptakes can be characterized as a function of solubility and diffusivity, assuming that physiological conditions remain constant.

The model must start with an exposure concentration entering the trachea, distribute that mass within the trachea, and determine the concentration leaving and entering the next generation. A concentration grid must be established within each region of transport (figure 2.7) which will control subsequent mass flux as inhalation

continues. The time of inhalation must be tracked to determine flow velocity and rate of convection. During exhalation the input concentration to the conductive zone is the alveolar concentration which is based on air/blood equilibration of the mass entering the alveoli during inhalation. One must also consider that the tissue concentration will eventually be influenced by rising blood concentrations from alveolar exchange.

We begin by considering the transport phenomenon on the level of a single bronchiole as shown in figure 2.7. Transport in the air phase is the most difficult to describe analytically. Air enters at one end with an existing concentration profile. As the model is moved forward over a time increment, the profile is influenced by laminar flow convection and radial diffusion with flux through the wall while experiencing a continually changing boundary condition at the air/liquid interface as it moves through the bronchiole. This is a complex analytical problem, and we must resort to considering a very small time increment over which the air advances only a small distance such that the condition of the liquid surface is considered constant. With this approach, we can consider an analytical expression describing the profile change for radial diffusion only, with constant boundary condition, and then adjust that profile according to the convective velocity distribution as shown in figure 5.1. The shape of the profile moved forward would depend on the profiles in upstream incremental volumes



CONVECTIVE-DIFFUSIVE TRANSPORT

FIGURE 5.1

and the fraction of those volumes moved forward at each radial point by the parabolic velocity distribution. The radial diffusion expression would be analogous to other transport problems in the literature such as heat flow in a cylindrical rod. Jaeger¹⁴ presents a heat conduction expression defining a profile as a function of distance from centerline [r], and initial profile [f(r)]. In terms of mass transport,

$$C = C_1 \left[1 - \frac{2}{RG} \sum_{n=1}^{\infty} \frac{J_0(r \alpha_n)}{\alpha_n J_0(RG \alpha_n)} \exp(-DA \alpha_n^2 t) \right] + \frac{2}{RG^2} \sum_{n=1}^{\infty} \frac{J_0(r \alpha_n)}{J_1^2(RG \alpha_n)} \exp(-DA \alpha_n^2 t) * \int_0^{RG} r' f(r') J_0(r' \alpha_n) dr' \quad (5.1)$$

where C_1 = constant surface concentration

t = time increment

J_0, J_1 = zero and first order Bessel functions of the first kind

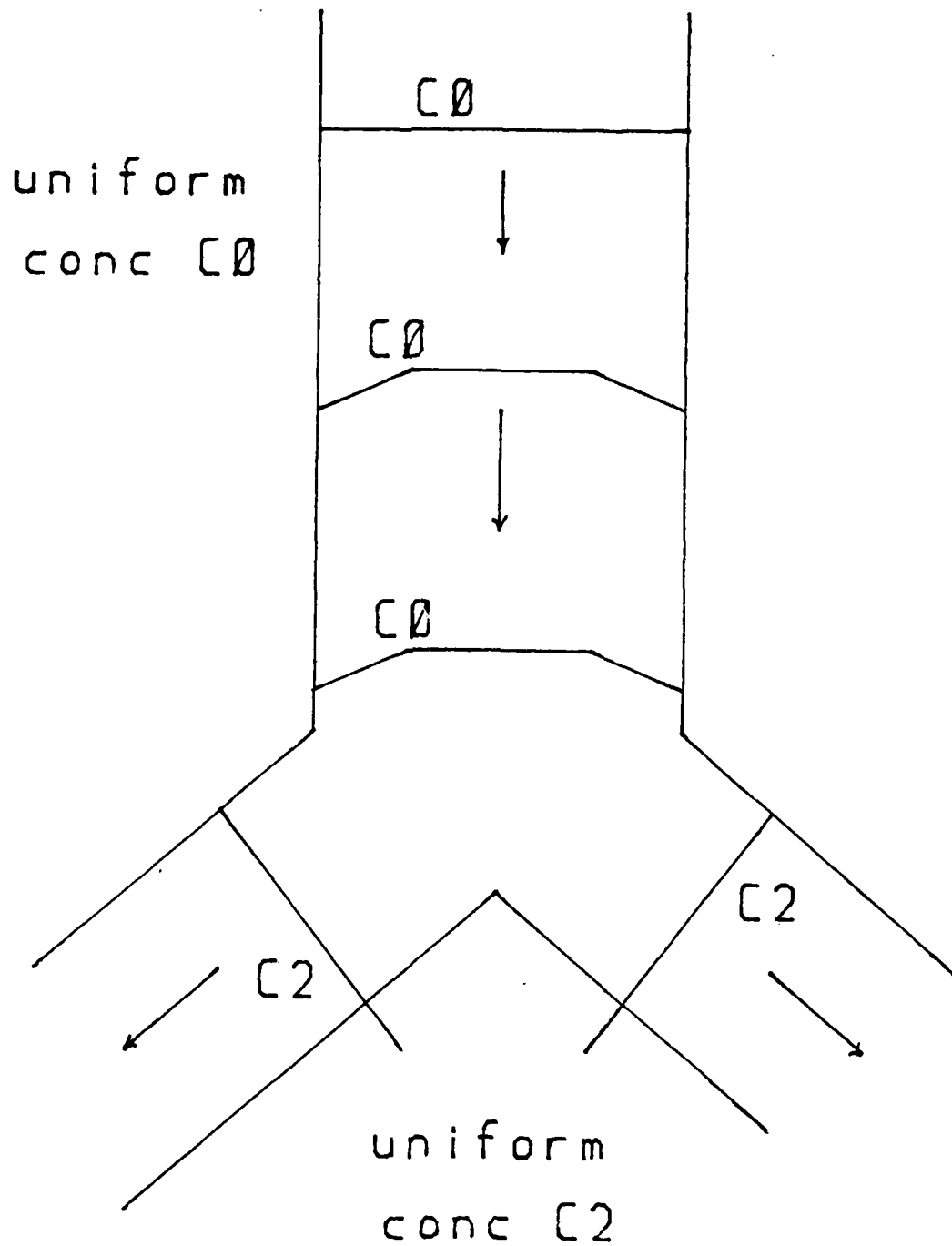
and the α_n 's are the real, positive roots of J_0 .

Use of the Bessel functions is necessitated by the cylindrical geometry of the problem. Unfortunately, Jaeger's expression (formulated for heat conduction problems) does not provide satisfactory results for many values of DA , t , and RG which are encountered in the lung mass transport problem.

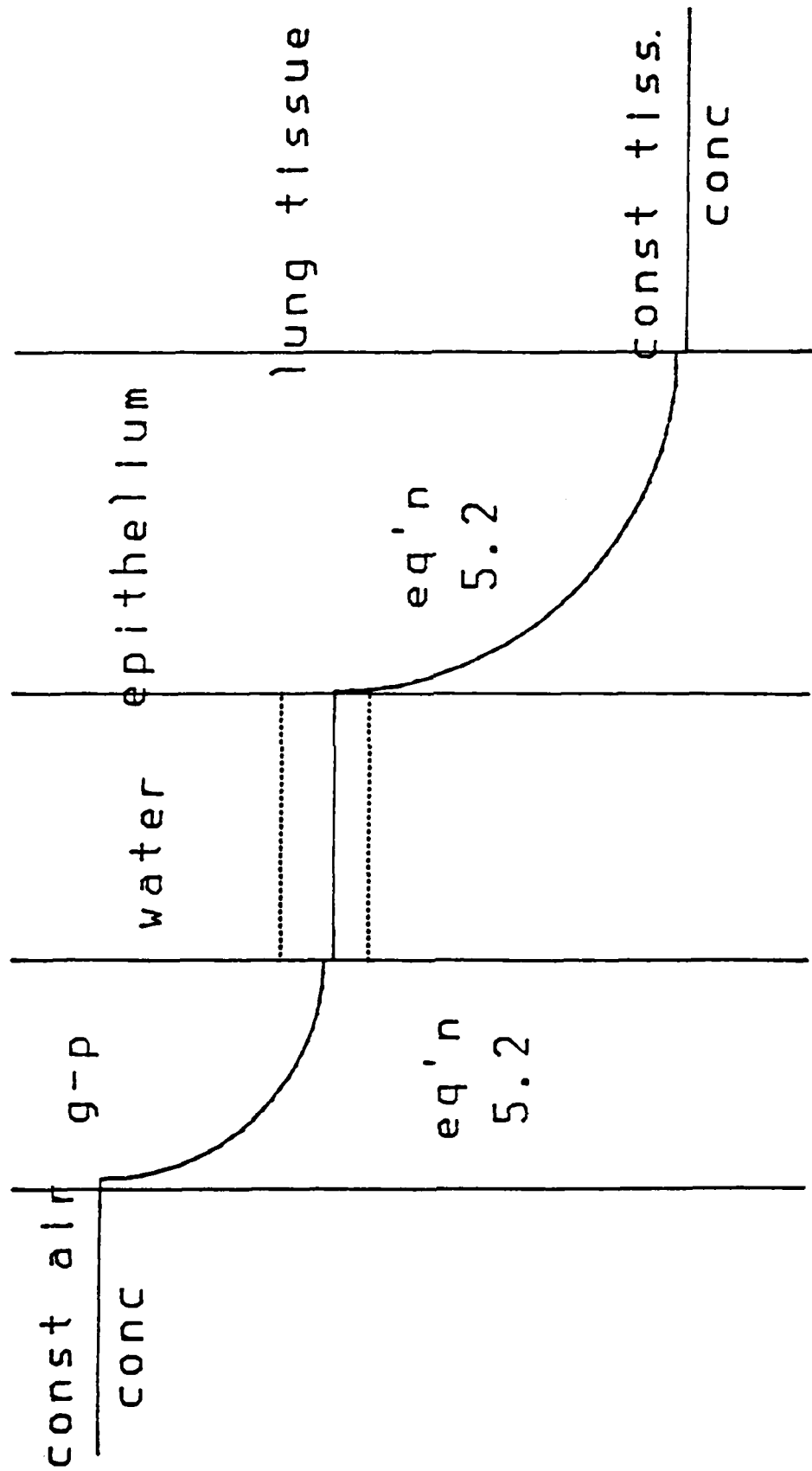
However, if we consider the case of a gas or vapor which is not highly soluble such that wall absorption is

small, then, over the length of a single bronchiole, wall flux would not significantly influence the concentration profile in air. If we further assume that mixing at bifurcations is sufficient to uniformly distribute the mass over the cross-section at entry, then a relatively uniform air concentration profile may be assumed within each bronchiole as shown in figure 5.2. In this way, an entire bronchiole may be treated as a unit which, over a small time increment, has a constant air concentration over its length which then serves as a constant boundary condition for transport into the fluid layers.

Transport in the fluid and tissue layers presents a much simpler analytical problem. The combined thickness of the fluid blanket and epithelium is small compared to the diameter of the airway. Thus, for purposes of mass transport modeling, we may neglect the cylindrical nature of the problem and assume that the ring of fluid and epithelium is stretched out along a smooth plane. This will allow use of trigonometric functions rather than the more complicated Bessel expressions. Furthermore, the upward movement of the glyco-protein layer due to ciliary action is very slow such that the overwhelmingly predominant influence on that layer's concentration is the concentration gradient due to radial diffusion, and the convective component can be neglected. Thus, the problem can be perceived as shown in figure 5.3. Since, over a small time increment, air concentration in a single airway is constant and tissue



SIMPLIFIED AIRWAY MODEL
FIGURE 5.2



FLUID AND EPITHELIAL MODEL

FIGURE 5.3

concentration is constant, we have a one dimensional diffusion problem across four infinite planes separating the air, fluid, and tissue regions. Crank⁶ presents an expression for mass transport between two infinite planes with constant boundary conditions C_1 and C_2 at the two planes, respectively, and initial concentration profile $f(X)$:

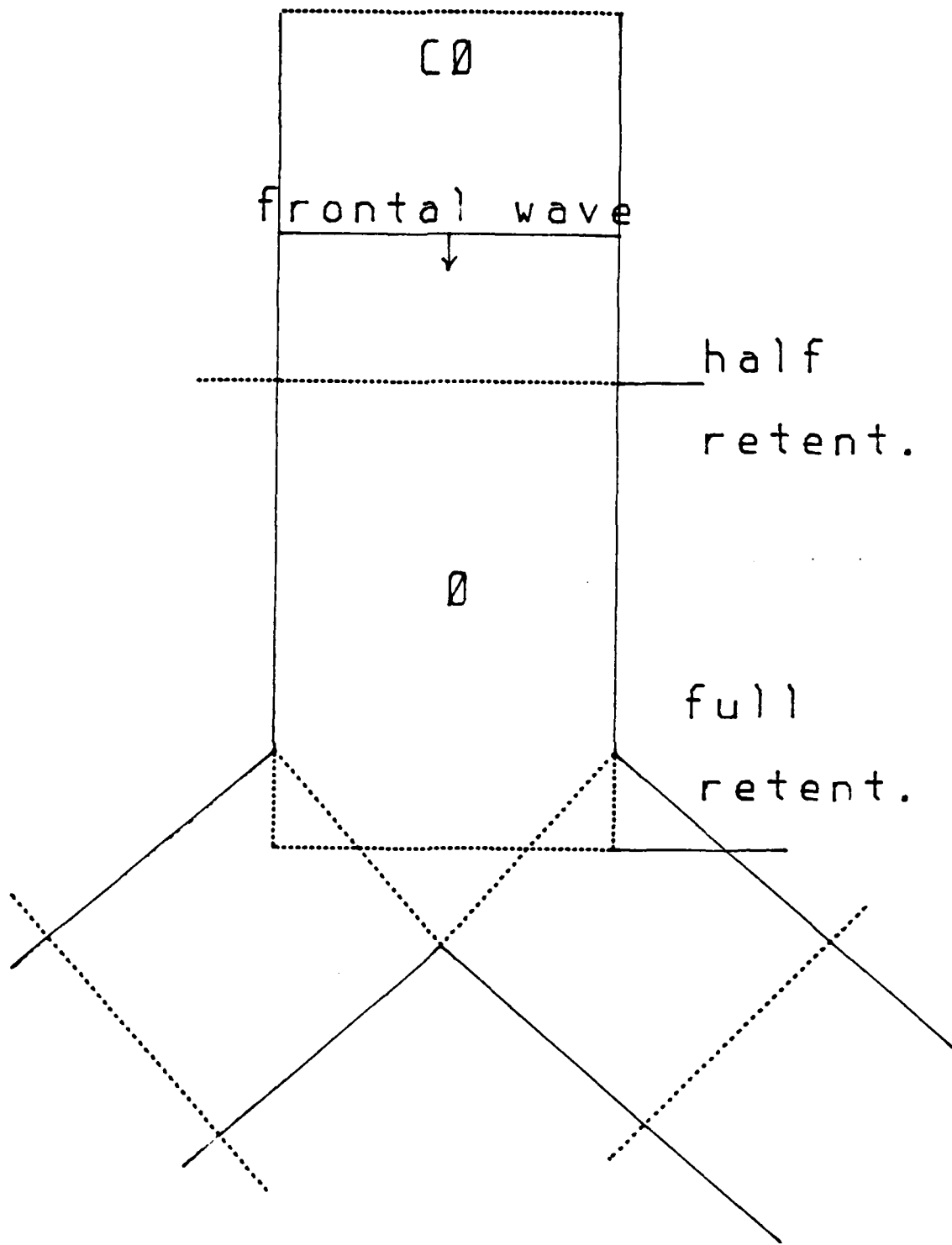
$$C = C_1 + (C_2 - C_1)X/L + 2/\pi \sum_{n=1}^{\infty} [C_2 \cos(n\pi) - C_1]/n * \sin(n\pi X/L) \exp(-DW n^2 \pi^2 t/L^2) + 2/L \sum_{n=1}^{\infty} \sin(n\pi X/L) * \exp(-DW n^2 \pi^2 t/L^2) \int_0^L f(X') \sin(n\pi X'/L) dX' \quad (5.2)$$

where L = distance between boundaries

and X = distance from lower boundary ($X=0$).

Since the water layer represents a reservoir of uniform concentration due to turbulent mixing by cilia, we can apply equation 5.2 across the glyco-protein layer with C_1 equal to the constant air concentration times the air/liquid partition coefficient and C_2 equal to the uniform water concentration during a small time increment. The same equation may be used to describe transport in the epithelium with C_1 and C_2 equal to the water concentration and tissue concentration respectively. The uniform water concentration must then be adjusted from time increment to time increment ($t = \text{say, } 0.01 \text{ sec}$) based on evaluation of the derivative of equation 5.2 at its boundaries and calculation of total mass

fluxing in or out of the known water volume during the time increment. It now remains to define the air concentration and tissue concentration. Consider the beginning of an inhalation exposure at which time a frontal wave of inspired air enters the trachea. At some time later, the wave has moved into the trachea such that the concentration behind it is C_0 (inspired air concentration) and the concentration ahead of it is 0, as shown in figure 5.4. Since the model considers a constant air concentration throughout the airway during a time increment, at some point the tracheal air concentration must be re-defined from 0 to C_0 . A reasonable approximation would be to establish that point at the time the wave extends half way into the trachea, or one-half tracheal retention time at the prevailing flow. Next, the model must re-define the concentration leaving the trachea (input concentration for next generation) based on the cumulative mass absorbed through the wall as determined by means described above. This definition should occur when the wave reaches the end of the trachea, or full retention time. The next generation will then use this value to define its air concentration when half retention is achieved for that generation. Wave entry times must be established for each generation at the beginning of exposure and redefined each time full retention is reached for the respective generation based on the triangular flow function over the course of inhalation or exhalation.



BRONCHIAL AIR CONCENTRATION
FIGURE 5.4

The concentration leaving generation 16 is averaged over the course of an inhalation and is used to define alveolar concentration (which is the input concentration during exhalation). We assume that the concentration entering alveolated space is instantaneously equilibrated in blood/gas exchange such that alveolar concentration is established by a simple distribution over the combined volume of the respiratory zone and blood flow. An appropriate expression is given by Fiserova-Bergerova⁸ as

$$\begin{aligned} C_{ALV} &= C_{in} [Q/(Q + F PN)] \\ &= C_{in} \frac{1}{1 + (F/Q)PN} \end{aligned} \quad (5.3)$$

where C_{ALV} = alveolar concentration

C_{in} = avg concentration leaving generation 16

F/Q = perfusion/ventilation ratio
= 1.25 in resting man

PN = blood/air partition coefficient (taken to be equal to the water/air partition coefficient for the inhaled gas)

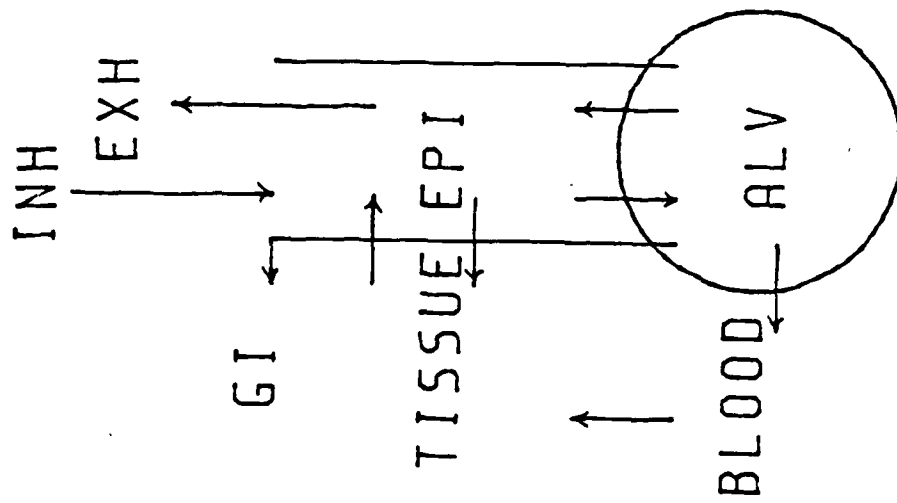
Inhaled gas or vapor concentration in the blood should be distributed back into lung tissue from the heart in a matter of seconds after undergoing alveolation. We must therefore consider its influence on lung tissue concentration. An expression for tissue concentration is taken from Ketty¹⁵: (We assume here that the tissue/blood partition coefficient is 1.0.)

$$C_i = C_a (1 - e^{-kt}) \quad (5.4)$$

where C_i = tissue concentration
 C_a = PN C_{ALV}
 k = F/V
 V = lung tissue volume
 = 600 cc (Fiserova-Bergerova⁸)
 F = bronchial tissue perfusion rate
 (estimated at 0.5 liters/min.)

By employing the model above with input values of diffusion coefficient, partition coefficient, exposure concentration, tidal volume, and respiratory rate, we can describe concentrations and magnitudes and directions of mass flux throughout the conductive zone over small time increments. Cumulative values can be formed such that, at the end of a complete inhalation/exhalation cycle, fractions of inhaled mass can be calculated for alveolar uptake, bronchial epithelial uptake, discharge to GI, and exhalation. Figure 5.5 summarizes the function of the model and lists the values ultimately produced. As shown, the fractional components of distribution should add to 1.0 for ideal results. The computed fractional values might be expected to change in proportion to each other in subsequent breaths as blood and tissue concentrations change but should stabilize fairly quickly such that concentrations and rates of flux remain the same from end-exhalation to end-exhalation.

Figure 5.6 lists the major assumptions of the model described and each is summarized below:



$$F_{REXH} = EXH / INH$$

$$F_{RGI} = \text{dischrg to GI} / INH$$

$$F_{REPI} = \text{net EPI uptake} / INH$$

$$F_{RALV} = \text{net ALV uptake} / INH$$

$$F_{REXH} + F_{RGI} + F_{REPI} + F_{RALV} = I$$

TRANSPORT MODEL OVERVIEW

FIGURE 5.5

MODEL ASSUMPTIONS

1. Regular dichotomy
2. Bronchial absorp. only
3. Uniform air conc. prfle
4. Air/liq interface equil.
5. Low concentration
6. Slow ciliary transport

FIGURE 5.6

1. Weibel's regular dichotomy model for lung morphology is used which assumes symmetrical bifurcation of airway branches with each airway of a particular generation having identical dimensions. Bifurcation in the human lung is known to be 'irregular'.

2. The model considers transport in the conductive zone only and does not deal with nasal-pharyngeal absorption or epithelial absorption in alveolated airways of the transitory and respiratory zones. Thus, tidal volume and exposure concentration refer to air entering the trachea at body temperature and humidity.

3. The solubility of the inhaled gas or vapor is assumed to be such that no significant air concentration profile is developed in the airways due to absorption at the wall. Furthermore, air flow patterns at bifurcations are such that mass is uniformly distributed across the airway cross-section upon entry into an airway generation.

4. The air and liquid concentrations at the air/liquid interface are in phase equilibrium at the airway wall.

5. The inhaled gas or vapor is at low concentration such that the phase equilibrium function is linear, being described by a partition coefficient, and molecular diffusion can be described using Fick's Law.

6. The convective motion of the mucus blanket due to ciliary action is slow and is not a significant factor in mass transport of gases and vapors.

Results of application of this model over a range of solubilities and diffusivities are presented in chapter 6.

Chapter 6

RESULTS

The model described in chapter 5 was implemented using fortran 77. A source listing of one version of the main routine (with comments) is provided in Appendix C. Significant cpu time was logged on the Cyber 205 at Colorado State University through the Institute for Computational Studies there and the services of Triangle Universities Computation Center. Most of the results, however, were generated by the MAP 6420 array processor by CSP Inc, Billerica, Mass. This system was hosted by a VAX 750 at the National Institutes of Health's National Biomedical Simulation Resource facility at Duke University. Results were cross-checked using the VAX 750 with a Digital Equipment Corp. fortran compiler.

Several trial runs were performed using various time increments for successive iterations. It was found that reducing the time increment from 0.01 second to 0.001 second gave concentration grid values which differed by less than 2%. Subsequent runs were performed at an iteration exposure time increment of 0.01 second to conserve cpu time.

The algorithm was constructed to continue generating data until such time as end-exhalation conditions differed

by less than 5% of conditions at the most previous end-exhalation, as discussed in chapter 5. Under this criterion, only the data generated for the last breath are reported as model results. In all cases, conditions stabilized within 15 breaths with most stabilizing in the range of 3 to 8 breaths, lower solubilities tending to require longer stabilization times.

Reasonable ranges of solubilities (PN) and diffusivities (DFW) were selected based on review of handbook data for hundreds of compounds. However, with higher solubilities, model results for some cases revealed 100% absorption in the conductive zone. Since this was considered inconsistent with a 'relatively insoluble' assumption, the solubility range was reduced and the ranges studied were as follows:

$$[6.26 \times 10^{-6} < \text{DFW} < 4.74 \times 10^{-5}] \text{ cm}^2/\text{sec}$$

$$[0.62 < \text{PN} < 13.0]$$

where the partition coefficient (PN) is defined as described in chapter 4. Above a PN value of 13 the uniform air concentration assumption would not be expected to hold with high diffusivity values ($> 4 \times 10^{-5} \text{ cm}^2/\text{sec}$). Under these conditions, high bronchial absorption would likely produce a significant parabolic air concentration profile. The resulting lower air concentration at the bronchial walls would limit further absorption and, thus, bronchial

absorption would be lower and alveolar uptake would be higher relative to model predictions. However, diffusivity values greater than 3×10^{-5} are rare and in the range of $1-2 \times 10^{-5}$, which holds for most compounds, the PN range for the model may be extended to approximately 20.

Operating within the above ranges 109 cases were studied with the following critical input data:

Exposure Concentration = 375 mg/l

Tidal Volume = 600 cc

Respiratory Rate = 15 breaths/min

G-P layer thickness = 7.0×10^{-4} cm

Water layer thickness = 7.0×10^{-4} cm.

(Note: Model output is in terms of concentrations based on exposure concentration. Fractional partitioning is then calculated from model output. Test runs at 10, 75, 125, and 250 mg/l exposure concentration gives identical fractional uptake data, showing that fractional partitioning is independent of concentration. Thus, as one might intuitively assume, total uptake is directly proportional to exposure concentration.)

Results were analyzed using SAS utilities (Statistical Analysis System) to sort, plot, and compare data, and to fit simple analytical expressions to some curves. Initial model results from above data are listed (sorted by PN and DFW) in Appendix D. The last column in the listing represents the sum of the fractional compartmental uptake values which

should ideally add to 1.0.

Figure 6.1 is a plot of model results showing total mass taken up by the lung (mass inhaled minus mass exhaled) as a fraction of mass inhaled vs solubility (PN). The three curves represent three values of the diffusion coefficient, the lower curve at the bottom of the DFW range, the middle curve at mid range, and the top curve at top of the DFW range. The curves show that solubility is the primary influencing factor in total uptake while diffusivity appears to govern slightly the asymptotic value approached at higher solubilities. Note also that uptake is significant, even at very low solubilities and climbs sharply up to a PN value of 4, nearing an asymptotic maximum beyond a PN of 8.

Figure 6.2 shows a plot of the fraction taken up through the epithelial walls of the conductive zone. Here we see a much greater dependence on diffusivity as this is the primary transport pathway in which diffusivity is a factor. Diffusivity may indeed play as important a role here as solubility. This is illustrated by a least squares non-linear regression fit to the plotted data. A reasonable fit is obtained with an expression giving equal weight to both variables:

$$\text{FREPI} = 1 - \exp(-3961 \text{ DFW PN}). \quad (6.1)$$

Figure 6.3 shows the same model results for two of the diffusivity values with curves overlayed, representing corresponding values predicted by equation 6.1. Appendix E

FIG 6.1: LUNG UPTAKE (fract. of inhaled)

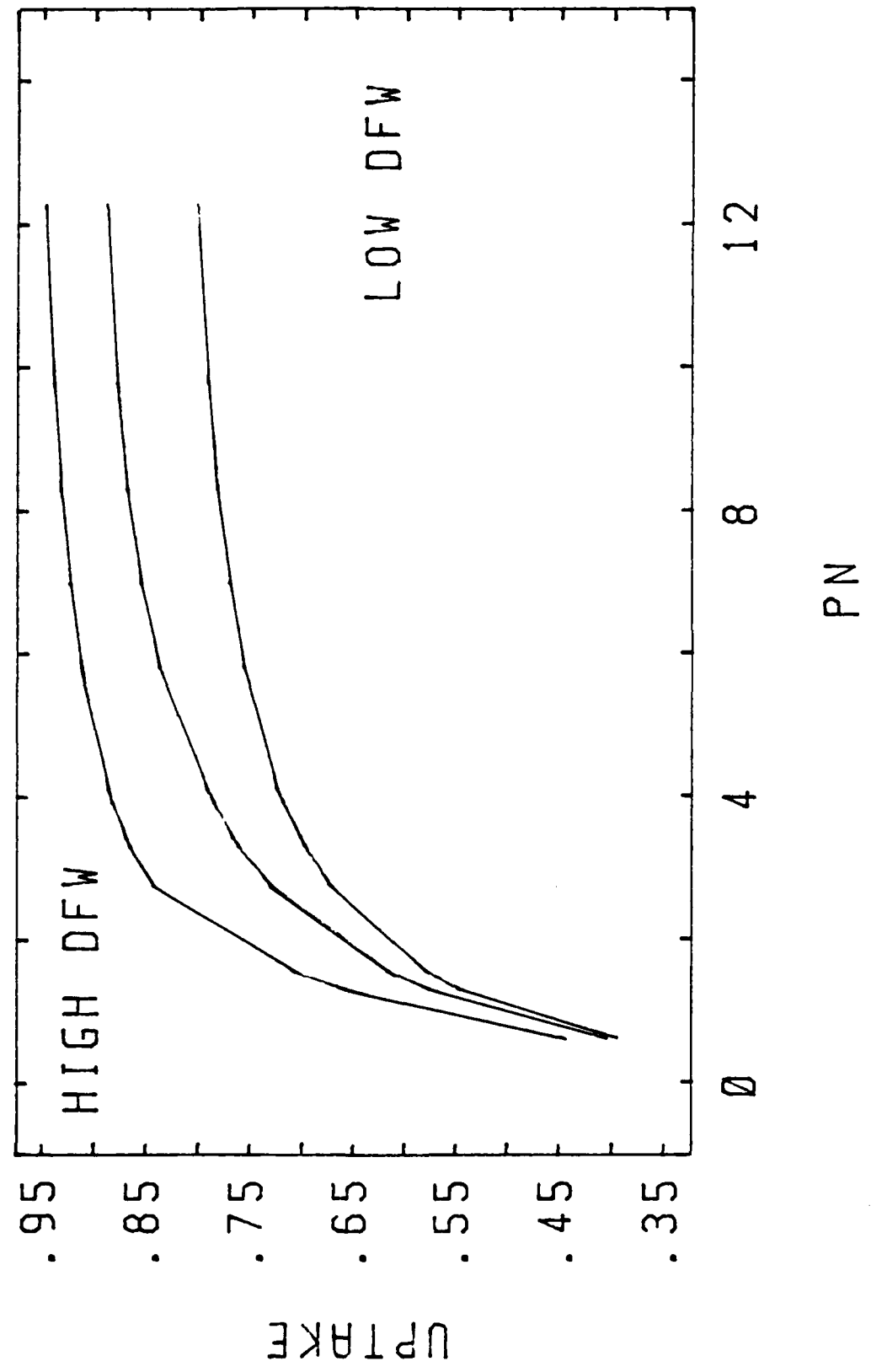


FIGURE 6.2: EPITHELIAL ABSORPTION

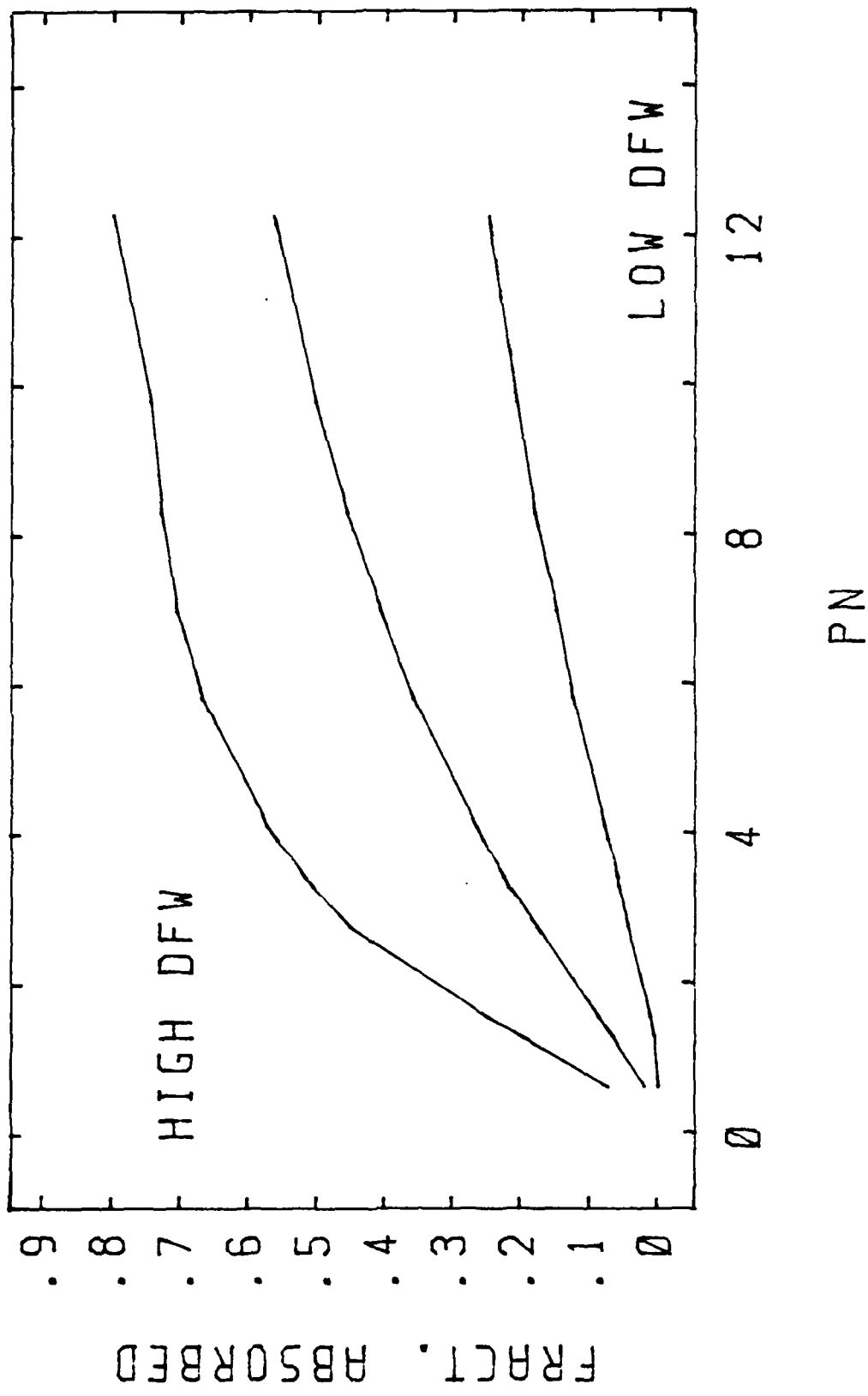
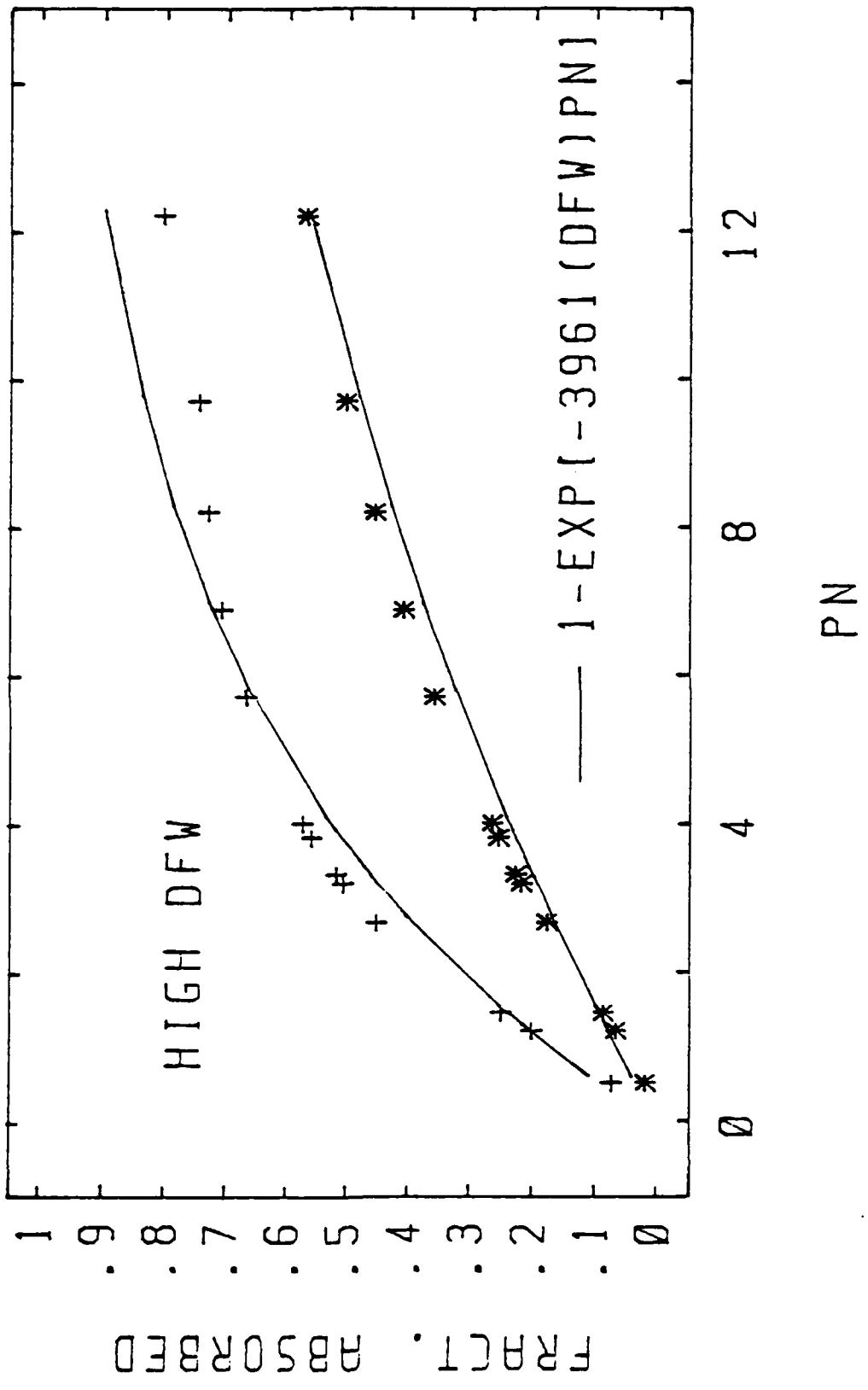


FIGURE 6.3: PREDICTED EPITH. ABSORP.



lists the complete model results for fractional epithelial uptake with corresponding values and residuals from equation 6.1.

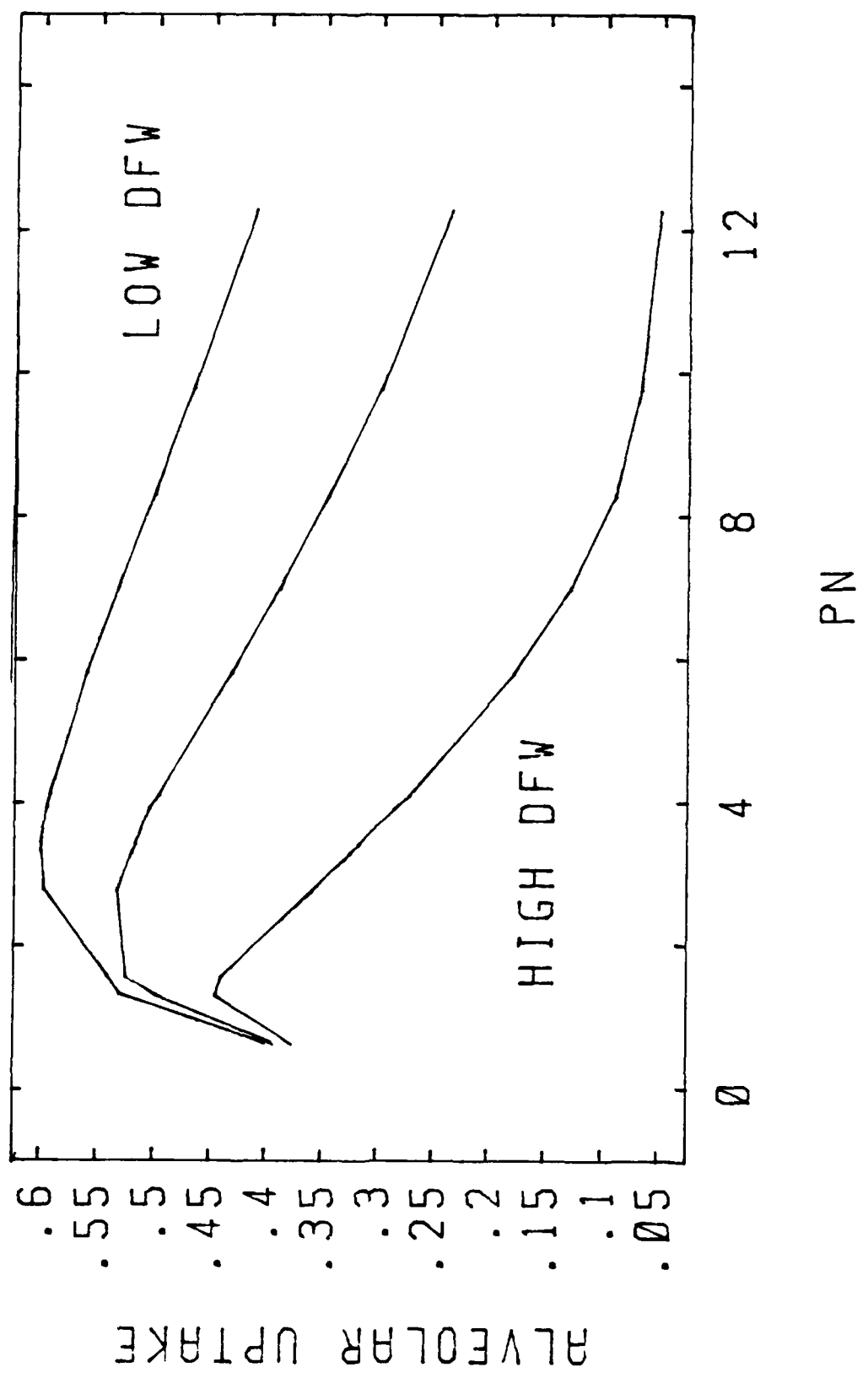
Figure 6.4 shows a plot of the fraction taken up by blood/gas exchange in the respiratory zone, again, for the same three diffusivity values. Here we can see evidence of two terms which are apparently affecting the shape of the curve. This can easily be explained when we consider that alveolar uptake is dependent not only on solubility in blood/gas partitioning but also on the mass allowed to reach the alveolar region from the conductive zone. This alveolar uptake rises with solubility up to point where uptake is limited by decreased input due to rising absorption in the conductive zone. Regression analysis provides the following empirical equation for alveolar uptake:

$$FRALV = \exp(-6282 DFW PN) - 1/(1 + 348.5 DFW^{0.5} PN) \quad (6.2)$$

Again, figure 6.5 and Appendix F compare model results with values predicted by equation 6.2 as in the case of bronchial absorption.

The fraction discharged to the GI tract by muco-ciliary clearance, as shown in figure 6.6, is not a significant component of distribution. Unlike particulate matter which is captured and accumulated by the mucus blanket and carried upward to the trachea, gas and vapor concentrations in the fluid layers conform to the concentrations in adjacent regions without a cumulative build up. Thus, the fluid

FIG 6.4: ALV UPTAKE (fract. of inhaled)



PN

FIGURE 6.5: PREDICTED ALVEOLAR UPTAKE

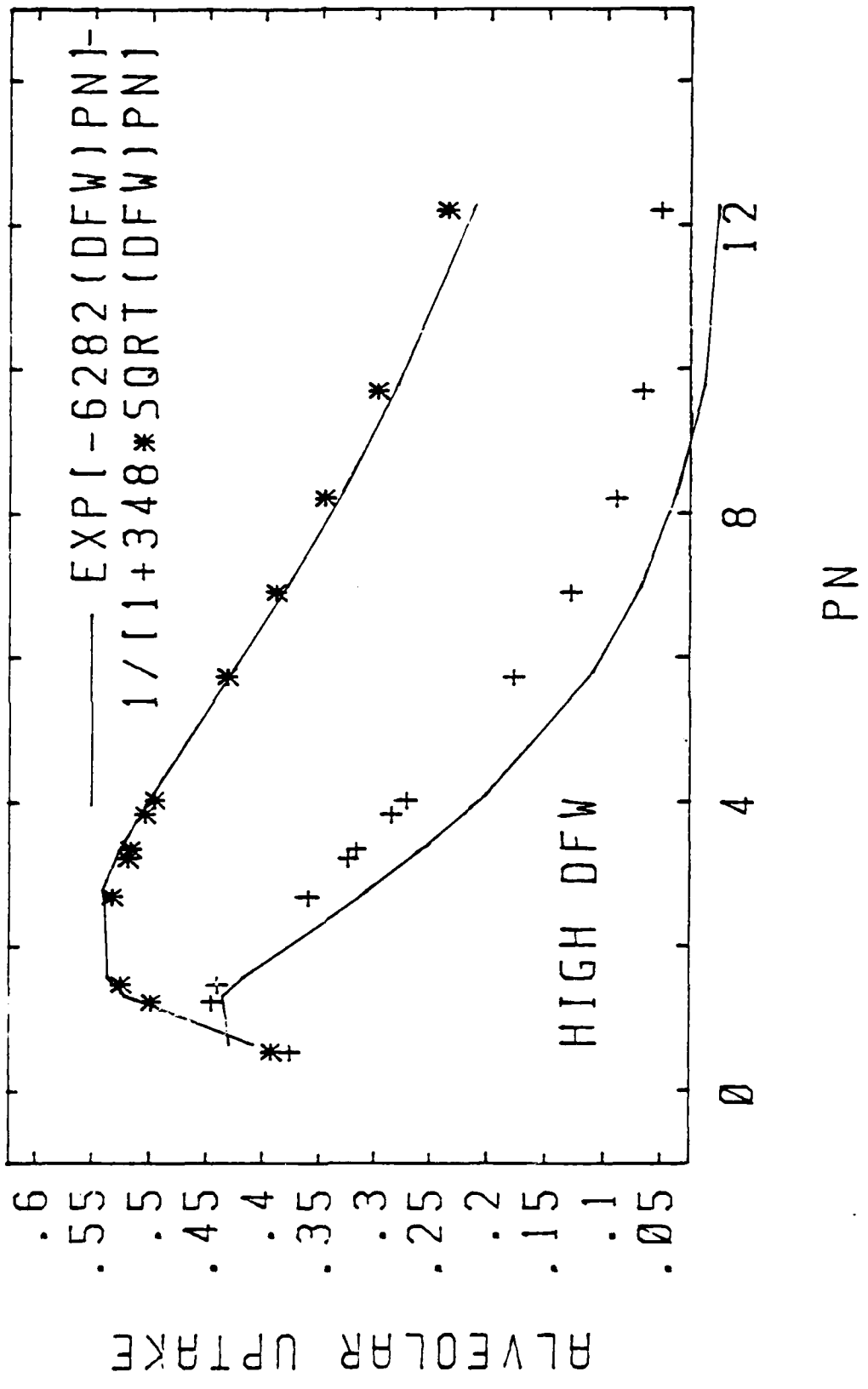
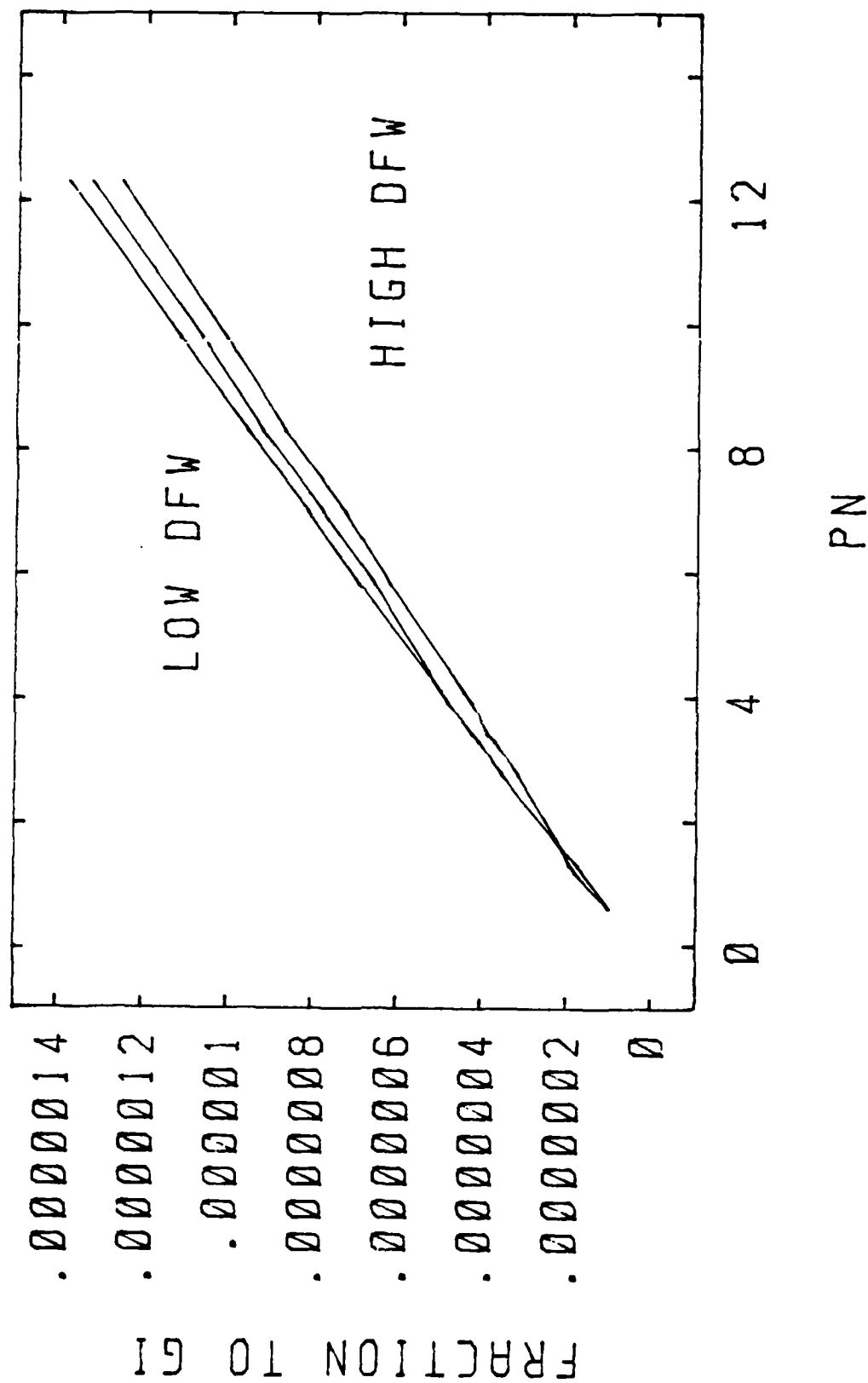


FIGURE 6.6: MUCO-CILIARY CLEARANCE



FRACTION TO GI

.0000014
.0000012
.000001
.0000008
.0000006
.0000004
.0000002
0

0

4

8

12

PN

layer concentration combined with a small volume of fluid discharged in the course of a single exposure limits discharge to the GI tract to extremely small values. However, prediction of the discharge may be valuable in some cases when the impact of toxic substances on the GI tract is a concern. Figure 6.6 shows that the fraction reaching the GI tract is almost solely dependent on solubility and can be practically estimated by a linear regression according to equation 6.3:

$$\text{FRGI} = 5.75 \times 10^{-8} \text{PN} \quad (6.3)$$

Sensitivity to Assumed Parameters

The model, as described, assumes constant values for certain key physiological parameters for simplicity. To evaluate the model's sensitivity to changes in these parameters, several model runs were performed at a constant, mid-range diffusion coefficient. For each parameter considered, thirteen runs were performed at thirteen representative solubility points within the model solubility range. Each run held the parameter in question constant at a value substantially changed from the model base-line value while holding all other parameters constant at the base-line value. Table 6.1 lists factors by which fractional bronchial epithelial absorption and fractional alveolar uptake were changed from the model base-line results at the same solubility and diffusivity point. The factors listed are averages of the thirteen values produced for that case,

but none of the calculated factors differed from their average by more than 5%. The results listed in table 6.1 are discussed below.

Respiratory Rate:

Increasing the respiratory rate from 15 to 25 breaths per minute substantially reduces the fraction absorbed in the upper airways (0.61 of base-line value) due to the higher flow rate and decreased retention time in this region. Less absorption increases the mass entering the alveolar region; however, this effect is offset somewhat by the higher alveolar ventilation rate which tends to lower alveolar uptake. Hence, only a slight increase in fractional alveolar uptake is effected. Thus, the combined effect of lower bronchial absorption and only slightly altered alveolar uptake would appear to lower total fractional uptake. At first, this appears to be incongruous with increased respiration. However, these figures are for uptake as a fraction of that inhaled. Since a higher respiratory rate increases the volume inhaled per minute, the total mass taken up per minute would not be expected to decrease and may in fact increase.

Tidal Volume:

Increasing the tidal volume is precisely analogous to increasing the respiratory rate (higher flow rate, smaller retention time). Thus, the same effect is observed. The smaller factor for tidal volume relative to that for

Table 6.1

Factors by which Baseline Model Results Change
with Indicated Parameter Change

<u>PARAMETER CHANGE</u>	<u>FRACT. BRONCH. ABSORP.</u>	<u>FRACT. ALV. UPTAKE</u>
Increase resp rate to 25	0.61	1.10
Double tidal volume	0.47	1.15
Double mucus layer thickness	0.97	0.98
Double perfusion/volume ratio in bronchial tissue	0.94	1.01
Half alveolar perfusion/ ventilation ratio (Q/V)	0.80	0.90

respiratory rate reflects the degree to which tidal volume was altered compared to that for respiratory rate.

Mucus Layer Thickness:

An increase in the thickness of the glyco-protein layer may be encountered, particularly in the case of upper respiratory disease or an irritant effect by the exposure gas. Wanner²⁸ points out that the walls and cilia of the upper airways can support a substantially greater mucus thickness than is normally found in healthy humans. For this test, the glyco-protein thickness in the trachea was doubled and linearly tapered down from generation to generation to the base-line value in generation 16. Results show only minor sensitivity.

Bronchial tissue perfusion/volume ratio:

The perfusion/volume ratio in bronchial tissue is used to calculate bronchial tissue concentration. Doubling this ratio (halving tissue volume or doubling perfusion rate) has only a minor influence on model results. The higher ratio produces a higher tissue concentration which slightly limits bronchial absorption and allows slightly more gas or vapor to reach the alveolar region.

Alveolar perfusion/ventilation ratio:

This test measured the effect of reducing the perfusion/ventilation ratio in the calculation of the alveolar equilibrium air concentration only, apart from any

change in respiratory rate or tidal volume (i.e. a lowering of the perfusion rate). The resulting higher concentration in arterial blood produces higher bronchial tissue concentrations (assuming the bronchial perfusion rate remains unchanged). Thus, bronchial absorption is reduced. Alveolar uptake also is reduced due to the smaller blood flow.

Conclusions

In summary, the present work sought to develop a simplified model of gas and vapor transport in the human lung to partition inhaled mass into compartments of alveolar blood/gas exchange, bronchial epithelial absorption, mucociliary clearance to the GI tract, and exhalation. The following statements summarize the results of the work:

1. Sufficient tools are available to construct a practical model of mass transport in the lung and to collect sufficient data for analysis.
2. Total uptake by the lung is significant even at very low solubilities. (fig 6.1)
3. Uptake by direct blood/gas exchange in the respiratory zone decreases with solubility after peaking at a relatively low solubility due to bronchial absorption in the upper airways. (fig 6.4)
4. Diffusivity in the fluid layers and epithelium of the bronchial wall is a significant factor in bronchial absorption, perhaps as much as solubility. (fig 6.3)

5. Muco-ciliary clearance of inhaled gas or vapor to the GI tract is insignificant as a fraction of mass inhaled.

6. Sufficient model results display a clear trend in uptake patterns allowing empirical development of equations estimating fractional compartmental uptake as a function of solubility and diffusivity (eq'ns 6.1 thru 6.3). These equations may then be employed in expanded modeling efforts.

7. In the absence of experimental data, sufficient methods exist for the estimation of solubilities and diffusivities using readily available handbook data for most gases and vapors (chapter 4).

SUMMARY OF CONCLUSIONS

1. Mass trans. model avail.
2. Total lung uptake signif.
3. Alveolar uptake decreases
with solubility
4. Diffusivity strongly
influences absorption

FIGURE 6.7(A)

SUMMARY OF CONCLUSIONS
(cont.)

5. Muco-ciliary clearance of
vapor not significant

6. Uptake trends allow dev.
of empirical expressions

7. Methods available for est.
physical character of gas

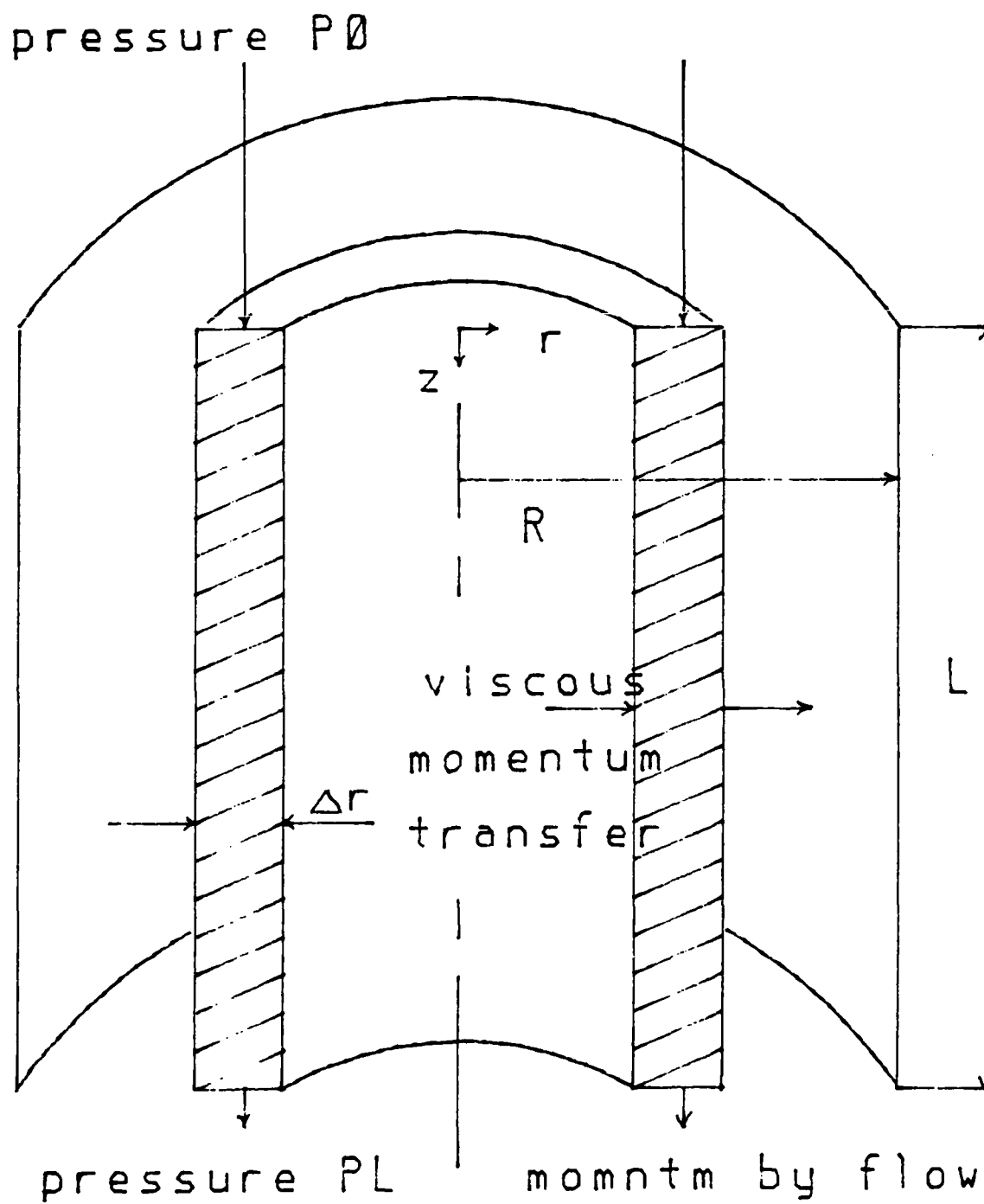
FIGURE 6.7(B)

APPENDIX A
LAMINAR FLOW VELOCITY PROFILE
IN A CIRCULAR TUBE

Expressions describing the velocity distribution in flow through various geometries are described in Bird, Stewart, and Lightfoot². For the case of laminar flow in a circular tube, consider a cylinder of length L and radius R as shown in figure A.1. We begin by assuming that ideal laminar flow exists, i.e. flow everywhere is parallel to the tube wall and entrance and exit perturbations in flow streamlines are absent. We consider an elemental volume within the tube as a hollow shell of thickness Δr and length L and seek to write an equation expressing a momentum balance over this volume. Since a parabolic velocity distribution is developed due to frictional resistance at the wall, a 'shearing force' per longitudinal area may be thought of along the surface of the shell which we will denote by τ . The rate of momentum transfer (force) across the shell may then be expressed in terms of this shearing force per area:

$$\text{Rate of momentum in} = 2\pi rL \tau|_r \quad (\text{A.1})$$

$$\text{Rate of momentum out} = 2\pi rL \tau|_{r+\Delta r} \quad (\text{A.2})$$



In the z direction, the rate of momentum (force or mass-velocity per time) can be expressed in terms of the mass entering or leaving and its velocity:

$$\text{Rate of momentum in} = 2\pi r \Delta r v(\rho v)|_{z=0} \quad (\text{A.3})$$

$$\text{Rate of momentum out} = 2\pi r \Delta r v(\rho v)|_{z=L} \quad (\text{A.4})$$

The sum of these rates of momentum transfer over the elemental volume must equal the total force acting on the element. These forces can be described as:

$$\text{Gravity force} = 2\pi r \Delta r L \rho g \quad (\text{A.5})$$

$$\text{Pressure force} = 2\pi r \Delta r P(0) \quad (\text{A.6})$$

at $z=0$

$$\text{Pressure force} = 2\pi r \Delta r P(L) \quad (\text{A.7})$$

at $z=L$

The sum of equations A.1 thru A.7 must be zero:

$$\begin{aligned} 2\pi r L \tau|_r - 2\pi r L \tau|_{r+\Delta r} + 2\pi r \Delta r \rho v^2|_{z=0} - \\ 2\pi r \Delta r \rho v^2|_{z=L} + 2\pi r \Delta r L \rho g + \\ 2\pi r \Delta r [P(0) - P(L)] = 0 \end{aligned} \quad (\text{A.8})$$

We now simplify the equation by assuming the compression of the air over the length of the tube, given small static pressure differences within the system, is negligible. Thus

we may consider the velocity at $z=0$ to equal the velocity at $z=L$ and the third and fourth terms above cancel. If we then divide by $2\pi L \Delta r$ and take the limit as Δr approaches zero, we have:

$$d/dr(r\tau) = [P(0) - P(L)]r/L + \rho gr \quad (\text{A.9})$$

Recognizing that gravity is acting in the same manner at $z=0$ and $z=L$, we may drop the right most term by assuming that $P(0)$ and $P(L)$ represent the combined effect of static pressure and gravity. Upon integration we then have

$$\tau = [P(0) - P(L)]r/2L, \quad (\text{A.10})$$

the constant of integration being zero to satisfy conditions at $r=0$.

The shearing force per area may also be described by Newton's law of viscosity as

$$\tau = -\mu dv/dr \quad (\text{A.11})$$

Combining equations A.10 and A.11, we have

$$dv/dr = -[P(0) - P(L)]r/2\mu L$$

and integrating,

AD-A168 829

A MODEL OF INHALED GAS AND VAPOR TRANSPORT IN THE HUMAN
LUNG(U) AIR FORCE INST OF TECH WRIGHT-PATTERSON AFB OH
M L SHELLEY 1985 AFIT/CI/NR-85-143D

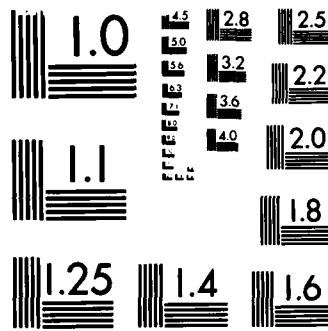
2/2

UNCLASSIFIED

F/G 6/16

NL

												END		
												FILMED		
												DTG		



MICROCOPY RESOLUTION TEST CHART
NATIONAL BUREAU OF STANDARDS-1963-A

$$v = -[P(0) - P(L)] r^2/4\mu L + C \quad (\text{A.12})$$

Since the velocity is zero at $r=R$

$$C = [P(0) - P(L)] R^2/4\mu L \quad (\text{A.13})$$

and

$$v = [P(0) - P(L)] R^2 [1 - (r/R)^2]/4\mu L \quad (\text{A.14})$$

To simplify this equation, one may use the above expression for v and calculate the average velocity over the cross-section by integrating $[v r dr d\theta]$ from 0 to R and from 0 to 2π and dividing by the cross-sectional area. This procedure will show that the average velocity is

$$v_{\text{AVG}} = [P(0) - P(L)] R^2/8\mu L \quad (\text{A.15})$$

Thus the velocity profile may be written in terms of the average velocity as

$$v = 2 v_{\text{AVG}} [1 - (r/R)^2] \quad (\text{A.16})$$

APPENDIX B

EQUATIONS OF CHANGE FOR TURBULENT AIR FLOW

Referring to figure 3.1, we desire to write a mass balance over the elemental volume for the case of turbulent flow. Here we consider the mass flux in the z direction to consist of a convective flux, which is an average flux over time, plus a turbulent flux, which represents variations from the time averaged value due to turbulence.

$$N_z = vC + v'C' \quad (B.1)$$

where v is the time averaged velocity at r . Likewise, since the turbulent flux is expected to act radially as well, the flux in the r direction consists of a diffusive flux plus the turbulent flux.

$$N_r = -D_A \frac{\partial C}{\partial r} + v'C' \quad (B.2)$$

For conditions in the turbulent core of the stream, we use the von Karman Similarity Hypothesis to describe the turbulent flux as follows: (see Bird, Stewart, and Lightfoot²)

$$N_z = vC - K^2 |(\partial v / \partial r)^3 / (\partial^2 v / \partial r^2)^2| \partial C / \partial z \quad (B.3)$$

$$N_r = -D_A \partial C / \partial r - K^2 |(\partial v / \partial r)^3 / (\partial^2 v / \partial r^2)^2| \partial C / \partial r \quad (B.4)$$

where $K = 0.36$ or 0.40 depending on the investigation referenced.

Experimental investigations have shown the velocity profile in a circular tube for turbulent flow to be roughly

$$v = 1.25 v_{AVG} [1 - r/RG]^{0.143} \quad (B.5)$$

Taking the first and second derivative of the above expression with respect to r , we may then substitute in equations B.3 and B.4, giving values of N_z and N_r which may now be used to evaluate equation 3.3 for the turbulent case.

$$-\partial N_z / \partial z - \partial(N_r r) / r \partial r = \partial C / \partial t \quad (3.3)$$

The resulting equation for mass transport in the turbulent core is

$$D_A [\partial^2 C / \partial r^2 + \partial C / r \partial r] + v_{AVG} (1 - r/RG)^{0.143} *$$

$$[0.032 RG (1 - r/RG) \partial^2 C / \partial z^2 - 1.25 \partial C / \partial z = 0.032 RG *$$

$$(1 - r/RG) \partial^2 C / \partial r^2 + 0.032 RG/r * (1 - r/RG) \partial C / \partial r -$$

$$-0.037 \partial C / \partial r] = \partial C / \partial t \quad (\text{B.6})$$

Near the wall of the tube (outside the turbulent core), motion is dampened by resistance at the wall, and the turbulent flux can be described by Deissler's Empirical Formula⁹ so that the fluxes are written as

$$N_z = vC - n^2 vr [1 - \exp(-n^2 vr / \nu)] \partial C / \partial z \quad (\text{B.7})$$

$$N_r = -D_A \partial C / \partial r - n^2 vr [1 - \exp(-n^2 vr / \nu)] \partial C / \partial r \quad (\text{B.8})$$

where ν = kinematic viscosity
and $n = 0.124$ (empirical constant).

Using equation B.5 for velocity and substituting equations B.7 and B.8 into equation 3.3, one arrives at the mass transport equation for the near-wall region. The resulting long expression is not reproduced here.

The location of the boundary separating the turbulent core from the near-wall region is a function of the medium's velocity and viscosity and can be determined in terms of the dimensionless value S^+ :

$$S^+ = 0.36 S^2 (\partial v / \partial S) / \nu \quad (\text{B.9})$$

Using equation B.5 for velocity and recognizing that $r = R_G - S$, the above equation can be re-written as

$$S+ = 0.064 v_{AVG} (RG - r)^{1.143} / (\nu RG^{0.143}) \quad (B.10)$$

Values of r for which $S+$ is less than 26 are considered to be in the near-wall region.

APPENDIX C
FORTRAN SOURCE LISTING

The following pages display a FORTRAN-77 source listing for the transport model described in chapter 5. Only the main routine showing the general model algorithm is listed. More detailed calculations from sub-routines are not shown.

C (* Model lung for insoluble case *)
PROGRAM INSOL

```

C*****
C*
C* This program performs a running calculation of the
C* concentration of a particular species (vapor or gas)
C* in various regions of the human lung. It is intended
C* to approximate the case of a relatively insoluble
C* vapor or gas in water such that no significant concen-
C* tration profile is developed within a single
C* bronchial segment. It relies on constant input values
C* of physiological parameters and species
C* characteristics.
C* Weibel's morphological model of the human lung is used.
C* The inner surface of each bronchiole is assumed to be
C* bathed with a smooth continuous bilayer fluid of
C* viscous glycoprotein on top and non-viscous water
C* beneath. A characteristic thickness is assumed for
C* the epithelia separating the fluid from well perfused
C* tissue. The transport equation employed is from Crank
C* (Eqn 4.16), 'The Mathematics of Diffusion'.
C*
C* PROGRAMMER: M. L. SHELLEY
C*
C* FUNCTIONS CALLED:
C* RAVG
C* RINTGR
C* FLOW
C* RETNTN
C* TRMIII
C* TERMIV
C* DERVTV
C*
C* PROCEDURES CALLED:
C* PRTCON
C* CHKCND
C*****

```

```

CHARACTER*20 SPEC
C (* exposure gas or vapor *)
REAL PNCDEF
C (* water/air partition coef *)
REAL*8 DFCDFW
C (* diffusion coef of species *)
C (* in water *)
REAL ATCDEF
C (* activity coef for solubility in water *)
REAL PS
C (* saturation vapor pressure *)
REAL VC

```

```

C          (* critical volume *)
REAL*8 EXPCON
C          (* exposure conc (micro-grams/cc) *)
REAL MAXTIM
C          (* exposure time signalling termination *)
REAL*8 TRDIA
C          (* dimensions of trachea *)
REAL*8 TRLEN
C          (*
           "
           *)
REAL*8 PTRDIA
C          (* emperical value for gen 4 to 16 *)
REAL*8 PTRLEN
C          (*
           "
           *)
REAL*8 TIDVOL
C          (* tidal volume of lung *)
REAL*8 GLYC0
C          (* layer thickness in extreme generation *)
REAL*8 GLYC16
C          (*
           "
           *)
REAL*8 WATR0
C          (*
           "
           *)
REAL*8 WATR16
C          (*
           "
           *)
REAL*8 EPIT0
C          (*
           "
           *)
REAL*8 EPIT16
C          (*
           "
           *)
REAL DELTIM
C          (* time increment for iteration *)
REAL PCTSTA
C          (* acceptable signrif for lung stability *)
REAL*8 GLYVEL
C          (* mucus transport rate *)
INTEGER MAXPNT
C          (* number of points defining conc prfle *)
INTEGER RESRAT
C          (* respiratory rate *)
INTEGER MXTERM
C          (* terms for series approximations *)
CHARACTER*80 ASTRSK
REAL*8 PI
REAL*8 AIRCJN(0:16,2)
C          (* bronchial air concentration *)
REAL ENTIME(0:16)
C          (* time from beginning of exposure at *)
C          (* which the frontal wave enters a *)
C          (* bronchiole *)
REAL*8 AMASTR(0:16)
C          (* cum mass transported from air to *)
C          (* glyco throughout a generation *)
C          (* during one retention time *)
REAL*8 FLUXTO(0:16,4)
C          (* current flux across interface *)
REAL*8 NFLXTO(0:16,4)

```

```

C          (* flux across interface at next time incr *)
REAL*8 MASSTO(0:16,4)
C          (* mass transfered across interface in *)
C          (* an individual bronchiole in one *)
C          (* time increment *)
REAL*8 LNGCON(0:16,2,30)
C          (* conc prfle in lung region *)
REAL*8 LNGCO1(17)
C          (* for MAP application only *)
INTEGER JMAP, KMAP
C          (*
C          "
C          *)
REAL*8 NLNCON(0:16,2,30)
C          (* conc one time increment later *)
REAL*8 WATCON(0:16)
C          (* conc in water layer *)
REAL*8 NWTCON(0:16)
C          (* conc one time increment later *)
REAL*8 LNGDIM(0:16,6)
C          (* dimensions of lung *)
REAL*8 CI(0:50)
C          (* avg conc discharged to resp in breath *)
REAL*8 UPTAKE(0:50)
C          (* avg uptake rate over breath (mass/sec) *)
REAL*8 GIDSCR(0:50)
C          (* avg discharge rate to GI over breath, m/s *)
REAL*8 EPDSCR(0:50)
C          (* avg discharge rate thru epi wall *)

INTEGER GLY, WAT, EPI, TIS, GLYCO, EPITHL, DIA, VOL,
1      LEN, GLYTH,
1      WATTH, EPITH, TOGI, TOEXH, TOTIS, STRD, IN,
1      OUT
C          (* array subscripts *)

REAL*8 TLCGLY(30), TLCEPI(30), NTCGLY(30)
C          (* temporary arrays for parameter passing *)

REAL CURTIM
C          (* elapsed exposure time *)
REAL*8 ALVCON
C          (* alveolar concentration *)
REAL*8 SYSCON
C          (* systemic concentration *)
REAL*8 MASTOG
C (* mass transfered to GI during current time increment *)
REAL*8 CMSTOG
C          (* cummulative mass discharged to GI *)
REAL*8 CMSTOR
C          (* cum mass passed to respiratory zone *)
C          (* in current breath *)
REAL*8 MASTOE
C          (* mass passed to exhalation in current time incr *)
REAL*8 CMSTOE
C          (* cum mass exhaled in current breath *)

```

```

REAL*8 CMSTOT
C      (* cum mass transfered to tissue *)
REAL TMBRTH
C      (* time from beginning of exposure at which *)
C      (* the current inhalation or exhalation began *)
REAL CUMVOL
C      (* cumulative volume for calc initial entry times *)
INTEGER I
C      (* loop counter *)
INTEGER GEN
C      (* generation number (trachea = 0) *)
INTEGER POINT
C      (* evaluation point for conc function *)
INTEGER ITERTN
C      (* iteration counter *)
INTEGER BREATH
C      (* number of full breath (inh + exh) from *)
C      (* beginning of exposure *)
LOGICAL INHLTN
C      (* states whether inh or exh *)
LOGICAL STBLZD
C      (* states condition of lung *)

REAL*8 EPSI
C      (* zero variable *)

```

```

C*****
C      INITIALIZE CONSTANTS
C*****

```

```
DATA SPEC/'111'/
```

```
DATA  ATCOEF,  PS,      EXPCON,  MAXTIM,  TRDIA
1      /0.1,    0.01,   3.75D+02,  60.05,   1.8D+00/
```

```
DATA  TRLEN
1      /12.0D+00/
```

```
DATA  PTRDIA,  PTRLEN,  TIDVOL,  GLYC0,   GLYC16
1      /1.3D+00,  2.5D+00,  6.0D+02,  7.0D-04,  7.0D-04/
```

```
DATA  WATR0
1      /7.0D-04/
```

```
DATA  WATR16,  EPIT0,   EPIT16,  DELTIM,  PCTSTA
1      /7.0D-04,  3.0D-03,  3.0D-03,  0.01,   0.05/
```

```
DATA  GLYVEL
1      /8.3D-03/
```

```
DATA  MAXPNT,  RESRAT,  MXTERM,  VC
1      /15,     15,     12,     40.0/
```

C*****)

DATA PI/3.1415926536D+00/

DATA EPSI/1.0D-06/

DATA IN, OUT, GLY, WAT, EPI, TIS, GLYCOF, EPITHL, DIA
1 /1, 2, 1, 2, 3, 4, 1, 2, 1/

DATA VOL, LEN
1 /2, 3/

DATA GLYTH, WATTH, EPITH, TOGI, TOEXH, TOTIS, STRD
1 /4, 5, 6, 1, 2, 3, 4/

C*****
C* (* MAIN PROGRAM *) *
C*****

C (* Initialize program variables *)

PNCDEF = 1243/(ATCDEF * PS)

DFCOFW = 2.27D-04/(0.285 * VC**1.048)**0.6

SYSCON = 0

DO 110 GEN = 0, 16

AIRCON(GEN, IN) = 0

AIRCON(GEN, OUT) = 0

AMASTR(GEN) = 0

WATCON(GEN) = 0

DO 120 POINT = 1, MAXPNT

LNGCON(GEN, GLYCOF, POINT) = 0

LNGCON(GEN, EPITHL, POINT) = 0

120 CONTINUE

FLUXTO(GEN, GLY) = 0

FLUXTO(GEN, WAT) = 0

FLUXTO(GEN, EPI) = 0

FLUXTO(GEN, TIS) = 0

110 CONTINUE

C (* Calculate morphological dimensions of lung *)

DO 70 GEN = 0, 3

LNGDIM(GEN, DIA) = TRDIA * EXP(-0.388 * GEN)

LNGDIM(GEN, LEN) = TRLEN * EXP(-0.920 * GEN)

LNGDIM(GEN, VOL) = PI/4 * (LNGDIM(GEN, DIA))**2 *
1 LNGDIM(GEN, LEN) * 2.0**GEN

70 CONTINUE

DO 80 GEN = 4, 16

LNGDIM(GEN, DIA) = PTRDIA * EXP(GEN *
1 (0.0062 * GEN - 0.293))

LNGDIM(GEN, LEN) = PTRLEN * EXP(-0.17 * GEN)

LNGDIM(GEN, VOL) = PI/4 * (LNGDIM(GEN, DIA))**2 *
1 LNGDIM(GEN, LEN) * 2.0**GEN

```

80    CONTINUE

C      (* Calculate layer thicknesses *)
      DO 90 GEN = 0,16
          LNGDIM(GEN, GLYTH) = GLYC0 - GEN *
1          (GLYC0 - GLYC16)/16
          LNGDIM(GEN, WATTH) = WATR0 - GEN *
1          (WATR0 - WATR16)/16
          LNGDIM(GEN, EPITH) = EPIT0 - GEN *
1          (EPIT0 - EPIT16)/16
90    CONTINUE

C      (* Initialize all entry times *)
      ENTIME(0) = 0
      CUMVOL = 0
      DO 100 GEN = 1,16
          CUMVOL = CUMVOL + LNGDIM(GEN - 1, VOL)
          ENTIME(GEN) = SQRT(450 * CUMVOL/(RESRAT**2 *
1          TIDVOL))
100   CONTINUE

      CI(0) = 0.0
      UPTAKE(0) = 0.0
      EPDSCR(0) = 0.0
      GIDSCR(0) = 0.0
      ALVCON = 0
      CURTIM = 0
      INHLTN = .TRUE.
      CMSTOG = 0
      CMSTOR = 0
      CMSTOE = 0
      CMSTOT = 0
      TMBRTH = 0
      BREATH = 1
      STELZD = .FALSE.
      WRITE(ASTRSK, '(2A40)')
1          '*****',
1          '*****'
      MASTOE = 0

C      (* Write program heading *)
      WRITE(6,510) ASTRSK, SPEC, ASTRSK, ASTRSK
      WRITE(6,511) EXPCON, DFDFW, PNCDEF,
1          MAXPNT, MAXTIM, TIDVOL, RESRAT, DELTIM,
1          MXTERM,
1          PCTSTA, TRDIA, TRLEN, ATCOEF, PS, VC
510   FORMAT(///1X, A80/1X, 8X, 'RESULTS OF LUNG TRANSPORT ',
1          'MODEL FOR ',
1          'INSOLUBLE SPECIES ',
1          A20/1X, A80///1X, A80//1X, 38X, 'CASE'///)
511   FORMAT(1X, 8X,
1          'EXP CONC = ', D8.2, 6X, 'DIFF COEF = ', D9.2, 1X,
1          'PARTITION COEF = ',

```

```

1      E8.2//1X,2X,'PROFILE POINTS = ',I7,2X,
1      'TOTAL EXP TIME = ',F7.2,
1      4X,'TIDAL VOLUME = ',D8.2//' RESPIRATORY ',
1      'RATE = ',I7,2X,
1      'TIME INCREMENT = ',F8.4,2X,
1      ' SERIES TERMS = ',I7//
1      ' STABILITY SIGNIF = ',F7.2,5X,
1      'TR DIAMETER = ',D7.2,7X,
1      'TR LENGTH = ',D7.2//
1      ' ACTIVITY COEF = ',F7.2,1X,
1      'SAT VAPOR PRESS = ',F7.2,1X,
1      'CRITICAL VOLUME = ',F7.2//

      ITERTN = 0

C      (* Begin exposure and cummulative calculation *)
270    CONTINUE

      ITERTN = ITERTN + 1

C      (* Begin single iteration *)
      DO 290 GEN = 0,16

C      (* If time to re-assign concentration in *)
      IF (CURTIM .GE. (ENTIME(GEN) +
1          RETNTN('HALF',LNGLDIM(GEN,VOL),
1          TMBRTH,ENTIME(GEN),TRDIA,TRLEN,PTRDIA,
1          PTRLEN,RESRAT,TIDVOL)))
1      THEN
1          IF (INHLTN)
1              THEN
1                  IF (GEN .NE. 0)
1                      THEN
1                          AIRCON(GEN,IN) = AIRCON(GEN - 1,OUT)
1                      ELSE
1                          AIRCON(GEN,IN) = EXPCON
1                      ENDIF
1                  ELSE
C                      (* NOT INHALATION *)
1                      IF (GEN .NE. 16)
1                          THEN
1                              AIRCON(GEN,IN) = AIRCON(GEN + 1,OUT)
1                          ELSE
1                              AIRCON(GEN,IN) = ALVCON
1                          ENDIF
1                      ENDIF
1                  ENDIF
1              ENDIF
1          ENDIF
1          (* if inhalation *)
1      ENDIF
1      (* if time to re-aassign *)

C      (* If time to re-assign conc out and entry time *)
1      IF (CURTIM .GE. (ENTIME(GEN) +
1          RETNTN('FULL',LNGLDIM(GEN,VOL),

```

```

1          TMBRTH, ENTIME (GEN), TRDIA, TRLEN, PTRDIA,
1          PTRLEN, RESRAT, TIDVOL))
1      THEN

C          (* Calculate concentration out *)
          AIRCON (GEN, OUT) = (AIRCON (GEN, IN) *
1              LNGDIM (GEN, VOL) -
1              AMASTR (GEN)) / LNGDIM (GEN, VOL)
          IF (AIRCON (GEN, OUT) .LT. 0.0)
1              THEN
                  AIRCON (GEN, OUT) = 0.0D+00
          ENDIF

C          (* Re-initialize cum mass transfered *)
          AMASTR (GEN) = 0

C          (* Re-assign entry time *)
          ENTIME (GEN) = CURTIM

      ENDIF

C      (* Create temporary array variable for param passing *)
      DO 310 I = 1, MAXPNT
          TLCGLY (I) = LNGCON (GEN, GLYCOP, I)
          TLCEPI (I) = LNGCON (GEN, EPITHL, I)
310      CONTINUE

C      (* Calculate next f(r) points for glyco and epi regions *)
      DO 300 POINT = 1, MAXPNT

          IF ((AIRCON (GEN, IN) .LT. EPSI) .AND. (WATCON (GEN)
1              .LT. EPSI))
1              THEN
                  NLNCON (GEN, GLYCOP, POINT) = 0
          ELSE
                  NLNCON (GEN, GLYCOP, POINT) = PNCOEF *
1                      AIRCON (GEN, IN) +
1                      (WATCON (GEN) - PNCOEF * AIRCON (GEN, IN)) *
1                      POINT / (MAXPNT + 1) +
1                      TRMIII (POINT, AIRCON (GEN, IN) *
1                      PNCOEF, WATCON (GEN), LNGDIM (GEN, GLYTH),
1                      MAXPNT,
1                      MXTERM, DFCOFW, DELTIM, PI) +
1                      TERMIV (POINT, TLCGLY, LNGDIM (GEN, GLYTH),
1                      MAXPNT, MXTERM, DFCOFW, DELTIM, PI)
          ENDIF

          IF ((WATCON (GEN) .LT. EPSI) .AND. (SYSCON .LT.
1              EPSI))
1              THEN
                  NLNCON (GEN, EPITHL, POINT) = 0
          ELSE
                  NLNCON (GEN, EPITHL, POINT) = WATCON (GEN) +

```

```

1          (SYSCON - WATCON(GEN)) * POINT/
1          (MAXPNT + 1) +
1          TRMIII(POINT, WATCON(GEN), SYSCON,
1          LNGDIM(GEN, EPITH), MAXPNT,
1          MXTERM, DFPCOFW, DELTIM, PI) +
1          TERMIV(POINT, TLCEPI,
1          LNGDIM(GEN, EPITH), MAXPNT,
1          MXTERM, DFPCOFW, DELTIM, PI)
1          ENDIF

```

```

300      CONTINUE

```

```

C      (* Calculate fluxes between regions *)
      IF ((AIRCON(GEN, IN) .LT. EPSI) .AND. (WATCON(GEN)
1      .LT. EPSI))
1      THEN
1      NFLXTO(GEN, GLY) = 0
1      NFLXTO(GEN, WAT) = 0
1      ELSE
1      NFLXTO(GEN, GLY) = -DFPCOFW * DERVTV('LOWER',
1      TLCGLY, AIRCON(GEN, IN) * PNCOEF,
1      WATCON(GEN), LNGDIM(GEN, GLYTH),
1      MAXPNT, MXTERM, DFPCOFW,
1      DELTIM, PI)
1      NFLXTO(GEN, WAT) = -DFPCOFW * DERVTV('UPPER',
1      TLCGLY, AIRCON(GEN, IN) * PNCOEF,
1      WATCON(GEN), LNGDIM(GEN, GLYTH),
1      MAXPNT, MXTERM, DFPCOFW,
1      DELTIM, PI)
1      ENDIF

```

```

      IF ((WATCON(GEN) .LT. EPSI) .AND. (SYSCON .LT.
1      EPSI))
1      THEN
1      NFLXTO(GEN, EPI) = 0
1      NFLXTO(GEN, TIS) = 0
1      ELSE
1      NFLXTO(GEN, EPI) = -DFPCOFW * DERVTV('LOWER',
1      TLCEPI, WATCON(GEN), SYSCON,
1      LNGDIM(GEN, EPITH), MAXPNT,
1      MXTERM, DFPCOFW, DELTIM, PI)
1      NFLXTO(GEN, TIS) = -DFPCOFW * DERVTV('UPPER',
1      TLCEPI, WATCON(GEN), SYSCON,
1      LNGDIM(GEN, EPITH), MAXPNT,
1      MXTERM, DFPCOFW, DELTIM, PI)
1      ENDIF

```

```

C      (* Calculate mass transfered between regions *)
      MASSTO(GEN, GLY) = (NFLXTO(GEN, GLY) +
1      FLUXTO(GEN, GLY))/2 *
1      DELTIM * PI * LNGDIM(GEN, LEN) * LNGDIM(GEN, DIA)

      MASSTO(GEN, WAT) = (NFLXTO(GEN, WAT) +

```

```

1      FLUXTO(GEN,WAT))/2 *
1      DELTIM * PI * LNGDIM(GEN,LEN) * LNGDIM(GEN,DIA)

      MASSTO(GEN,EPI) = (NFLXTO(GEN,EPI) +
1      FLUXTO(GEN,EPI))/2 *
1      DELTIM * PI * LNGDIM(GEN,LEN) * LNGDIM(GEN,DIA)

      MASSTO(GEN,TIS) = (NFLXTO(GEN,TIS) +
1      FLUXTO(GEN,TIS))/2 *
1      DELTIM * PI * LNGDIM(GEN,LEN) * LNGDIM(GEN,DIA)

290    CONTINUE
C      (* end GEN loop *)

C      (* Update concentration and cummulative values *)
C      (* Create temp array variable for param passing *)
      DO 320 I = 1,MAXPNT
          TLCGLY(I) = LNGCON(0, GLYCOP, I)
          NTCGLY(I) = NLNCON(0, GLYCOP, I)
320    CONTINUE
      MASTOG = (RAVG(TLCGLY,MAXPNT,AIRCON(0,IN) * PNCOEF,
1          WATCON(0)) + RAVG(NTCGLY,MAXPNT,
1          AIRCON(0,IN) * PNCOEF,(WATCON(0) * PI *
1          LNGDIM(0,DIA) * LNGDIM(0,LEN) *
1          LNGDIM(0,WATTH) +
1          MASSTO(0,WAT) - MASSTO(0,EPI))/(PI *
1          LNGDIM(0,DIA) *
1          LNGDIM(0,LEN) * LNGDIM(0,WATTH)))/2 * PI *
1          TRDIA *
1          LNGDIM(0, GLYTH) * GLYVEL * DELTIM

      CMSTOG = CMSTOG + MASTOG

      IF (INHLTN)
1      THEN
          CMSTOR = CMSTOR + AIRCON(16,OUT) * DELTIM *
1          FLOW(CURTIM,TMBRTH,RESRAT,TIDVOL)
      ELSE
          MASTOE = AIRCON(0,OUT) * DELTIM *
1          FLOW(CURTIM,TMBRTH,
1          RESRAT,TIDVOL)
          CMSTOE = CMSTOE + MASTOE
      ENDIF

      DO 330 GEN = 0,16

          CMSTOT = CMSTOT + MASSTO(GEN,TIS) * 2.0**GEN

          AMASTR(GEN) = AMASTR(GEN) + MASSTO(GEN, GLY) *
1          2.0**GEN

          WATCON(GEN) = (WATCON(GEN) * PI * LNGDIM(GEN,DIA) *
1          LNGDIM(GEN,LEN) * LNGDIM(GEN,WATTH) +
1          MASSTO(GEN,WAT) - MASSTO(GEN,EPI))/(PI

```

```

1          * LNGDIM(GEN, DIA) * LNGDIM(GEN, LEN) *
1          LNGDIM(GEN, WATTH))
1      IF (WATCON(GEN) .LT. 0.0)
1      THEN
1          WATCON(GEN) = 0.0D+00
1      ENDIF

1      DO 340 POINT = 1, MAXPNT
1          LNGCON(GEN, GLYCOP, POINT) =
1              NLNCON(GEN, GLYCOP, POINT)
1          LNGCON(GEN, EPITHL, POINT) =
1              NLNCON(GEN, EPITHL, POINT)
340      CONTINUE

1          FLUXTO(GEN, GLY) = NFLXTO(GEN, GLY)
1          FLUXTO(GEN, WAT) = NFLXTO(GEN, WAT)
1          FLUXTO(GEN, EPI) = NFLXTO(GEN, EPI)
1          FLUXTO(GEN, TIS) = NFLXTO(GEN, TIS)

330      CONTINUE
C          (* end GEN loop *)

C          (* Increment time *)
1          CURTIM = CURTIM + DELTIM

C          (* If end of inhalation or exhalation *)
1          IF (CURTIM .GE. (TMBRTH + 30/RESRAT))
1      THEN

1          TMBRTH = CURTIM

1          DO 370 GEN = 0, 16
1              ENTIME(GEN) = CURTIM
370          CONTINUE

1          IF (INHLTN)
1      THEN
1          ALVCON = CMSTOR/TIDVOL * (1/(1 + 1.25 *
1              PNCDEF))
1          SYSCON = PNCDEF * ALVCON * (1 - EXP(-0.0139 *
1              CURTIM))
1          CI(BREATH) = CMSTOR/TIDVOL
1          CMSTOR = 0.0
1          INHLTN = .FALSE.
1          CALL PRCON(ITERTN, CURTIM, ASTRSK,
1              BREATH, INHLTN, TMBRTH,
1              SYSCON, LNGCON, WATCON, AIRCON, GLYCOP,
1              EPITHL,
1              IN, ALVCON, CMSTOR, CMSTOE, CMSTOT, CMSTOG)
1          ELSE
C          (* exhalation *)

```

```

1          UPTAKE(BREATH) = (EXPCON * TIDVOL - CMSTOE) *
          RESRAT/60
          CMSTOE = 0.0
          GIDSCR(BREATH) = CMSTOG * RESRAT/60
          CMSTOG = 0.0
          EPDSCR(BREATH) = CMSTOT * RESRAT/60
          CMSTOT = 0.0

          INHLTN = .TRUE.

          CALL CHKCND(CI, UPTAKE, STBLZD, EPDSCR, GIDSCR,
1          ASTRSK, BREATH, CURTIM, PCTSTA, EPSI)

          BREATH = BREATH + 1

          ENDIF
C          (* if inhalation else exhalation *)

          ENDIF
C          (* If end inhalation or exhalation *)

C          (* end iteration loop *)
          IF ((CURTIM .LT. MAXTIM) .AND. (.NOT. STBLZD)) THEN
          GO TO 270
          ENDIF

C          (* Write program heading *)
          WRITE(6,512) ASTRSK, SPEC, ASTRSK, ASTRSK
          WRITE(6,513) EXPCON, DFPCOFW, PNCDEF,
1          MAXPNT, MAXTIM, TIDVOL, RESRAT, DELTIM,
1          MXTERM,
1          PCTSTA, TRDIA, TRLEN, ATCOEF, PS, VC
512  FORMAT(///1X,A80/1X,8X,'RESULTS OF LUNG TRANSPORT ',
1          'MODEL FOR INSOLUBLE SPECIES ',
1          A20/1X,A80///1X,A80//1X,38X,'CASE'///)
513  FORMAT(1X,8X,
1          'EXP CONC = ',D8.2,6X,'DIFF COEF = ',D9.2,1X,
1          'PARTITION COEF = ',
1          E8.2//1X,2X,'PROFILE POINTS = ',I7,2X,
1          'TOTAL EXP TIME = ',F7.2,
1          4X,'TIDAL VOLUME = ',D8.2//
1          'RESPIRATORY RATE = ',I7,2X,
1          'TIME INCREMENT = ',F8.4,2X,
1          'SERIES TERMS = ',I7//
1          'STABILITY SIGNIF = ',F7.2,5X,
1          'TR DIAMETER = ',D7.2,7X,
1          'TR LENGTH = ',D7.2//
1          'ACTIVITY COEF = ',F7.2,1X,
1          'SAT VAPOR PRESS = ',F7.2,1X,
1          'CRITICAL VOLUME = ',F7.2/)

          CALL PRTCN(ITERTN, CURTIM, ASTRSK, BREATH, INHLTN,
1          TMBRTH,

```

```

1          SYSCON, LNGCON, WATCON, AIRCON,
1          GLYCON, EPITHL,
1          IN, ALVCON, CMSTOR, CMSTOE, CMSTOT,
1          CMSTOG)

C      (* List stabilization parameters *)
        WRITE(6,389) ASTRSK
389     FORMAT(1X,A80/1X,'BREATH',9X,'CI',9X,'UPTAKE RATE',5X,
1         'EPI DSCH RATE',3X,'GI DSCH RATE'//)
        DO 380 I = 0, BREATH-1
            WRITE(6,390) I, CI(I), UPTAKE(I), EPDSCR(I),
1             GIDSCR(I)
390     FORMAT(3X,I3,5X,D13.7,3X,D13.7,3X,D13.7,3X,D13.7//)
380     CONTINUE

C      (* Write condition of normal job termination *)
        IF (CURTIM .GE. MAXTIM)
1       THEN
            WRITE(6,350) CURTIM
350     FORMAT(//////////1X,'TIME = ',F8.4,
1         ' ***** NORMAL TERMINATION'//)
        ELSE
            IDUMMY = BREATH - 1
            WRITE(6,241) ASTRSK, IDUMMY, CURTIM, CI(IDUMMY),
1             UPTAKE(IDUMMY), EPDSCR(IDUMMY),
1             GIDSCR(IDUMMY)
241    FORMAT(////1X,A80//1X,30X,'STABILITY PARAMETERS' /1X,
1         31X,'END OF ',I4,
1         ' BREATHS' /1X,28X,
1         ' EXPOSURE TIME = ',F8.4//1X,24X,
1         ' CNC DISCHARGING TO ALV = ',D11.4//1X,16X,
1         '          UPTAKE PER SECOND =
1         ',D11.4//1X,20X,
1         ' DISCHARGE RATE TO TISSUE = ',D11.4//1X,26X,
1         ' DISCHARGE RATE TO GI = ',D11.4//)
            WRITE(6,360) CURTIM, BREATH
360    FORMAT(//////////1X,'CONDITIONS STABLE AT ',F8.4,
1         ' (BREATH ',I4,')',
1         ' ***** NORMAL TERMINATION'//)
        ENDIF

        STOP
        END

C      (* MAIN PROGRAM *)

```

APPENDIX D

TABULATED MODEL RESULTS

The following pages list model results for 109 hypothetical gases or vapors (OBS). The columns are defined as follows:

PN = Partition coefficient (as defined in chapter 4)

DFW = Diffusion coefficient in water (cm²/sec)

BRTN = Number of breaths required to reach stable conditions

FRUPTK = Fraction of inhaled mass taken up (1 - fract exhaled)

FREPI = Fraction of inhaled mass taken up through epithelial absorption in the conductive zone

FRALV = Fraction of inhaled mass taken up by alveolar blood/gas exchange

FRGI = Fraction of inhaled mass taken up by muco-ciliary discharge to the GI tract

CHK = (1 - FRUPTK) + FREPI + FRALV + FRGI
(ideally equal to 1.0)

OBS	PN	DFW	BRTH	FRUPTK	FREPI	FRALV	FRGI	CHK
1	0.617	6.26E-6	13	0.39	0.00	0.40	1.01E-7	1.00
2	0.617	1.03E-5	13	0.40	0.01	0.40	1.03E-7	1.00
3	0.617	1.72E-5	11	0.40	0.02	0.39	1.03E-7	1.01
4	0.617	2.85E-5	10	0.42	0.04	0.38	1.03E-7	1.00
5	0.617	4.74E-5	9	0.44	0.07	0.38	1.01E-7	1.00
6	0.885	7.16E-6	15	0.47	0.00	0.46	1.39E-7	0.99
7	0.885	8.49E-6	12	0.47	0.01	0.45	1.39E-7	0.99
8	0.885	1.07E-5	11	0.48	0.02	0.45	1.39E-7	0.99
9	0.885	1.57E-5	9	0.48	0.03	0.47	1.39E-7	1.01
10	1.080	7.16E-6	12	0.51	0.01	0.49	1.62E-7	0.99
11	1.080	8.49E-6	11	0.51	0.01	0.49	1.64E-7	0.99
12	1.080	1.07E-5	10	0.52	0.02	0.49	1.64E-7	0.99
13	1.080	1.57E-5	9	0.53	0.04	0.50	1.64E-7	1.01
14	1.100	7.16E-6	12	0.52	0.01	0.49	1.65E-7	0.98
15	1.100	8.49E-6	11	0.52	0.01	0.49	1.67E-7	0.98
16	1.100	1.07E-5	9	0.52	0.03	0.51	1.67E-7	1.01
17	1.100	1.57E-5	9	0.53	0.05	0.50	1.67E-7	1.01
18	1.310	6.26E-6	12	0.55	0.01	0.53	1.96E-7	0.99
19	1.310	1.72E-5	8	0.58	0.07	0.50	1.96E-7	0.99
20	1.310	4.74E-5	7	0.66	0.20	0.45	1.78E-7	0.99
21	1.340	7.16E-6	10	0.56	0.01	0.53	1.96E-7	0.98
22	1.340	8.49E-6	10	0.56	0.02	0.52	1.96E-7	0.99
23	1.340	1.07E-5	9	0.56	0.04	0.52	1.96E-7	0.99
24	1.340	1.57E-5	8	0.58	0.06	0.53	1.96E-7	1.01
25	1.400	7.16E-6	10	0.56	0.02	0.55	1.96E-7	1.00
26	1.400	8.49E-6	9	0.57	0.03	0.54	1.95E-7	1.00
27	1.400	1.07E-5	8	0.57	0.04	0.54	1.96E-7	1.00
28	1.400	1.57E-5	8	0.59	0.07	0.52	1.96E-7	1.00
29	1.490	7.16E-6	10	0.57	0.02	0.54	2.13E-7	0.99
30	1.490	8.49E-6	9	0.58	0.03	0.54	2.13E-7	0.99
31	1.490	1.07E-5	8	0.59	0.04	0.53	2.13E-7	0.99
32	1.490	1.57E-5	8	0.60	0.07	0.51	2.13E-7	0.99
33	1.560	6.26E-6	11	0.58	0.01	0.54	2.13E-7	0.97
34	1.560	1.72E-5	7	0.62	0.09	0.53	2.13E-7	1.00
35	1.56	4.74E-5	6	0.71	0.25	0.44	2.13E-7	0.98
36	1.75	7.16E-6	9	0.60	0.03	0.56	2.49E-7	0.98
37	1.75	8.49E-6	8	0.61	0.04	0.56	2.49E-7	0.99
38	1.75	1.07E-5	8	0.62	0.05	0.55	2.49E-7	0.99
39	1.75	1.57E-5	7	0.64	0.09	0.54	2.49E-7	0.99
40	1.81	7.16E-6	9	0.61	0.03	0.57	2.49E-7	0.99
41	1.81	8.49E-6	8	0.62	0.04	0.56	2.49E-7	0.99
42	1.81	1.07E-5	7	0.62	0.06	0.55	2.49E-7	0.99
43	1.81	1.57E-5	7	0.64	0.09	0.54	2.49E-7	0.99
44	2.01	7.16E-6	8	0.63	0.03	0.58	2.67E-7	0.98
45	2.01	8.49E-6	8	0.63	0.05	0.57	2.67E-7	0.98
46	2.01	1.07E-5	7	0.64	0.07	0.56	2.67E-7	0.99
47	2.01	1.57E-5	6	0.66	0.11	0.54	2.67E-7	0.99
48	2.25	7.16E-6	8	0.65	0.04	0.58	3.02E-7	0.98
49	2.25	8.49E-6	7	0.65	0.06	0.58	3.02E-7	0.98
50	2.25	1.07E-5	7	0.66	0.08	0.57	3.02E-7	0.99
51	2.25	1.57E-5	6	0.67	0.13	0.55	3.02E-7	0.99
52	2.35	7.16E-6	8	0.65	0.04	0.59	3.20E-7	0.98

OBS	PN	DFW	BRTH	FRUPTK	FREPI	FRALV	FRGI	CHK
53	2.35	8.49E-6	7	0.66	0.06	0.58	3.20E-7	0.98
54	2.35	1.07E-5	7	0.67	0.08	0.57	3.20E-7	0.98
55	2.35	1.57E-5	6	0.69	0.13	0.55	3.02E-7	0.99
56	2.51	7.16E-6	7	0.66	0.05	0.59	3.38E-7	0.98
57	2.51	8.49E-6	7	0.67	0.07	0.58	3.38E-7	0.98
58	2.51	1.07E-5	6	0.68	0.09	0.57	3.38E-7	0.98
59	2.51	1.57E-5	6	0.71	0.14	0.55	3.20E-7	0.98
60	2.74	7.16E-6	7	0.68	0.06	0.59	3.56E-7	0.97
61	2.74	8.49E-6	6	0.69	0.08	0.59	3.56E-7	0.98
62	2.74	1.07E-5	6	0.70	0.10	0.57	3.56E-7	0.98
63	2.74	1.57E-5	5	0.72	0.16	0.54	3.56E-7	0.98
64	2.77	6.26E-6	7	0.67	0.05	0.60	3.56E-7	0.97
65	2.77	1.72E-5	5	0.73	0.18	0.53	3.56E-7	0.98
66	2.77	6.26E-6	3	0.84	0.45	0.36	3.20E-7	0.97
67	3.30	6.26E-6	7	0.70	0.06	0.60	4.09E-7	0.96
68	3.30	1.72E-5	4	0.76	0.22	0.53	4.09E-7	0.98
69	3.30	4.74E-5	3	0.87	0.51	0.33	3.73E-7	0.97
70	3.37	7.16E-6	6	0.71	0.08	0.59	4.27E-7	0.96
71	3.37	8.49E-6	6	0.71	0.10	0.58	4.27E-7	0.96
72	3.37	1.07E-5	5	0.73	0.13	0.57	4.27E-7	0.97
73	3.37	1.57E-5	5	0.75	0.20	0.53	4.27E-7	0.98
74	3.43	6.26E-6	7	0.70	0.06	0.60	4.27E-7	0.96
75	3.43	1.03E-5	5	0.73	0.13	0.57	4.27E-7	0.97
76	3.43	1.72E-5	4	0.77	0.23	0.52	4.27E-7	0.98
77	3.43	2.85E-5	3	0.82	0.36	0.43	4.09E-7	0.97
78	3.43	4.74E-5	3	0.87	0.52	0.32	3.91E-7	0.97
79	3.57	7.16E-6	6	0.71	0.08	0.59	4.45E-7	0.97
80	3.57	8.49E-6	5	0.72	0.11	0.58	4.45E-7	0.97
81	3.57	1.07E-5	5	0.74	0.14	0.56	4.45E-7	0.97
82	3.57	1.57E-5	4	0.77	0.22	0.52	4.45E-7	0.97
83	3.92	6.26E-6	6	0.72	0.08	0.59	4.80E-7	0.95
84	3.92	1.72E-5	4	0.79	0.26	0.50	4.80E-7	0.97
85	3.92	4.47E-5	3	0.88	0.56	0.29	4.27E-7	0.96
86	4.11	6.26E-6	6	0.72	0.08	0.59	4.98E-7	0.95
87	4.11	1.03E-5	5	0.75	0.16	0.56	4.98E-7	0.96
88	4.11	1.72E-5	4	0.79	0.27	0.50	4.98E-7	0.97
89	4.11	2.85E-5	3	0.85	0.41	0.40	4.62E-7	0.97
90	4.11	4.47E-5	3	0.89	0.58	0.27	4.45E-7	0.96
91	5.12	7.16E-6	5	0.75	0.13	0.57	6.22E-7	0.94
92	5.12	8.49E-6	4	0.76	0.16	0.54	6.22E-7	0.94
93	5.12	1.07E-5	4	0.78	0.21	0.53	6.05E-7	0.95
94	5.12	1.57E-5	3	0.82	0.30	0.47	6.05E-7	0.96
95	5.82	6.26E-6	4	0.76	0.13	0.56	6.93E-7	0.93
96	5.82	1.72E-5	3	0.84	0.36	0.43	6.58E-7	0.95
97	5.82	4.47E-5	3	0.91	0.67	0.18	6.22E-7	0.93
98	6.99	6.26E-6	4	0.77	0.15	0.53	8.17E-7	0.91
99	6.99	1.72E-5	3	0.86	0.41	0.39	7.82E-7	0.94
100	6.99	4.74E-5	3	0.92	0.71	0.13	7.29E-7	0.91
101	8.30	6.26E-6	3	0.78	0.18	0.50	9.60E-7	0.90
102	8.30	1.72E-5	3	0.87	0.46	0.35	9.25E-7	0.93
103	8.3	4.74E-5	3	0.93	0.73	0.09	8.71E-7	0.89
104	9.79	6.26E-6	3	0.79	0.21	0.47	1.12E-6	0.88

OBS	PN	DFW	BPTH	FRUPTK	FREPI	FRALV	FRGI	CHK
105	9.79	1.72E-5	3	0.88	0.51	0.30	1.06E-6	0.92
106	9.79	4.74E-5	3	0.94	0.74	0.07	1.01E-6	0.87
107	12.30	6.26E-6	3	0.80	0.25	0.41	1.38E-6	0.86
108	12.30	1.72E-5	3	0.89	0.57	0.24	1.33E-6	0.92
109	12.30	4.74E-5	3	0.95	0.81	0.05	1.26E-6	0.91

APPENDIX E

BRONCHIAL ABSORPTION UPTAKE
(MODEL RESULTS vs PREDICTED)

The following pages list model results for 109 hypothetical gases or vapors (OBS) with corresponding predicted values from an empirically derived expression.

PN = Partition coefficient (as defined in chapter 4)

DFW = Diffusion coefficient in water (cm²/sec)

FREPI = Fraction of inhaled mass taken up through epithelial absorption in the conductive zone (model results)

PFREPI = Predicted FREPI
= $1 - \exp(-3961 \text{ DFW PN})$

PRESID = Predicted residual

OBS	PN	DFW	FREPI	PFREPI	PRESID
1	0.617	6.26E-6	0.00	0.015	-0.01956
2	0.617	1.03E-5	0.01	0.025	-0.01975
3	0.617	1.72E-5	0.02	0.041	-0.02200
4	0.617	2.85E-5	0.04	0.067	-0.02731
5	0.617	4.74E-5	0.07	0.109	-0.03550
6	0.885	7.16E-6	0.00	0.025	-0.02228
7	0.885	8.49E-6	0.01	0.029	-0.02157
8	0.885	1.07E-5	0.02	0.037	-0.02111
9	0.885	1.57E-5	0.03	0.054	-0.02064
10	1.080	7.16E-6	0.01	0.030	-0.02295
11	1.080	8.49E-6	0.01	0.036	-0.02210
12	1.080	1.07E-5	0.02	0.045	-0.02102
13	1.080	1.57E-5	0.04	0.065	-0.02047
14	1.100	7.16E-6	0.01	0.031	-0.02286
15	1.100	8.49E-6	0.01	0.036	-0.02193
16	1.100	1.07E-5	0.03	0.046	-0.01986
17	1.100	1.57E-5	0.05	0.066	-0.01996
18	1.310	6.26E-6	0.01	0.032	-0.02438
19	1.310	1.72E-5	0.07	0.085	-0.01740
20	1.310	4.74E-5	0.20	0.218	-0.01625
21	1.340	7.16E-6	0.01	0.037	-0.02266
22	1.340	8.49E-6	0.02	0.044	-0.02169
23	1.340	1.07E-5	0.04	0.055	-0.01959
24	1.340	1.57E-5	0.06	0.080	-0.01704
25	1.400	7.16E-6	0.02	0.039	-0.02280
26	1.400	8.49E-6	0.03	0.046	-0.02097
27	1.400	1.07E-5	0.04	0.058	-0.01819
28	1.400	1.57E-5	0.07	0.083	-0.01681
29	1.490	7.16E-6	0.02	0.041	-0.02308
30	1.490	8.49E-6	0.03	0.049	-0.02115
31	1.490	1.07E-5	0.04	0.061	-0.01824
32	1.490	1.57E-5	0.07	0.089	-0.01668
33	1.560	6.26E-6	0.01	0.038	-0.02457
34	1.560	1.72E-5	0.09	0.100	-0.01267
35	1.56	4.74E-5	0.25	0.254	-0.00315
36	1.75	7.16E-6	0.03	0.048	-0.02219
37	1.75	8.49E-6	0.04	0.057	-0.01942
38	1.75	1.07E-5	0.05	0.071	-0.01708
39	1.75	1.57E-5	0.09	0.103	-0.01186
40	1.81	7.16E-6	0.03	0.050	-0.02223
41	1.81	8.49E-6	0.04	0.059	-0.01938
42	1.81	1.07E-5	0.06	0.074	-0.01693
43	1.81	1.57E-5	0.09	0.106	-0.01156
44	2.01	7.16E-6	0.03	0.055	-0.02088
45	2.01	8.49E-6	0.05	0.065	-0.01888
46	2.01	1.07E-5	0.07	0.082	-0.01395
47	2.01	1.57E-5	0.11	0.117	-0.00617
48	2.25	7.16E-6	0.04	0.062	-0.02042
49	2.25	8.49E-6	0.06	0.073	-0.01629
50	2.25	1.07E-5	0.08	0.091	-0.01263
51	2.25	1.57E-5	0.13	0.131	-0.00410
52	2.35	7.16E-6	0.04	0.064	-0.02022

OBS	PN	DFW	FREPI	PFREPI	PRESID
53	2.35	8.49E-6	0.06	0.076	-0.01596
54	2.35	1.07E-5	0.08	0.095	-0.01210
55	2.35	1.57E-5	0.13	0.136	-0.00328
56	2.51	7.16E-6	0.05	0.069	-0.01844
57	2.51	8.49E-6	0.07	0.081	-0.01569
58	2.51	1.07E-5	0.09	0.101	-0.00863
59	2.51	1.57E-5	0.14	0.145	-0.00252
60	2.74	7.16E-6	0.06	0.075	-0.01783
61	2.74	8.49E-6	0.08	0.088	-0.01217
62	2.74	1.07E-5	0.10	0.110	-0.00731
63	2.74	1.57E-5	0.16	0.157	0.00473
64	2.77	6.26E-6	0.05	0.066	-0.02027
65	2.77	1.72E-5	0.18	0.172	0.00700
66	2.77	6.26E-6	0.45	0.406	0.04842
67	3.30	6.26E-6	0.06	0.079	-0.01946
68	3.30	1.72E-5	0.22	0.201	0.01878
69	3.30	4.74E-5	0.51	0.462	0.04606
70	3.37	7.16E-6	0.08	0.091	-0.01412
71	3.37	8.49E-6	0.10	0.107	-0.01027
72	3.37	1.07E-5	0.13	0.133	-0.00033
73	3.37	1.57E-5	0.20	0.189	0.00892
74	3.43	6.26E-6	0.06	0.082	-0.01935
75	3.43	1.03E-5	0.13	0.131	-0.00242
76	3.43	1.72E-5	0.23	0.208	0.01933
77	3.43	2.85E-5	0.36	0.321	0.04289
78	3.43	4.74E-5	0.52	0.475	0.04480
79	3.57	7.16E-6	0.08	0.096	-0.01375
80	3.57	8.49E-6	0.11	0.113	-0.00603
81	3.57	1.07E-5	0.14	0.140	0.00046
82	3.57	1.57E-5	0.22	0.199	0.01718
83	3.92	6.26E-6	0.08	0.093	-0.01645
84	3.92	1.72E-5	0.26	0.234	0.02168
85	3.92	4.47E-5	0.56	0.521	0.03982
86	4.11	6.26E-6	0.08	0.097	-0.01607
87	4.11	1.03E-5	0.16	0.154	0.00169
88	4.11	1.72E-5	0.27	0.244	0.02275
89	4.11	2.85E-5	0.41	0.371	0.04311
90	4.11	4.47E-5	0.58	0.538	0.03781
91	5.12	7.16E-6	0.13	0.135	-0.00795
92	5.12	8.49E-6	0.16	0.158	0.00241
93	5.12	1.07E-5	0.21	0.195	0.01089
94	5.12	1.57E-5	0.30	0.273	0.03058
95	5.82	6.26E-6	0.13	0.134	-0.00703
96	5.82	1.72E-5	0.36	0.327	0.03343
97	5.82	4.47E-5	0.67	0.665	0.00558
98	6.99	6.26E-6	0.15	0.159	-0.00711
99	6.99	1.72E-5	0.41	0.379	0.03103
100	6.99	4.74E-5	0.71	0.731	-0.02285
101	8.30	6.26E-6	0.18	0.186	-0.00235
102	8.30	1.72E-5	0.46	0.432	0.02625
103	8.3	4.74E-5	0.73	0.789	-0.05781
104	9.79	6.26E-6	0.21	0.216	-0.00467

OBS	PN	DFW	FREPI	PFREPI	PRESID
105	9.79	1.72E-5	0.51	0.487	0.01878
106	9.79	4.74E-5	0.74	0.841	-0.09294
107	12.30	6.26E-6	0.25	0.263	-0.01025
108	12.30	1.72E-5	0.57	0.567	0.00293
109	12.30	4.74E-5	0.81	0.901	-0.09547

APPENDIX F

ALVEOLAR UPTAKE
(MODEL RESULTS vs PREDICTED)

The following pages list model results for 109 hypothetical gases or vapors (OBS) with corresponding predicted values from an empirically derived expression.

PN = Partition coefficient (as defined in chapter 4)

DFW = Diffusion coefficient in water (cm /sec)²

FRALV = Fraction of inhaled gas or vapor taken up by alveolar blood/gas exchange

PFRALV = Predicted FRALV

$$= \exp(-6282 \text{ DFW PN}) - 1 / (1 + 348.5 \text{ DFW}^{0.5} \text{ PN})$$

PRESID = Predicted residual

OBS	PN	DFW	FRALV	PFRALV	PRESID
1	0.617	6.26E-6	0.400	0.326	0.07418
2	0.617	1.03E-5	0.397	0.369	0.02816
3	0.617	1.72E-5	0.392	0.407	-0.01489
4	0.617	2.85E-5	0.376	0.430	-0.05384
5	0.617	4.74E-5	0.376	0.429	-0.05299
6	0.885	7.16E-6	0.456	0.413	0.04289
7	0.885	8.49E-6	0.453	0.427	0.02613
8	0.885	1.07E-5	0.451	0.444	0.00622
9	0.885	1.57E-5	0.467	0.466	0.00029
10	1.080	7.16E-6	0.493	0.454	0.03898
11	1.080	8.49E-6	0.491	0.467	0.02359
12	1.080	1.07E-5	0.485	0.482	0.00356
13	1.080	1.57E-5	0.501	0.498	0.00378
14	1.100	7.16E-6	0.491	0.458	0.03259
15	1.100	8.49E-6	0.488	0.471	0.01736
16	1.100	1.07E-5	0.509	0.485	0.02428
17	1.100	1.57E-5	0.499	0.500	-0.00152
18	1.310	6.26E-6	0.531	0.483	0.04769
19	1.310	1.72E-5	0.499	0.522	-0.02372
20	1.310	4.74E-5	0.445	0.436	0.00971
21	1.340	7.16E-6	0.525	0.497	0.02836
22	1.340	8.49E-6	0.523	0.507	0.01525
23	1.340	1.07E-5	0.517	0.518	-0.00089
24	1.340	1.57E-5	0.528	0.525	0.00264
25	1.400	7.16E-6	0.549	0.505	0.04411
26	1.400	8.49E-6	0.544	0.515	0.02890
27	1.400	1.07E-5	0.539	0.525	0.01370
28	1.400	1.57E-5	0.523	0.530	-0.00743
29	1.490	7.16E-6	0.544	0.517	0.02734
30	1.490	8.49E-6	0.539	0.526	0.01300
31	1.490	1.07E-5	0.531	0.534	-0.00345
32	1.490	1.57E-5	0.515	0.536	-0.02159
33	1.560	6.26E-6	0.541	0.517	0.02453
34	1.560	1.72E-5	0.525	0.538	-0.01229
35	1.56	4.74E-5	0.440	0.418	0.02242
36	1.75	7.16E-6	0.563	0.544	0.01832
37	1.75	8.49E-6	0.560	0.551	0.00922
38	1.75	1.07E-5	0.555	0.555	-0.00045
39	1.75	1.57E-5	0.539	0.549	-0.01010
40	1.81	7.16E-6	0.568	0.550	0.01823
41	1.81	8.49E-6	0.563	0.556	0.00707
42	1.81	1.07E-5	0.555	0.559	-0.00433
43	1.81	1.57E-5	0.541	0.551	-0.00940
44	2.01	7.16E-6	0.579	0.566	0.01302
45	2.01	8.49E-6	0.571	0.570	0.00117
46	2.01	1.07E-5	0.563	0.570	-0.00712
47	2.01	1.57E-5	0.544	0.555	-0.01130
48	2.25	7.16E-6	0.584	0.581	0.00303
49	2.25	8.49E-6	0.579	0.582	-0.00380
50	2.25	1.07E-5	0.571	0.579	-0.00845
51	2.25	1.57E-5	0.549	0.557	-0.00815
52	2.35	7.16E-6	0.587	0.586	0.00032

OBS	PN	DFW	FRALV	PFRALV	PRESID
53	2.35	8.49E-6	0.581	0.587	-0.00555
54	2.35	1.07E-5	0.571	0.582	-0.01139
55	2.35	1.57E-5	0.549	0.558	-0.00821
56	2.51	7.16E-6	0.589	0.594	-0.00455
57	2.51	8.49E-6	0.584	0.593	-0.00891
58	2.51	1.07E-5	0.571	0.586	-0.01509
59	2.51	1.57E-5	0.547	0.557	-0.01011
60	2.74	7.16E-6	0.592	0.603	-0.01075
61	2.74	8.49E-6	0.587	0.600	-0.01297
62	2.74	1.07E-5	0.573	0.589	-0.01593
63	2.74	1.57E-5	0.544	0.554	-0.01013
64	2.77	6.26E-6	0.597	0.604	-0.00665
65	2.77	1.72E-5	0.533	0.541	-0.00813
66	2.77	6.26E-6	0.360	0.308	0.05250
67	3.30	6.26E-6	0.600	0.620	-0.02038
68	3.30	1.72E-5	0.520	0.527	-0.00673
69	3.30	4.74E-5	0.325	0.262	0.06317
70	3.37	7.16E-6	0.592	0.618	-0.02594
71	3.37	8.49E-6	0.581	0.609	-0.02800
72	3.37	1.07E-5	0.565	0.591	-0.02541
73	3.37	1.57E-5	0.533	0.540	-0.00699
74	3.43	6.26E-6	0.600	0.623	-0.02323
75	3.43	1.03E-5	0.571	0.594	-0.02352
76	3.43	1.72E-5	0.517	0.522	-0.00510
77	3.43	2.85E-5	0.432	0.406	0.02637
78	3.43	4.74E-5	0.317	0.252	0.06559
79	3.57	7.16E-6	0.592	0.621	-0.02865
80	3.57	8.49E-6	0.581	0.610	-0.02907
81	3.57	1.07E-5	0.563	0.589	-0.02672
82	3.57	1.57E-5	0.523	0.535	-0.01188
83	3.92	6.26E-6	0.595	0.631	-0.03611
84	3.92	1.72E-5	0.504	0.505	-0.00067
85	3.92	4.47E-5	0.285	0.215	0.07024
86	4.11	6.26E-6	0.592	0.633	-0.04058
87	4.11	1.03E-5	0.557	0.588	-0.03047
88	4.11	1.72E-5	0.496	0.497	-0.00130
89	4.11	2.85E-5	0.400	0.363	0.03658
90	4.11	4.47E-5	0.272	0.202	0.06999
91	5.12	7.16E-6	0.565	0.621	-0.05578
92	5.12	8.49E-6	0.544	0.600	-0.05571
93	5.12	1.07E-5	0.525	0.563	-0.03720
94	5.12	1.57E-5	0.472	0.480	-0.00758
95	5.82	6.26E-6	0.560	0.631	-0.07080
96	5.82	1.72E-5	0.432	0.427	0.00507
97	5.82	4.47E-5	0.178	0.110	0.06823
98	6.99	6.26E-6	0.533	0.619	-0.08536
99	6.99	1.72E-5	0.389	0.380	0.00954
100	6.99	4.74E-5	0.129	0.068	0.06087
101	8.30	6.26E-6	0.501	0.600	-0.09876
102	8.30	1.72E-5	0.347	0.331	0.01577
103	8.30	4.74E-5	0.090	0.037	0.05350
104	9.79	6.26E-6	0.467	0.576	-0.10891

OBS	PN	DFW	FRALV	PFRALV	PRESID
105	9.79	1.72E-5	0.298	0.281	0.01722
106	9.79	4.74E-5	0.067	0.013	0.05332
107	12.30	6.26E-6	0.411	0.531	-0.12025
108	12.30	1.72E-5	0.235	0.211	0.02401
109	12.30	4.74E-5	0.050	0.000	0.05725

APPENDIX G

The following tables list equations and coefficients used in the prediction of activity coefficients and hydrogen bonding factors for use in determining the partition coefficient (PN) as described in chapter 4. The tables are adapted from Reid, Prausnitz, and Sherwood²¹ and from Hayduk¹³.

TABLE G.1

Correlating Constants for the Calculation
of Activity Coefficients in Water
(adapted from Reid, Prausnitz, and Sherwood²¹)

(All values are for 25 degrees C unless otherwise stated.)

<u>SOLUTE</u>	<u>J</u>	<u>K</u>	<u>M</u>	<u>EQ'N</u>
n-Acids	-1.000	0.622	0.490	(a)
n-Primary Alcohols	-0.995	0.622	0.558	(a)
n-Secondary Alcohols	-1.220	0.622	0.170	(b)
n-Tertiary Alcohols	-1.740	0.622	0.170	(c)
Alcohols, General	-0.525	0.622	0.475	(d)
n-Allyl Alcohols	-1.180	0.622	0.558	(a)
n-Aldehydes	-0.780	0.622	0.320	(a)
n-Alkene Aldehydes	-0.720	0.622	0.320	(a)
n-Ketones	-1.475	0.622	0.500	(b)
n-Acetals	-2.556	0.622	0.486	(e)
n-Ethers (20 deg C)	-0.770	0.640	0.195	(b)
n-Nitriles	-0.587	0.622	0.760	(a)
n-Alkene Nitriles	-0.520	0.622	0.760	(a)
n-Esters (20 deg C)	-0.930	0.640	0.260	(b)
n-Formates (20 deg C)	-0.585	0.640	0.260	(a)
n-Monoalkyl Chlorides (20 deg C)	1.265	0.640	0.073	(a)
n-Paraffins (16 deg C)	0.688	0.642	0	(a)
n-Alkyl Benzenes	3.554	0.622	-0.466	(f)

TABLE G.1 (cont.)

EQUATIONS

$$(a) \text{ LOG } \gamma = J + K(N) + M/N$$

$$(b) \text{ LOG } \gamma = J + K(N) + M(1/N' + 1/N'')$$

$$(c) \text{ LOG } \gamma = J + K(N) + M(1/N' + 1/N'' + 1/N''')$$

$$(d) \text{ LOG } \gamma = J + K(N) + M(1/N' + 1/N'' + 1/N''' - 3)$$

$$(e) \text{ LOG } \gamma = J + K(N) + M(1/N' + 1/N'' + 2/N''')$$

$$(f) \text{ LOG } \gamma = J + K(N) + M(1/N - 4)$$

Where N = total number of carbon atoms in solute molecule

N', N'', N''' = number of carbon atoms in respective branches of branched compounds, counting the polar grouping; thus, for t-butanol, $N' = N'' = N''' = 2$

TABLE G.2

Hydrogen Bonding Factors for Gases in Water at 25 deg C
(adapted from Hayduk¹³)

<u>GAS</u>	<u>σ</u>
C4H10	0.0452
C2H3CL	0.0031
SO2	0.103
NH3	2.46
C3H8	0.0326
C2H6	0.0012
C2H2	0.0359
N2O	0.0247
C2H4	0.0053
CO2	0.0359
KR	0.0071
CH4	0.0069
NO	0.0175
A	0.0158
O2	0.0175
CO	0.0134
N2	0.0119
H2	0.0355
NE	0.0410
HE	0.0454
H	39.0

REFERENCES

1. Baker, Lon G., Ultman, James S., and Rhodes, Rodney A., "Simultaneous Gas Flow and Diffusion in a Symmetric Airway System: A Mathematical Model," Respiration Physiology, Vol. 21, No. 1, July, 1974, pg 119-138.
2. Bird, R.B., Stewart, W.E., and Lightfoot, E.N., Transport Phenomena, Wiley, New York, 1960
3. Boucher, Stutts, Bromberg, and Gatzky, "Regional Differences in Airway Surface Liquid Composition," Journal of Applied Physiology, Vol. 50 (1981)
4. Boyd, Eldon M., and Ronan, Alice, "The Excretion of Respiratory Tract Fluid," The American Journal of Physiology, Vol. 135, No. 2, January, 1942, pg 383-386.
5. Comroe, Julius H., Physiology of Respiration, 2nd Ed., Year Book Medical Publishers, Chicago, 1974.
6. Crank, John, The Mathematics of Diffusion, Clarendon Press, Oxford, 1956.
7. Davies, C.N., "Absorption of Gases in the Respiratory Tract," The Annals of Occupational Hygiene, Vol. 29, No. 1, 1985, pp. 13-25.
8. Fiserova-Bergerova, Vera, Modeling of Inhalation Exposure to Gases and Vapors, Chemical Rubber Company, 1983.
9. Gill, W.N., and Sankarasubramanian, R., "Exact Analysis of Unsteady Convective Diffusion," Proceedings of the Royal Society of London, Vol. 316, Series A, 1970.
10. Haggard, H.W., "The Absorption, Distribution, and Elimination of Ethyl Ether," Journal of Biology and Chemistry, Vol. 59, 1924.
11. Handbook of Physiology, Sect 3, Respiration, Vol. 1, American Physiological Society, 1964.
12. Hatch, Theodore, Cook, Kenneth M., and Palm, Paul E., "Respiratory Dead Space," Journal of Applied Physiology, Vol. 5, No. 7, January, 1953, pg 341-347.

13. Hayduk, Walter and Laudie, Harry, "Solubilities of Gases in Water and Other Associated Solvents", AICHE Journal, Vol. 19, No. 6, November, 1973, pg 1233-1238.
14. Jaegar, J.C., "Radial Heat Flow in Circular Cylinders," Proceedings of the Royal Society of New South Wales, Vol. 74, 1940, pp. 342-352.
15. Ketty, Seymour S., "The Theory and Application of the Exchange of Inert Gas at the Lung and Tissue," Pharmacological Review, Vol. 31, 1951.
16. Miller, F. and Menzel, D., Fundamentals of Extrapolation Modeling of Inhaled Toxicants, Hemisphere Publishing, 1984.
17. Morales and Smith, "On the Theory of Blood-Tissue Exchange of Inert Gases," Bulletin of Mathematics and Biophysics, Vol. 10, 1948.
18. Olson, Dan E., Sudlow, Michael F., Horsfield, Keith, and Filley, Giles F., "Convective Patterns of Flow During Inspiration", Archives of Internal Medicine, Vol. 131, No. 1, January, 1973, pg 51-57.
19. Panwitz, K., "Diffusion Coefficients," Drager Review, Vol. 52, January, 1984.
20. Reid, Lynne, "The Secondary Lobule in the Adult Human Lung, with Special Reference to Its Appearance in Bronchograms", Thorax, Vol. 13, No. 2, June, 1958, pg 110-115.
21. Reid, Robert C., Prausnitz, John M., and Sherwood, Thomas K., Properties of Gases and Liquids, 3rd Ed., McGraw-Hill, N.Y., 1977.
22. Scherer, P. W., Shendalman, L. H., Green, N. M., and Bouhuys, A., "Measurement of Axial Diffusivities in a Model of the Bronchial Airways," Journal of Applied Physiology, Vol. 38, No. 4, April, 1975, pg 719-723.
23. Schroter, R. C., and Sudlow, M. F., "Flow Patterns in Models of the Human Airways," Respiration Physiology, Vol. 7, No. 3, October, 1969, pg 341-355.
24. Tashiro, R., "Gas Absorption into the Human Respiratory Tract Fluid - Mathematical Model and Computer Calculation," Masters Technical Report, Department of Environmental Science and Engineering, University of North Carolina at Chapel Hill, 1979.

25. Taylor, Geoffrey, "Dispersion of Soluble Matter in Solvent Flowing Slowly through a Tube," Proceedings of the Royal Society of London, Vol. A219, 1953.
26. Teorell, T., "Kinetics of Distribution of Substances Administered to the Body," Arch. Internat. de Pharmacodyn. et de Therap. Vol. 57, 1937.
27. Ultman, James S. and Blatman, Hal S., "Longitudinal Mixing in Pulmonary Airways. Analysis of Inert Gas Dispersion in Symmetric Tube Network Models", Respiration Physiology, Vol. 30, No. 3, August, 1977, pg 349-367.
28. Wanner, Adam, "Clinical Aspects of Muco-Ciliary Transport," American Review of Respiratory Diseases, Vol. 116, 1977.
29. Weibel, E.R., Morphology of the Human Lung, Academic Press, 1963.
30. Widmark, E.M.P., "Studies in Concentration of Indifferent Narcotics in Blood and Tissues," Acta Med. Scandinav, Vol. 52, 1919.
31. Wilke, C. R. and Chang, Pin, "Correlation of Diffusion Coefficients in Dilute Solutions", AIChE Journal, Vol. 1, No. 2, June, 1955, pg 264-270.

END

FILMED

12-85

DTIC